TRANSPORT THROUGH
MACROMOLECULAR SOLUTIONS AND GELS

by

Chunhai Wang

B.S. (ENG.) ZHEJIANG UNIVERSITY, PRC (1982)

M.S. (ENG.) UNIVERSITY OF ROCHESTER (1989)

SUBMITTED TO THE DEPARTMENT OF MECHANICAL ENGINEERING IN
PARTIAL FULFILLMENT OF THE REQUIREMENTS FOR THE DEGREE OF

DOCTOR OF PHILOSOPHY

at the

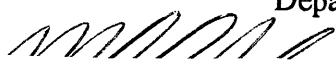## MASSACHUSETTS INSTITUTE OF TECHNOLOGY

December, 1993

(February 1994)

© Massachusetts Institute of Technology, 1993

Signature of Author _____
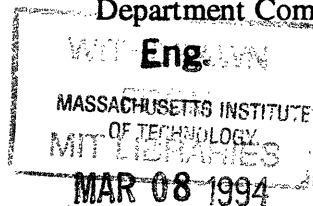Department of Mechanical Engineering
December, 1993

Certified by _____
Mark Johnson
Thesis Supervisor

Certified by _____
Professor Roger D. Kamm
Thesis Supervisor

Accepted by _____
Professor Ain A. Sonin, Chairman
Department Committee on Graduate Students

TRANSPORT THROUGH MACROMOLECULAR SOLUTIONS AND GELS

by

CHUNHAI WANG

Submitted to the Department of Mechanical Engineering on December 18, 1993 in partial fulfillment of the requirements for the Degree of Doctor of Philosophy

ABSTRACT

Transport of nutrients and fluids through body tissues is vital for the normal function of all multi-cellular organisms. Materials that need to be transported through this biological macromolecular network range from pure solvent, small molecular weight substances and nutrients to macromolecular substances. While transport through macromolecular networks is especially relevant to living organisms, the phenomenon is also found in a variety of medical and industrial processes. In all applications it is important to understand the mechanism of transport, and to know quantitative parameters such as the resistance of the network to the moving species, the species delivery rate and species distributions within the network.

One distinctive feature of transport through a macromolecular network is the interaction between the flow field, the macromolecular conformation and the structure of the network, as well as the chemical potential of the macromolecules. Previous studies have dealt with one aspect or another of this complex mechanochemical transport problem, but the mechanism of transport is not well understood and there are no reliable methods to predict transport parameters of practical importance in the multi-component systems.

In this study, transport equations derived from non-equilibrium thermodynamics were adopted. Analysis, literature data and additional measurements were then used to provide five additional "constitutive relations" for closure. Theoretical and experimental studies of binary and ternary systems of saline / albumin, saline / hyaluronic acid, saline / collagen gel, and saline / albumin / hyaluronic acid were carried out. Comparisons reveal that theory agrees well with experimental data for both binary and ternary solution systems. Several very interesting experimental observations as well as possible problems are discussed when matrix stress is involved.

Thesis Committee: Dr. Mark Johnson (Co-Chairman)
Prof. Roger D. Kamm (Co-Chairman)
Prof. Robert E. Cohen
Professor Ain A. Sonin
Professor Ioannis V. Yannas

Acknowledgment

Each Ph.D. experience is unique. Mine is no exception. To acknowledge everyone in one sheet of paper seems impossible, but I do know that I have been very lucky to have so many wonderful people in my life -- parents, mentors, colleagues and friends -- constantly providing for me, guiding me and encouraging me. My love and sincere gratitude to them all.

At MIT, I want to thank my advisers, Professor Roger Kamm and Dr. Mark Johnson for their guidance. Special appreciation goes to Roger for his understanding and support during critical times. It has been a very stressful period, but I am grateful that I have a very supportive thesis committee. I want to sincerely thank Professor Sonin for his guidance and support, much of which came at times when I needed it the most. Thanks also goes to Professor Cohen and Professor Yannas for their constant encouragement. A big thank you goes to Mr. Richard Fenner for his support in the Fluids Lab.

In seeking advice over the years, I have talked to many people. On the technical side, I would like to thank Professor Tim Pedley of Leeds, England, Professor Ronald Probstein and Professor Forbes Dewey of Mechanical Engineering, Professor Alan Grodzinsky of EECS, Professor John Deutch of Chemistry and Dr. David Edwards of Chemical Engineering. On the extracurricular side, I would like to thank Professor Edward Roberts of Sloan School, Director Robert K. Weatherall of MIT Career Office and Executive Director William Hecht of MIT Alumni Association. I immensely enjoyed my MIT experience, of which my non-technical activities were no small part.

My colleagues in the Fluids Lab and friends in and outside MIT made my stay in Cambridge a delight. In the lab, I have had so much fun with my office mates and close friends, Frank Espinosa and David Otis. Frank and Dave have done many proof-readings for me. Apparently they enjoyed it so much that they sometimes even insisted on proof-reading my letters to girlfriend(s). My thanks go to Jian Shen for his friendship and his help upon my first arrival; to Fuquan Gao for his friendship; to John Fowler for inviting me to his home state West Virginia for the wonderful white water rafting; to Ken Wesley for his Canadian lumber-jack hand shaking; to James Shin for the annual basketball pool which I never won; to Arthur, Barbara, Barry, Gregg, Edwin, James, Jim, John, Kathy, Mac, Manuel, Mariano, Mick, Naomi, Sanjay, Serhat, Stefano and Wilson for the numerous "beer seminars", poke and softball games ... Thanks to fellows, whom I cannot possibly list, for being helpful and cheerful friends. I missed those who already left and I will miss everyone who are still here. Keep in touch!

I endured graduate school largely because of the constant encouragement from so many close friends. I truly am thankful to my girlfriend Wendy for sharing with me the hardships and occasionally, the excitement. My close friends Zhihong and Li, Xiaomin and Peiying, Lei and Hui, Xiaohong and Jia, Tomorrow, Guy and Molly, and many others, were always there for me, and together we have had a lot of fun. *"Graduate school is hell"* and that has been surely the case at MIT, but thanks God, I made it and enjoyed it.

To the late Professor

T. C. LIN

Who guided me like a father to a son,

during my five year residence at

the Institute of Mechanics, Chinese Academy of Sciences

Table of Contents

List of Figures

List of Tables

Chapter 1

Introduction

1.1 Background

Transport of nutrients and fluids through body tissues is vital for the normal functions of all multi-cellular organisms. This transport takes place through the extracellular matrix, a biological macromolecular network. The extracellular matrix is comprised of the hydrophobic, fibrous proteins elastin and collagen and the hydrophilic, highly charged proteoglycans. The materials that need to be transported through this matrix range from pure solvent, small molecular weight substances and nutrients to macromolecular substances that may be either hydrophilic or hydrophobic (Bert and Pearce, 1984; Ganger, 1981). Transport through tissues is thus a permeation process of complex solutions through macromolecular networks.

While permeation through macromolecular networks is especially relevant to living organisms, the phenomenon is also found in a variety of medical and industrial processes. Membrane separation processes (Albertsson, 1986), transport in bio-reactors (Klibanov, 1983), artificial organ design (Deen et al, 1979), hemodialysis (Colton and Lowrie, 1981), controlled drug delivery (Langer, 1980) and gel chromatography (Yamamoto et al, 1990) are some examples.

Whether designing a synthetic kidney, a drug delivery system, or an industrial membrane separation device, one needs to understand the mechanism of transport through

macromolecular networks. In most applications, it is also important to know quantitative parameters such as the resistance of the matrix to the transporting species, the species delivery rate and species distributions within the network.

Permeation through macromolecular networks, especially transport in living organisms, is usually very complex. One distinctive feature of transport through the macromolecular network is that the structure of the network is determined by both the flow field and the molecular conformation. The structure affects the flow and the flow alters the structure. In addition to the forces one commonly encounters in traditional transport problems, the permeation occurs on a molecular scale where the chemical activities play an important role. If a network is cross-linked, then the flow will cause deformation in the matrix and the matrix stress will also play a role. Thus the transport through macromolecular networks is a complex mechanochemical problem. Simplified models have been developed in the earlier studies in order to understand certain aspects of the process. We review these studies briefly next.

1.2 Previous Studies

1.2.1 Porous Media Theory

Studies on how network structures affect transport are described as porous media theory. Central to porous media theory is an empirical equation known as Darcy's Law, valid for creeping flows, that relates the pressure gradient to flow rate through a parameter called the "specific hydraulic conductivity", or the "permeability" (Bear, 1972). Hence the determination of the permeability coefficient has been a main subject of porous media

theory.

The transport of fluids through low porosity porous medium has been modeled as internal flow as the flow paths are describable torturous pores. The permeability of the low porosity porous medium was given by Carmen-Kozeny formula which relates the permeability to porosity and average pore radius square through an empirical coefficient, the tortuosity factor (Bird, et al, 1960). The transport through a porous medium of high porosity where fluids flow around the matrix component, on the other hand, has been modeled as external flow (Happel and Brenner, 1965). The unit cell model (Kuwabara, 1959), the method of reflections (Kirkwood and Riseman, 1948) and the "average field" approach such as Debye-Brinkman method (Debye and Buche, 1948; Brinkman, 1948) are examples of external flow modeling. Permeability of a variety of materials has also been calculated from sedimentation and ultrafiltration experiments. The data are generally in good agreement with the predictions for monodispersed porous media (Bear and Corapcioglu, 1984).

For a polydispersed matrix, however, there are relatively few studies. Either (1991) applied the Debye-Brinkman method to calculate permeability of a media composed of two types of macromolecules. The hindering effect of macromolecular network on the moving proteins has been discussed experimentally. These experimental studies established that the sedimenting speed of albumin in hyaluronic acid solution decreases exponentially with the increase of the square root of hyaluronic acid concentration (Laurent, 1960, 1963; Winlove and Parker 1984). Analyses, many of which based on the mean field theory (Flory, 1953), gives the same exponential relation reported in the experimental studies (Altenberger et al, 1985; Jansons and Phillips, 1989).

14

1.2.2 The Effect of Chemical Activity Gradient

Chemical activity for a dilute solution is its solute concentration (Gyftopoulos, 1991). In a solution where each component is free to move, chemical activity gradients drive diffusional fluxes (Truesdell, 1962). In a solution where the solute is blocked by a membrane, the chemical activity difference across the membrane gives rise to an osmotic pressure difference (Hiemanz, 1986). Since both diffusion and osmosis are caused by the chemical activity gradient, the diffusivity and the osmotic pressure are related; this relationship is characterized by the Stokes-Einstein equation (Wijmans et al, 1985). In general, the chemical activity gradient is one of the driving forces for species transport in a microscopic system (Tanford, 1963). Transport through macromolecular networks occurs at molecular length scale and hence chemical activity plays a very important role (Silberberg, 1980, 1989).

1.2.3 The Effect of Matrix Stress

The deformation of an elastic matrix is associated with the development of an elastic stress within the matrix. For a matrix composed of random coils of macromolecules, rubber elasticity theory (Treloar, 1975) and Flory-Huggins theory (Flory, 1953) with scaling modification (de Gennes, 1979) has been used to derive a stress and strain relation (Horkay and Zrinyi, 1986, 1988). For a matrix under a small deformation in general, a linear stress-strain relation may be determined experimentally (Mow et al, 1984).

During transport through cross-linked macromolecular networks, flow causes the deformation of the matrix and the matrix stress in turn plays a role in determining the flow. The effect of the matrix stress in transport processes are discussed primarily in gel swelling kinetics (Tanaka and Fillmore, 1979; Horkey and Zrinyi, 1986, 1988) and cartilage related studies (Biot, 1962; Rice and Cleary, 1976; Mow, 1984; Eisenberg and Grodzinsky, 1987; Holemes and Mow, 1990; Lai et al, 1991; Gu et al, 1993). The former application motivated the derivation of a diffusion equation that describes the displacement of the gel. The effect of the matrix stress has been lumped into an "effective diffusion coefficient" which is determined experimentally (Tanaka and Fillmore, 1979). Cartilage studies, based on biphasic model (Mow et al, 1984), employed an empirical linear stress-strain relation for the combined media of solvent and solute; and the solvent transport rate was determined indirectly through the deformation of the media (Eisenberg and Grodzinsky, 1987). Both approaches are geared towards determining the stress and deformation of a matrix rather than the species transport. Based on the biphasic cartilage theory, a triphasic model has been proposed recently for cartilage studies. The elastic stress was treated as part of a total stress tensor which represents the combined effect of solute concentration, electric charge and the matrix deformation (Lai et al, 1991; Gu et al, 1993).

1.2.4. Transport Equations from Non-Equilibrium Thermodynamics

Linear phenomenological equations for species transport in a mixture have been described in non-equilibrium thermodynamics (Katchalsky and Curran, 1965). The application of the linear phenomenological equations in a binary macromolecular solution system gave rise to a modified version of Darcy's law (Wijmans et al, 1985; Wales, 1981), in which

the driving force for the flow is the combination of the hydrodynamic and osmotic pressure. The same principle is the underpinning of the triphasic theory in recent cartilage studies (Lai et al, 1991, Gu et al, 1993). For transport through multi-component macromolecular networks involving matrix stresses, the linear phenomenological equations were used in conjunction with the local equilibrium assumption to derive a set of transport equations (Silberberg, 1980, 1989). This model has the capacity to solve the transport problem of multi-component macromolecular systems. However, the model requires additional expressions for the chemical activities, the frictional coefficients, and the stress-strain relation for closure. For multi-component systems where forces acting on one component are affected by the existence of the other components, it is not straight-forward how to determine the required expressions. An attempt was made to produce closure and to solve for a three-component system, but the calculation was admittedly ad hoc (Silberberg, 1989).

In summary, a variety of theories and experimental data are available in the literature related to one aspect or another of transport through macromolecular networks. There is no theoretical framework to date, however, which could allow us to have a comprehensive understanding of the transport process. The transport equations of multi-component macromolecular systems based on non-equilibrium thermodynamics is promising, but unfortunately it is still incomplete, and has not been verified experimentally. Further studies are required.

1.3 Objectives and Approaches

Based on the previous discussion, the objectives of this thesis are three-fold:

To develop a comprehensive theoretical framework to describe the transport of fluid and macromolecules in a multi-component system that incorporates non-equilibrium thermodynamics, fluid mechanics and porous media theory

To develop a closure scheme which would allow us to obtain all necessary "constitutive relations" for the theoretical framework, whether by theoretical or by experimental means

To verify the framework we proposed experimentally

In short, we seek to provide a reliable framework and a systematic method to study steady-state transport processes through multi-component macromolecular networks.

To achieve our goals, we choose a one-dimensional steady state ultrafiltration shown in Fig. 1.1 as our model. This one-dimensional steady state model allows us to examine the interplay of major factors affecting transport. The disadvantage of the ultrafiltration experiment is that it requires a long time to reach equilibrium. Although sedimentation experiments will achieve equilibrium much faster under high centrifugal force, it seems that it would not allow us to examine the transport mechanism in detail. For example, under centrifugation the chemical activities are negligible compared with the dominant centrifugal force (Tanford, 1963) which is not the case in most natural transport processes in living tissues.

Using the steady-state one-dimensional ultrafiltration model, two-component ultrafiltration will be studied to elucidate the essential features of the transport process. Three-component ultrafiltration will then be studied. This approach will ensure the model and methods developed in this study can be generalized easily to solve for transport through multi-component macromolecular systems. With the bio-engineering applications

18

in mind, we choose albumin, hyaluronic acid and collagen to be the sample macromolecules. Hyaluronic acid is a long chain molecule and is a member of the glycosaminoglycan family (GAGs). Collagen is a structural protein which is usually found in a cross-linked form in nature. Both GAGs and collagen are the main constituents of the extracellular matrix (Ogston, 1970; Granger, 1981; Grodzinsky, 1983). Albumin is a widely distributed globular protein found in plasma and tissues and is transported through the extracellular matrix (Katz et al, 1970; Bill, 1960).

Overall, five distinct transport environments will be considered.

• *Saline filtration through an albumin solution layer*

• *Saline filtration through a hyaluronic acid solution layer*

• *Saline filtration through a collagen gel, a cross-linked macromolecular network which can support elastic load layer*

• *Saline filtration through a layer of albumin and hyaluronic acid mixture*

• *Mixture of Saline, albumin and hyaluronic acid filtration through a membrane which partially blocks both albumin and hyaluronic acid*

1.4 Outline of Thesis

Chapter Two and Three constitute the theoretical framework of this study. The transport equations are presented in Chapter Two with theories and methods for determining various "constitutive relations" discussed in Chapter Three. The design and fabrication of the main experimental apparatus will be described in Chapter Four. Chapter Five through Chapter Nine will describe the experiments, the analysis and the comparison of

the data for the five model systems listed in Section 1.3. The last chapter will include comments, conclusions and suggestions for future studies on the transport through macromolecular networks.

$$\Delta P = P_1 - P_0$$

P1

Solvent

Macromolecular
solution or gel

x

0

P0

Semi-permeable
Membrane

Q
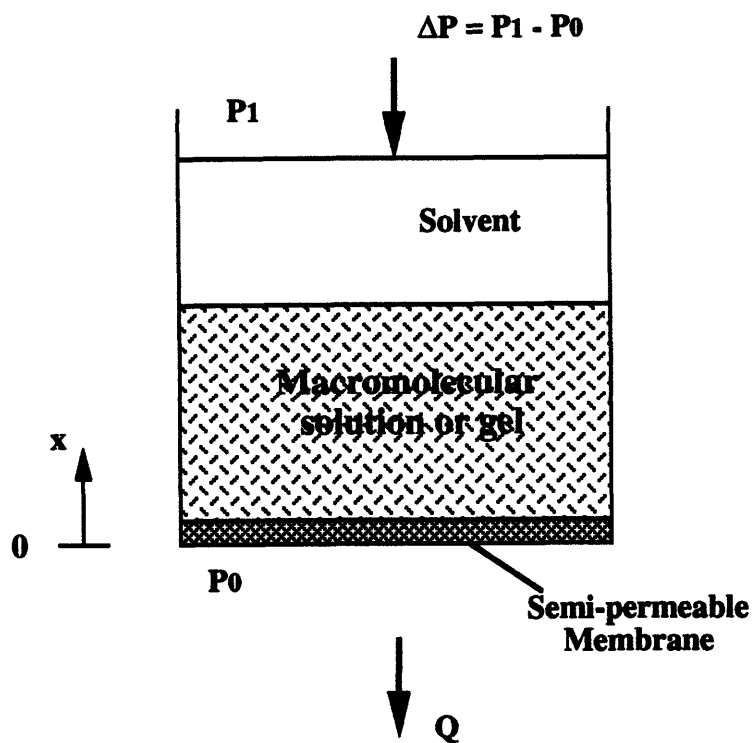
Fig. 1.1 Schematics of the One-Dimensional Steady-State Filtration Model

Chapter 2

Transport Equations in Macromolecular Systems

As discussed in Section 1.2.4, several formulations have been proposed in the literature to describe transport in macromolecular networks and they are all based on non-equilibrium thermodynamics. In this chapter, we will follow Silberberg's approach (1980, 1989) to derive a set of transport equations from the fundamental relations of thermodynamics. We only consider transport problems under constant temperature.

2.1 Thermodynamic Relations

Transport equations can be derived from the linear phenomenological equations, chemical potential relations and the Gibbs-Duhem equation. A general n-component system will be considered. In a macromolecular network, some components may be in a gelled state which can support mechanical load. We will lump these components into one and designate it as the matrix component. Furthermore, we assume that each fiber in the matrix component can only support tensile or compressive stress. Thus, our model is an n-component system with possibly one matrix-like species which can support tensile or compressive stresses.

2.1.1 Linear Phenomenological Equations

Transport through macromolecular networks is typically a flow with very low Reynolds number. Frictional forces between components at slow relative motion can be expressed linearly through Newton's friction law. The balance on each component of the frictional forces and the driving force, the chemical potential gradient, gives the linear phenomenological equations (Tanford, 1964)

$$\nabla \mu_i + \sum_{j \neq i} f_{ij}(\bar{v}_i - \bar{v}_j) = 0 \qquad i = 1, 2, \ldots n \qquad (2.1)$$

where

μ_i: chemical potential per unit mass of species i

f_{ij}: frictional coefficient between species i and j, $i \neq j$

$\bar{v}_i$: velocity of species i

To determine the transport velocity of each species, one needs to provide expressions for the chemical potentials as well as the frictional coefficients.

2.1.2 Expression of Chemical Potential

The chemical potential of the ith species, μ_i, is given by

$$\mu_i = \left(\frac{\partial G}{\partial n_i} \right)_{T, p, n_j} \qquad (2.2)$$

22

where n_i is the mass of ith component and G is the Gibbs free energy defined as

$$G = E + pV - TS \qquad (2.3)$$

with E, p, V, T, S being energy, pressure, volume, temperature and entropy of the system, respectively.

For a macromolecular system involving one matrix component, the first law, including the elastic energy, is found as (Katchalsky and Curran, 1965)

$$dE = TdS - pdV + \sigma dV_m + \sum_i \mu_i dn_i \qquad (2.4)$$

where σ is stress per unit cross sectional area of matrix (positive if tensile) and V_m is the total volume of the matrix component

$$V_m = n_m \upsilon_m$$

where υ_m is its partial specific volume.

From (2.3) and (2.4),

$$dG = -SdT + Vdp + (\sum_{i \neq m} \mu_i dn_i) + (\mu_m + \sigma \upsilon_m) dn_m \qquad (2.5)$$

From (2.2) and (2.5), we have (Silberberg, 1980, 1989)

$$d\mu_i = -s_i dT + \upsilon_i dp + RTd(\ln a_i) \quad , \quad i \neq m$$

$$d\mu_m = -s_m dT + \upsilon_m(dp - d\sigma) + RTd(\ln a_m)$$

(2.6)

where R is the universal gas constant, s_i is the partial specific entropy of component i and a_i is defined as "chemical activity" of the ith component. For dilute solutions, chemical activity of the ith component is the concentration of that component (Gyftopoulos and Beretta, 1991).

The combination of (2.6) and (2.1) provides a set of equations governing species transport through macromolecular networks. The equations involve a total of n(n-1) unknown frictional coefficients. In the following section, we will derive Onsager reciprocal relations which will reduce the number of unknown frictional coefficients by half.

2.1.3 Onsager's Reciprocal Relations

Since entropy, volume and mass are all additive, we can derive Eulers equation from the energy equation (2.4) (Gyftopoulos and Beretta, 1991):

$$E = TS - pV + \sigma V_m + \sum_i \mu_i n_i$$

(2.7)

Take differential of Eulers equation (2.7) and subtract from it the energy equation (2.4), we have the Gibbs-Duhem equation

$$-dp + \phi_m d\sigma + \sum_i c_i d\mu_i + \frac{S}{V} dT = 0 \qquad (2.8)$$

where ϕ_m and c_i are matrix volume fraction and the concentration of ith component, respectively,

$$\phi_m = \frac{V_m}{V} \quad , \quad c_i = \frac{n_i}{V}$$

The balance of mechanical forces, on the other hand, gives (Silberberg, 1980)

$$-dp + \phi_m d\sigma = 0 \qquad (2.9)$$

Hence at constant temperature, (2.8) reduces to

$$\sum_i c_i d\mu_i = 0 \qquad (2.10)$$

Combining (2.1) and (2.10), we have Onsager's reciprocal relation

$$c_i f_{ij} = c_j f_{ji}$$

or

$$\gamma_{ij} = \gamma_{ji} \qquad (2.11)$$

where

$$\gamma_{ij} = c_i f_{ij}$$

Truesdell (1962) has argued that this derivation is not strictly correct for multi-component ($n \geq 3$) mixture. The Onsager's reciprocal relation, however, may be regarded as a well-established law based on experimental verifications (Katchalsky and Curran, 1965).

Noticing that

$$\bar{F}_{ij} = c_i f_{ij}(\bar{v}_i - \bar{v}_j) \ , \ \bar{F}_{ji} = c_j f_{ji}(\bar{v}_j - \bar{v}_i)$$

are the action and reaction between component i and j in a unit volume of the mixture, Onsager's reciprocal relation is equivalent to Newton's Third Law.

Several additional relations are useful. By definition, species conservation is

$$\phi_i = c_i \upsilon_i \ , \ \sum_i \phi_i = 1 \tag{2.12}$$

where υ_i is the partial specific volume of the ith component.

Substitution of (2.6), (2.9) and (2.12) into (2.10), we have

$$\sum_i c_i d(\ln a_i) = 0 \tag{2.13}$$

Among the n equations in (2.1) and equation (2.9), there are only n independent equations because the sum of n equations of (2.1) gives equation (2.9). Physically, the summation of all n equations in (2.1) represents the total force balance in a mixture. After all internal forces, namely the chemical activity gradients and the frictional forces, cancel out, the remaining force balance is the mechanical force balance. Hence, we can choose any n equations out of this set of (n+1) equations at our convenience.

26

Now we are prepared to derive transport equations for n-component macromolecular systems. Although general transport equations of n-component system can be derived (Silberberg, 1980, 1989), we will derive transport equations for two and three-component systems so that the underlying physics is more apparent. We will use subscript 1 for the solvent phase and 2 for the solute phase. Subscript 3 or m stands for the matrix phase. In two-component systems where solute is in matrix form, 2 and m are used interchangeably.

2.2   Transport Equations for Two-component Systems

As stated earlier in the last section, for tow-component system, only two equations of the three represented in (2.1) and (2.9) are independent in two-component systems. From the first equation (i=1) of (2.1) with chemical activity given by (2.6), we have

$$\nabla(p + \frac{RT}{\upsilon_1}\ln a_1) + \frac{f_{12}}{\upsilon_1}\bar{v} = 0 \tag{2.14}$$

where $\bar{v}$ is the relative velocity between component 1 and 2. Equation (2.14) can be written in the more familiar Darcy's law form. Together with (2.9), we have

$$\nabla(p - \pi) = -\frac{\mu}{K}\bar{v}_{av}$$

$$\tag{2.15}$$

$$\nabla p = \phi_m \nabla \sigma$$

where the osmotic pressure π, the average velocity $\bar{v}_{av}$ and the hydraulic conductivity K

27

are defined as

$$\pi = -\frac{RT}{\upsilon_1}\ln a_1 \quad, \quad \bar{v}_{av} = \frac{\bar{Q}}{A} = \phi_1\bar{v} \quad, \quad K = \frac{\mu\phi_1^2}{\gamma_{12}} \tag{2.16}$$

with Q and A being solvent flux relative to solute and the cross-sectional area, respectively. a_1 is the chemical activity of solvent. The reference state of the osmotic pressure is chosen as pure solvent where a_1 equals 1.

Equations in (2.15) are transport equations for a two component system. In order to solve transport rate and species distribution, one has to provide the relations for the osmotic pressure and the specific hydraulic conductivity. When matrix stress is involved, one needs a stress-strain relation as well.

2.3   Transport Equation for Ternary System

From the first two equations of (2.1) with the substitution of (2.6), we have , for one-dimensional transport as shown in Fig. 1.1,

$$\upsilon_1\frac{dp}{dx} + RT\frac{d(\ln a_1)}{dx} + f_{12}(v_1 - v_2) + f_{13}(v_1 - v_3) = 0$$

$$\tag{2.17}$$

$$\upsilon_2\frac{dp}{dx} + RT\frac{d(\ln a_2)}{dx} + f_{21}(v_2 - v_1) + f_{23}(v_2 - v_3) = 0$$

Using (2.13), and noticing that

$$v_1 - v_2 = (v_1 - v_3) - (v_2 - v_3)$$

$$\upsilon_i = \frac{\phi_i}{c_i}, \quad \gamma_{ij} = c_i f_{ij}, \quad \gamma_{ij} = \gamma_{ji}$$

the velocities in (2.17) can be expressed as follows

$$v_1 - v_3 = \alpha \frac{dp}{dx} + \beta \frac{d\pi_2}{dx} + \vartheta \frac{d\pi_3}{dx}$$

(2.18)

$$v_2 - v_3 = \xi \frac{dp}{dx} + \eta \frac{d\pi_2}{dx} + \zeta \frac{d\pi_3}{dx}$$

where

$$\alpha = -\frac{\phi_1 \gamma_{12} + \phi_1 \gamma_{23} + \phi_2 \gamma_{12}}{\delta}$$

$$\beta = \frac{\phi_1 \gamma_{23}}{\delta}$$

$$\theta = \frac{\phi_1 \gamma_{12} + \phi_1 \gamma_{23}}{\delta}$$

$$\xi = -\frac{\phi_2 \gamma_{12} + \phi_2 \gamma_{13} + \phi_1 \gamma_{12}}{\delta}$$

$$\eta = -\frac{\phi_1 \gamma_{23}}{\delta}$$

$$\zeta = \frac{\phi_1 \gamma_{12}}{\delta}$$

$$\delta = \gamma_{12} \gamma_{23} + \gamma_{12} \gamma_{13} + \gamma_{13} \gamma_{23}$$

γ_{ij} are the frictional coefficients per unit volume of the mixture. $\alpha, \beta, \theta, \xi, \eta, \zeta$ are all functions of frictional coefficients and volume fractions. π_i is the "partial osmotic pressure" of component i defined as follows

29

$$\frac{d\pi_2}{dx} = \frac{\phi_2}{\phi_1}\frac{RT}{\upsilon_2}\frac{d}{dx}(\ln a_2)$$

$$\frac{d\pi_3}{dx} = \frac{\phi_3}{\phi_1}\frac{RT}{\upsilon_3}\frac{d}{dx}(\ln a_3)$$

(2.19)

Although the chemical activity of component 1 does not explicitly appear in the above equations, it plays a role through equation (2.13). From Eqs. (2.15) and (2.16), in an osmometer with a membrane blocking all solutes of a multi-component mixture, it is the solvent chemical activity which give rise to the osmotic pressure of the mixture. Defining the partial osmotic pressure of component 1 in a multi-component mixture as the conventional osmotic press with pure solvent as its reference state, namely

$$\pi = \pi_1 = -\frac{RT}{\upsilon_1}\ln a_1$$

(2.20)

then Eqs. (2.12), (2.13), (2.19) and (2.20) give

$$\frac{d}{dx}(\pi_1 - \pi_2 - \pi_3) = 0 \ , \text{or} \ (\pi_1 - \pi_2 - \pi_3) = \text{Const.}$$

chose a reference state to be pure solvent at which all partial osmotic pressures are zero, we have

$$\pi = \pi_1 = \pi_2 + \pi_3$$

(2.21)

The transport rates of each moving species, as expected, depend linearly on the pressure gradient and the partial osmotic pressure gradients according to Eq. (2.18). Equations (2.18) may also be written in such a form that the conventional hydraulic conductivity

and reflection coefficient appear explicitly (Silberberg, 1980, 1989).

One more independent equation to compliment equation (2.18) is the equation of the mechanical force balance on the mixture

$$\frac{dp}{dx} = \phi_m \frac{d\sigma}{dx} \tag{2.22}$$

(2.18) and (2.22) constitutes a set of all independent transport equations of a three component system. To solve for the transport rates and the species distributions, we have to provide three frictional coefficients and the stress-strain relation as a function of concentrations. Also we have to provide osmotic pressure as functions of concentration of all species.

2.5 Conclusions

The explicit transport equations for two and three-component systems have been derived. The transport equations by themselves, however, are incomplete in the sense that there are more unknowns than the equations. "Constitutive relations", which can relate the friction coefficients, osmotic pressures and the matrix stress with concentrations of species, must be provided to produce a closure. Additional theory and experiments to provide these "constitutive relations" will be discussed in Chapter Three.

Chapter 3

Constitutive Relations

This chapter presents the theories and methods that provide closure for the transport equations derived in Chapter Two. As discussed earlier in Section 2.2 and 2.3, two-component systems require one osmotic pressure and one frictional coefficient, while three-component systems require two partial osmotic pressures and three frictional coefficients for closure. When a gelled component which can support a mechanical load is present, an additional stress-strain relation is necessary. In two-component mixtures, osmotic pressure as a function of solute concentration can be measured routinely by conventional membrane osmometers (Adams, 1985; Wagner, 1945). Hence, we will first focus on theories and schemes to determine partial osmotic pressures in three-component systems. Then we will discuss theories and methods to determine frictional coefficients for both two and three-component systems. A discussion of the stress-strain relation will be left for Chapter Eight where a gelled component is considered.

3.1   Determination of Partial Osmotic Pressures

Partial osmotic pressures, as given in Eq. (2.19), are defined by chemical activities. Although osmotic pressure can be easily measured by a membrane osmometer in a two-component mixture, the measurement of partial osmotic pressures, or equivalently the chemical activities, is not easy in a multi-component mixture. Based on the osmotic pressure measurement method for two-component mixtures, one might want to use a

membrane osmometer with membranes which can selectively block only one solute at a time to determine partial osmotic pressures. It is not known, however, that how these measurements relate to the partial osmotic pressures. In the following sections, we will develop a procedure to determine partial osmotic pressures of a three-component mixture with a membrane osmometer.

3.1.1   Equilibrium Thermodynamic Relations

Partial osmotic pressures can be obtained according to their definition (2.19) once we determine chemical activities as functions of solute concentrations. Hence we here discuss the determination of chemical activities in multi-component macromolecular systems.

At osmotic equilibrium, the hydrostatic pressure difference across the membrane is balanced by the chemical activity difference across the membrane. For species i at chemical equilibrium across the membrane, there can be no difference in chemical potential (Tanford, 1963):

$$D\mu_i = 0 \qquad\qquad (3.1)$$

For clarity, notation "D" is used for difference across the membrane, while "Δ" represents changes relative to the reference state "c".

Using the expression of (2.6) for chemical potentials, we have at constant temperature

$$Dp = -\frac{RT}{\upsilon_i} D(\ln a_i) \tag{3.2}$$

The relation between chemical activities in a mixture at equilibrium is given by (2.13), or equivalently

$$\sum_i \{\phi_i \frac{RT}{\upsilon_i} \Delta(\ln a_i)\} = 0 \tag{3.3}$$

Equation (3.2) and (3.3) will be used to determine the quantity:

$$\frac{RT}{\upsilon_i} \Delta(\ln a_i) \quad , \quad i = 1, 2, \ldots$$

3.1.2 Experimental Scheme and Analysis

We choose saline, albumin and hyaluronic acid mixture as an example and use subscript 1, 2 and 3 for saline, albumin and hyaluronic acid, respectively. Our objective is to determine the chemical activities of each component relative to a common reference state "c"

$$\frac{RT}{\upsilon_i} \Delta(\ln a_i) = \frac{RT}{\upsilon_i} (\ln a_i - \ln a_i^c)$$

where superscript "c" stands for the reference state

$$(\phi_1, \phi_2, \phi_3) = (1, 0, 0)$$

Let's now consider experimental schemes.

pa

pb $\varnothing 1, \varnothing 2, \varnothing 3$ $\varnothing 1, \varnothing 2$ $\varnothing 1$ pc

B   A   C
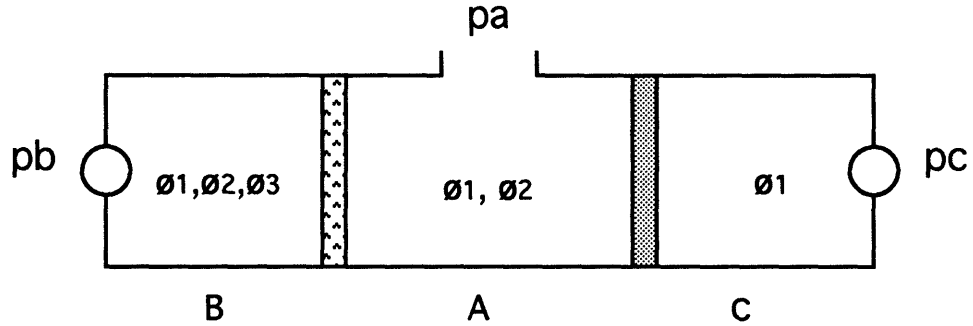
Fig. 3.1 Schematics of an Experimental Scheme for Determining Partial Osmotic Pressures in Ternary Mixtures. The three-component macromolecular mixture is made of saline, albumin and hyaluronic acid. Membrane between chamber A and B is permeable to both saline and albumin while membrane between chamber B and C is permeable to saline only. All three chambers are in equilibrium with each other. pb and pc are pressures measured by pressure transducers in chamber B and chamber C, respectively. pa is the ambient pressure.

Applying Eq. (3.2) across the membrane between chamber A and B for species 1 and 2 at the equilibrium state gives:

$$
\begin{aligned}
p^a - p^b &= \frac{RT}{\upsilon_1}(\ln a_1^b - \ln a_1^c) - \frac{RT}{\upsilon_1}(\ln a_1^a - \ln a_1^c) \\
p^a - p^b &= \frac{RT}{\upsilon_2}(\ln a_2^b - \ln a_2^c) - \frac{RT}{\upsilon_2}(\ln a_2^a - \ln a_2^c)
\end{aligned}
\tag{3.4}
$$

Superscript a, b and c stand for the equilibrium states in chamber A, B, and C. Chamber C has pure saline and hence is the reference state.

Applying Eq. (3.3) in chamber B at equilibrium with the same reference state c, we have:

$$\frac{RT}{\upsilon_3}\Delta(\ln a_3^b) = -\left(\frac{\phi_1^b}{\phi_3^b}\right)\frac{RT}{\upsilon_1}\Delta(\ln a_1^b) - \left(\frac{\phi_2^b}{\phi_3^b}\right)\frac{RT}{\upsilon_2}\Delta(\ln a_2^b) \tag{3.5}$$

Equations (3.3), (3.4) and (3.5) give:

$$\frac{RT}{\upsilon_1}\Delta(\ln a_1^b) = p^a - p^b + \frac{RT}{\upsilon_1}\Delta(\ln a_1^a)$$

$$\frac{RT}{\upsilon_2}\Delta(\ln a_2^b) = p^a - p^b + \frac{RT}{\upsilon_2}\Delta(\ln a_2^a) \tag{3.6}$$

$$\frac{RT}{\upsilon_3}\Delta(\ln a_3^b) = -\left(\frac{\phi_1^b}{\phi_3^b}\right)\frac{RT}{\upsilon_1}\Delta(\ln a_1^b) - \left(\frac{\phi_2^b}{\phi_3^b}\right)\frac{RT}{\upsilon_2}\Delta(\ln a_2^b)$$

Now, apply Eq. (3.2) for species 1 across membrane between chamber A and C:

$$\frac{RT}{\upsilon_1}\Delta(\ln a_1^a) = p^c - p^a \tag{3.7}$$

Applying Eq. (3.3) inside chamber A gives:

$$\frac{RT}{\upsilon_2}\Delta(\ln a_2^a) = -\left(\frac{\phi_1^a}{\phi_2^a}\right)\frac{RT}{\upsilon_1}\Delta(\ln a_1^a) = \left(\frac{\phi_1^a}{\phi_2^a}\right)(p^a - p^c) \tag{3.8}$$

36

Substitution of Eq. (3.7) and (3.8) to Eq. (3.6) gives:

$$\frac{RT}{\upsilon_1}\Delta(\ln a_1^b) = -p^{bc}$$

$$\frac{RT}{\upsilon_2}\Delta(\ln a_2^b) = -p^{ba} + \left(\frac{\phi_1^a}{\phi_2^a}\right)p^{ac}$$

$$\frac{RT}{\upsilon_3}\Delta(\ln a_3^b) = \left(\frac{\phi_1^b}{\phi_3^b}\right)p^{bc} + \left(\frac{\phi_2^b}{\phi_3^b}\right)\left(p^{ba} - \left(\frac{\phi_1^a}{\phi_2^a}\right)p^{ac}\right)$$

(3.9)

where

$$p^{ij} = p^i - p^j \quad , \quad i,j = a,b,c$$

(3.10)

In our example, the volume fraction of hyaluronic acid in chamber B is known since all hyaluronic acid is blocked by the membrane. The volume fraction of albumin in chamber A can be deduced by comparing p^{ac} with the osmotic pressure-concentration curve of two-component mixtures of albumin and saline. Given the initial concentrations, all other volume fractions can then be obtained from the species conservation.

Rewrite the first equation in Eq. (3.9) as

$$\pi^{bc} = \pi^{ba} + \pi^{ac}$$

(3.11)

where

$$\pi^{bc} = -\frac{RT}{\upsilon_1}\Delta(\ln a_1^b)$$

$$\pi^{ba} = p^b - p^a \tag{3.12}$$

$$\pi^{ac} = p^a - p^c$$

While by definition (2.20), π^{bc} is the osmotic pressure of the mixture, or the partial osmotic pressure of the solvent, π^{ba} and π^{ac} are only part of the partial osmotic pressures according to Eqs. (2.19) and (3.9).

Eq. (3.9) tells that the osmotic pressure between chamber B and C equals the osmotic pressure between chamber B and A plus the osmotic pressure between chamber A and C. We also know from Eq. (3.9) that for a general three-component mixture, when the volume fraction of component one approaches zero, we recover the relation between the measured pressure and the chemical potentials of a two-component mixture. Eqs. (2.19) and (3.9) give the partial osmotic pressure gradients required for closure in the transport equations (2.18) of three-component mixtures.

The direct measurement of volume fractions can be used as an independent check of the procedure developed here.

In conclusion, chemical activities and thus the partial osmotic pressures can be obtained from the theory and experimental scheme developed in this section for a three-component mixture of saline, albumin and hyaluronic acid. The implementation of the measurement procedure requires that there exists a membrane which can completely block hyaluronic acid while allowing albumin to pass freely. This approach can be generalized for other multi-component mixtures.

3.2 An Alternative Method to Determine Partial Osmotic Pressures

A semi-empirical method based on the excluded volume concept (Wielderhielm et al, 1976) can also be used to determine partial osmotic pressures in a mixture of saline, albumin and hyaluronic acid.

Consider a mixture of saline, albumin and hyaluronic acid at osmotic equilibrium with pure saline. The total volume of the mixture can be conceptually divided into two compartments, namely, the volume available to albumin and that available to the hyaluronic acid. In other words, in a three-component mixture composed of a solvent and two solutes, the existence of one solute "excludes" a certain volume of the solvent from the other and vice versa. As a result, the effective concentrations of both solutes increase. At osmotic equilibrium, the action exerted by the albumin compartment on the volume occupied by hyaluronic acid equals that exerted by the hyaluronic acid compartment on the volume occupied by albumin; and they both equal to the equilibrium osmotic pressure of the mixture.

Suppose we have determined experimentally the osmotic pressure in a two-component mixture of saline and albumin, and of saline and hyaluronic acid

$$\pi_{bsa} = f(c_b)$$
$$\pi_{ha} = g(c_h) \tag{3.13}$$

where π_{bsa} and c_b are the osmotic pressure and the concentration of albumin and saline mixture respectively, whereas π_{ha} and c_h are the counterparts for the hyaluronic acid and

saline mixture.

Then at osmotic equilibrium of the three-component mixture of saline, albumin and hyaluronic acid, we find that

$$\pi_{eq} = f(c_b^{eff}) = g(c_h^{eff}) \tag{3.14}$$

where π_{eq} is the equilibrium osmotic pressure of saline, albumin and hyaluronic acid mixture, and

$$c_b^{eff} = \frac{c_b}{\lambda} \ , \ c_h^{eff} = \frac{c_h}{1-\lambda}$$
$$\lambda = \frac{V_b}{V} \ , \ V = V_b + V_h \tag{3.15}$$

V_b and V_h are the volumes available to albumin and hyaluronic acid in the mixture respectively. V is the total volume of the mixture.

From (3.14) and (3.15), we can solve λ

$$\lambda = \lambda(c_b, c_h) \tag{3.16}$$

Substitution of (3.15) and (3.16) back into (3.14) gives the equilibrium osmotic pressure of the three component mixture. Experimental data agree well with the calculated equilibrium osmotic pressure in the mixture of saline, albumin and hyaluronic acid (Wiederhielm, 1976).

To calculate the partial osmotic pressures, I further postulate, according to Eq. (2.21):

$$\pi_b = \lambda \pi_{eq} \quad , \quad \pi_h = (1 - \lambda)\pi_{eq} \qquad (3.17)$$

where π_b and π_h are the partial osmotic pressures of albumin and hyaluronic acid in the three-component mixture respectively.

At first glance, assumption (3.17) resembles Dalton's law of partial pressure for ideal mixtures (Gyftopoulos & Beretta, 1991). The hypothesis, however, has included the excluded volume effect as has been discussed at the beginning of this section. According to Flory-Huggins mean field theory, the first two terms of the viral expansion of osmotic pressure represent the ideal behavior and the excluded volume effect (Flory, 1953). Unless the concentration of the mixture is really high or the energetic interactions dominate, one would expect a good agreement between the second order viral expansion and experimental data. In fact, as long as we can conceptually divide the three-component mixture into effective saline/albumin and saline/hyaluronic acid compartments, Eq. (3.17) is rigorous. In reality, however, the validity of Eq. (3.17) has to be checked experimentally.

3.3   Determining Frictional Coefficient in Binary Mixtures

The hydraulic conductivity (K) of bovine serum albumin has been determined from sedimentation experiments in physiological saline as a function of concentration (Kim et al, 1991)

$$K = 1.6 \times 10^{-14} c_b^{-1} (1 - 1.348 c_b)^{5.1} \quad (cm^2)$$
$$\text{for } c_b < 0.3 \ g/ml \tag{3.18}$$

The hydraulic conductivity K apparently does not depend on solution pH in the concentration range under consideration.

The hydraulic conductivity K of hyaluronic acid has been determined by sedimentation experiments in buffered physiological saline (Ethier, 1986).

$$K = 2.92 \times 10^{-16} c_h^{-1.47} \quad (cm^2)$$
$$\text{for } 10^{-4} g/ml < c_h < 2 \times 10^{-2} g/ml \tag{3.19}$$

The hydraulic conductivity of collagen can be obtained by fiber matrix model (Ethier, 1986) as a function of volume fraction and fiber radius of collagen. In a homogeneous concentration regime of collagen in physiological buffered saline under which our experiment will be carried out, we have (Ethier, 1986; Johnson, 1987)

$$K = 0.31 a^2 \phi_c^{-1.17} \tag{3.20}$$

Sedimentation experiments of collagen have also been carried out in saline under physiological pH and ionic strength (Obrink, 1971). Moreover, the relation between hydraulic conductivity K and sedimentation coefficient s was given as (Mijnlieff & Jaspers, 1971)

$$K = \frac{\mu_1 s}{c_2 (1 - \upsilon_2 \rho)} \tag{3.21}$$

where μ_1, υ_2, c_2 and ρ are viscosity of the solvent, specific volume and concentration of solute, and density of the mixture, respectively.

From sedimentation data and Eq. (3.21), we can calculate the hydraulic conductivity of collagen. By comparison of the hydraulic conductivity calculated from sedimentation data and from the fiber matrix model, the fiber radius of collagen is determined to be 9 Å. The calculated fiber radius is in good agreement with literature data of tropocollagen's fiber radius (Yannas, 1972; Visvanadham et al, 1978).

Thus we have expressions of hydraulic conductivity of albumin, hyaluronic acid and collagen as functions of concentration as discussed above. The relation between the frictional coefficient and the hydraulic conductivity, Eq. (2.16), can be rewritten as

$$\gamma_{12} = \frac{\mu_1 (1 - \upsilon_2 c_2)^2}{K} \tag{3.22}$$

Eq. (3.18), (3.19), (3.20) and (3.22) will give us the frictional coefficients of albumin, hyaluronic acid and collagen in the physiological buffered saline.

3.4 Determining Frictional Coefficients in Ternary Mixtures: I

There are two types of frictional interaction in the ternary mixture of saline, albumin and

hyaluronic acid. The interaction between saline and albumin, and that between saline and hyaluronic acid are interactions between fluid and solid-like solute. The interaction between albumin and hyaluronic acid is a solid-solid like interaction which has to be determined experimentally. I will first discuss interactions between solvent and solute in this section. The interaction between solutes will be dealt with in the next section.

The interaction between saline and albumin, and that between saline and hyaluronic acid can be obtained by summing up separately all frictional interactions of saline on albumin and of saline on hyaluronic acid in the three-component mixture. At the dilute limit where the interaction between albumin and hyaluronic acid approaches zero, we would expect that γ_{12} and γ_{13} approach the frictional coefficients in the two-component mixture of albumin in saline; and of hyaluronic acid in saline. As a first approximation when both the albumin and the hyaluronic acid concentrations are small, we will neglect the influence of albumin on the frictional coefficient between saline and hyaluronic acid. Likewise, we will neglect the influence of hyaluronic acid on the frictional coefficient between saline and albumin. Hence, we will use the corresponding experimentally determined formulas given in Section 3.3 for the frictional coefficients between saline and albumin, and between saline and hyaluronic acid in the three-component mixture.

3.5 Determining Frictional Coefficients in Ternary Mixtures: II

As we have mentioned in the introduction, there is no theory analyzing the interaction between albumin and hyaluronic acid in the three-component mixture of saline, albumin and hyaluronic acid. The sedimentation and diffusion experiments of albumin through

44

hyaluronic saline solution (Laurent et al, 1961; Laurent et al, 1963; Winlove and Parker, 1984), however, reveal the hindering effect of hyaluronic acid on albumin. In this section, we will first model the process of albumin sendimenting under centrifugal force through a mixture of hyaluronic acid and saline. Then we will use this model to determine the frictional coefficient between albumin and hyaluronic acid using literature data given by Laurent et al (1961, 1963).

3.5.1   Modeling Sedimentation Under Centrifuge

We use the force balance approach, once again. The centrifugal force per unit mass at location x away from the center of rotation is

$$f_{cent} = -\omega^2 x \tag{3.24}$$

where ω is the angular velocity of rotation.

Including the centrifugal force into the balance equation for the unit mass of each species, we have, from Eqs. (2.1) (2.6) and (2.11)

$$-\omega^2 x + \upsilon_i \nabla p + kT \nabla(\ln a_i) + \sum_{j \neq i} f_{ij}(\bar{v}_i - \bar{v}_j) = 0$$
$$i = 1, 2, \ldots n \tag{3.25}$$

Let's now first apply Eq. (3.25) for a solute sedimentation in a solvent, a two-component case.

3.5.2 The Relationship between the Permeability and the Sedimentation Coefficient in Binary Mixtures

Using the balance equation (3.25) on solute, we have

$$\bar{v}_2 - \bar{v}_1 = \frac{1}{f_{21}}(\omega^2 x - v_2 \nabla p - kT\nabla(\ln a_i)) \tag{3.26}$$

Recall Stokes-Einstein's formula of diffusivity (Wijmans et al, 1985), as well as the definition of osmotic pressure in two-component mixture in (2.16)

$$D = \frac{K\phi_2}{\mu_1} \frac{d\pi}{d\phi_2}$$

$$d\pi = -\frac{kT}{v_1} d(\ln a_1) = \frac{kT}{v_2} \frac{\phi_2}{\phi_1} d(\ln a_2) \tag{3.27}$$

where D is diffusivity and K is hydraulic conductivity which can be expressed by the frictional coefficient through formula (2.16).

With Eq. (3.27), we can re-write the third term in (3.26) as

$$\frac{kT}{f_{12}} \nabla(\ln a_2) = \frac{D}{\phi_1\phi_2} \frac{d\phi_2}{dx} \tag{3.28}$$

Therefore, the third term of Eq. (3.26) represents diffusion which only affects the width of the sedimenting front while the first two terms determine the velocity of the moving front. Because we are only interested in the velocity of the sedimenting front, the third

term can be neglected. Hence, we have

$$\bar{v}_2 - \bar{v}_1 = \frac{1}{f_{21}}(\omega^2 x - v_2 \nabla p) \tag{3.29}$$

Furthermore, the mixture as a whole during sedimentaion is static and we have the pressure gradient

$$\nabla p = \rho \omega^2 x \tag{3.30}$$

where ρ is the density of the *whole mixture*.

From Eq. (3.29), (3.30), (2.16), we obtain

$$K = \frac{\mu_1 s^0 (\phi_1^0)^2}{c_2^0 (1 - \rho^0 v_2)} = \frac{\mu_1 (\phi_1^0)^2}{\gamma_{12}^0} \tag{3.31}$$

or

$$s^0 = \frac{c_2^0 (1 - \rho^0 v_2)}{\gamma_{12}^0} \tag{3.32}$$

The superscript "0" stands for a two-component system and s is the sedimentation coefficient defined as

$$s = \frac{v_2}{\omega^2 x} \tag{3.33}$$

In deriving (3.31), I assumed that the velocity of the solvent is negligible compared to the

47

sedimentation velocity of the solute. This assumption is valid according to flux conservation if the concentration of the sedimenting solute is small. As expected, a derivation using the balance equation of (3.25) on the solvent gives the same result.

In summary, the force balance approach reproduced formula (3.31), which is well known in the literature relating the sedimentation coefficient and the hydraulic conductivity in a dilute two-component systems. We are now ready to apply this approach for a three-component mixture.

3.5.3 Sedimentation Coefficient in a Ternary System

Following analogous steps of the analysis of two-component systems, we can solve velocities of albumin sedimentation in the mixture of hyaluronic acid and saline

$$
\frac{v_1 - v_3}{\omega^2 x} = -\frac{\alpha}{\upsilon_1}(1 - \rho \upsilon_1)
$$

$$
\frac{v_2 - v_3}{\omega^2 x} = -\frac{\xi}{\upsilon_2}(1 - \rho \upsilon_2) \tag{3.34}
$$

where ρ is again the density of the whole mixture, and α and ξ are functions of the volume fractions and frictional coefficients we defined earlier in (2.18).

Subtraction of the first equation in (3.34) from the second gives

$$
s = \frac{\alpha}{\upsilon_1}(1 - \rho \upsilon_1) - \frac{\xi}{\upsilon_2}(1 - \rho \upsilon_2) \tag{3.35}
$$

where I neglected v_1 again given that the concentration of albumin and hyaluronic acid are both small.

3.5.4 Frictional Coefficient between Albumin and Hyaluronic Acid in the Ternary Mixture

From Eqs. (3.32), (3.35) and the definition of α and ξ, the ratio of s over s^0 can be expressed as a function of frictional coefficients γ^0_{12}, γ^0_{13}, γ_{12}, γ_{13} and γ_{23}.

$$\frac{s}{s_0} = \text{func}(\gamma^0_{12}, \gamma^0_{13}, \gamma_{12}, \gamma_{13}, \gamma_{23}) \tag{3.36}$$

The frictional coefficients γ^0_{12}, γ^0_{13}, γ_{12}, γ_{13} are already known according to previous discussions. Hence the only unknown in (3.36) is the frictional coefficient between albumin and hyaluronic acid, γ_{23}.

Furthermore, experiments (Laurent et al, 1960, 1963, Winlove and Parker, 1984) have established that

$$\frac{s}{s^0} = 1.03e^{-6.05\sqrt{c_h}}$$
$$0 < c_h < 0.014 g/ml \tag{3.37}$$

It is also found that within the albumin concentration range $0<c_b<0.01g/ml$ tested, the ratio of s to s^0 is independent of albumin concentration (Laurent et al, 1960).

The frictional coefficient γ_{23} can thus be obtained through (3.36) and (3.37).

3.6 Summary

In this chapter, I first provided a rigorous theory and experimental scheme to determine partial osmotic pressures in a three-component mixture of saline, albumin and hyaluronic acid. An alternative approach to determine the partial osmotic pressures through the "excluded volume" concept is also discussed. In case we can not find a membrane which can completely block hyaluronic acid while letting albumin pass freely, we have to use the alternative approach to determine the partial osmotic pressures.

The method of determining the frictional coefficient between saline and albumin, and that between saline and hyaluronic acid in a binary system has been provided. These data were also used to approximate γ_{12} and γ_{13} in the three-component mixture of saline, albumin and hyaluronic acid in which both albumin and hyaluronic acid concentration are small.

Finally, sedimentation processes under centrifugal force are modeled. The process of albumin sedimenting in the saline, and that of albumin sedimenting in the mixture of hyaluronic acid and saline have been analyzed by the model. The analysis enables us to use literature sedimentation data to calculate the frictional coefficient between albumin and hyaluronic acid, γ_{23}, which is the last coefficient required for closure in any three-component system without any gelation.

The discussion in this chapter provides for the first time a complete procedure to produce

a closure for the transport equations of ternary systems. The methods and schemes developed in this chapter can be easily generalized to other multi-component macromolecular systems.

This chapter and Chapter Two together constitute the theoretical framework upon which the study of transport through macromolecular networks will be carried out.

Chapter 4

Design and Fabrication of Experimental Apparatus

In this chapter I will focus on the design and fabrication of a custom designed filtration cell. This filtration cell will allow us to measure the filtration flow rate, the pressure and the osmotic pressure distribution along the filtration path. Other experimental apparatus will be discussed in later chapters.

4.1 Unsteady Osmotic Processes

To determine the driving force loss during a filtration process, we have to measure the pressure and osmotic pressure. A moving needle probe was used successfully to measure the pressure distribution (Kim et al, 1989). Based on the idea of the needle probe, one would naturally think of an "osmotic probe", a needle probe with a piece of membrane affixed on its tip. To measure osmotic pressure of a solution, one would fill the probe with solvent and connect the probe to a pressure transducer. When the probe is brought into contact with a solution, osmotic equilibrium will eventually be established across the membrane and the transducer would give the osmotic pressure reading. The initial attempt by Kim, however, failed to build such an osmotic probe (Kim, 1989). Kim tried to form a copper ferrocyanide membrane inside a tube of one centimeter diameter and to epoxy a piece of Millipore membrane onto a 16 gage needle. The osmotic probes constructed using either method gave only a small fraction of the true osmotic pressure during calibration tests (Kim, 1989). We made our osmotic probes by

gluing a piece of hollow fiber membrane (P10, Amicon, Beverly, MA) across the opening of a 22 gage needle. Tests on these osmotic probes revealed that it would take an excessively long time to reach osmotic equilibrium (osmotic pressure readings reach only 30% of the equilibrium value after 150 hours). The failure of the test prompted a study of the unsteady osmotic processes encountered during the measurement.

The unsteady osmotic process can be modeled as follows:
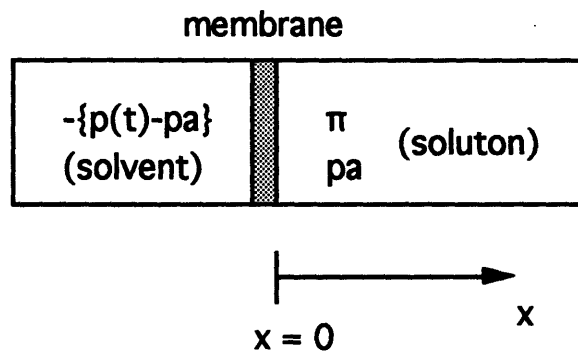
membrane

Fig. 4.1 Model of an Unsteady Osmotic process

The modified Darcy's law, as described in Section 2.2, applies across the membrane in Fig. 4.1

$$\Delta(p - \pi) = -\frac{\mu Q \Delta x}{KA}$$

Rearranging the equation, we have

$$Q = \frac{KA}{\mu \Delta x}(\pi - p) \tag{4.1}$$

The flow rate Q can be related to system compliance by definition

$$C = -\frac{dV}{dp} = \frac{Q}{dp/dt}$$

(4.2)

Combining (4.1) and (4.2) gives

$$\frac{dp}{dt} + \frac{1}{RC}p = \frac{1}{RC}\pi_{x=0^+}$$

(4.3)

where

$$R = \mu\,\Delta x / (AK)$$

The left hand side of Eq. (4.3) is identical to the voltage equation for an electrical RC circuit (Horowitz and Hill, 1989). From the well-known analysis of an RC circuit, we know that if the forcing term on the right hand side is a constant, the characteristic response time of the system is the product of the system resistance and compliance. Notice now that the forcing term on the right hand side of Equation (4.3) is time dependent. The osmotic potential at the membrane surface, $\pi(x=0+)$, is determined by the concentration of solute at that position. The concentration of solute in turn, is determined by the solvent flow across the membrane and diffusion of solute inside the solution chamber. Hence $\pi(x=0+)$ is determined by the combined effect of convection and diffusion, and we therefor expect to observe a phenomenon known as "unstirred layer effect" (Pedley, 1980, 1981). Hence, there are two time constants in the unsteady osmotic process under consideration. One is the RC time scale and the other is the diffusion time scale Δ^2/D, where Δ is the unstirred layer thickness and D is the solute

54

diffusivity in the solution. For a measurement system with very small resistance R and compliance C, we have a diffusion dominant case and the system response time is determined by Δ^2/D. On the other hand, the system response is determined by the RC time scale when the diffusion time scale is negligibly small in comparison. In general, the system response is determined by the system resistance R, system compliance C, the unstirred layer thickness Δ and the diffusion coefficient D of the solute in the mixture.

Our analysis of the unsteady osmotic processes has established that for a given solution, one has to reduce system resistance, compliance and the thickness of the unstirred layer in order to achieve a fast response.

4.2 The Osmotic Cell - An Ultrafiltration Cell with Osmotic Taps

Based on the analysis of unsteady osmotic processes, we have found that the failure of our initial tests on the osmotic probe was likely due to a large membrane resistance R, a large system compliance C and a large unstirred layer thickness Δ. Hence, a second osmotic probe was made by attaching a less resistive hollow fiber membrane (P30, Amicon, Beverly, MA) onto the tip of a 22 gage needle. All deformable connectors and tubing linking the probe to pressure transducer were replaced with more rigid connectors. The albumin/saline mixtures of known concentration, used as calibration solutions, were degassed with ultrasound bath for 20 minutes. During the calibration measurement, the solution around the probe was slowly stirred once each hour so as to minimize the effect of unstirred layer. After these painstaking steps, the osmotic probe gave true osmotic pressure readings of calibration solutions. However, because of the probe's large size

and the required cumbersome testing procedure, the osmotic probe is not feasible to measure the distribution of osmotic pressure during filtration experiments. Thus we decided to adopt the side-wall tap approach for measuring the pressure and osmotic pressure distributions. According to the criteria obtained from the unsteady osmotic processes analysis, a filtration cell with pressure and osmotic pressure taps was designed and fabricated. Made from Plexiglas, the osmotic cell is shown schematically in Fig. 4.2.
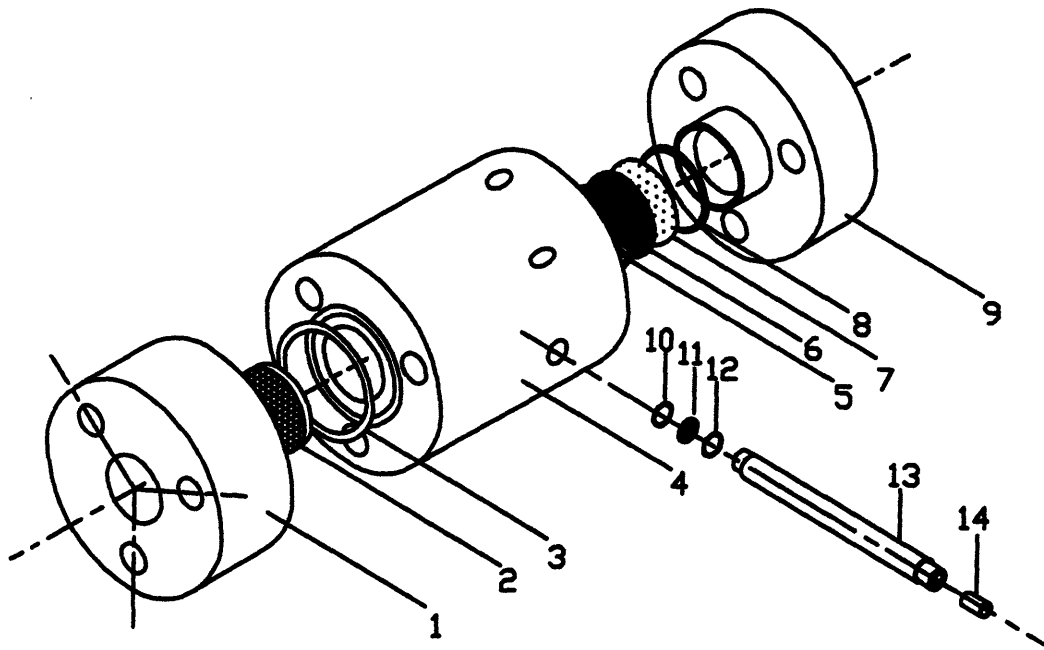
Fig. 4.2.1 The Exploded View of The Osmotic Cell

1: Top lid; 2: Porous disc; 3: O-ring; 4: Filtration chamber; 5: O-ring; 6: Main membrane; 7: Stainless steel screen disc; 8: O-ring; 9: Bottom lid; 10: O-ring; 11: Tap membrane; 12: O-ring; 13: Measurement tap; 14: Shouldering stainless tube
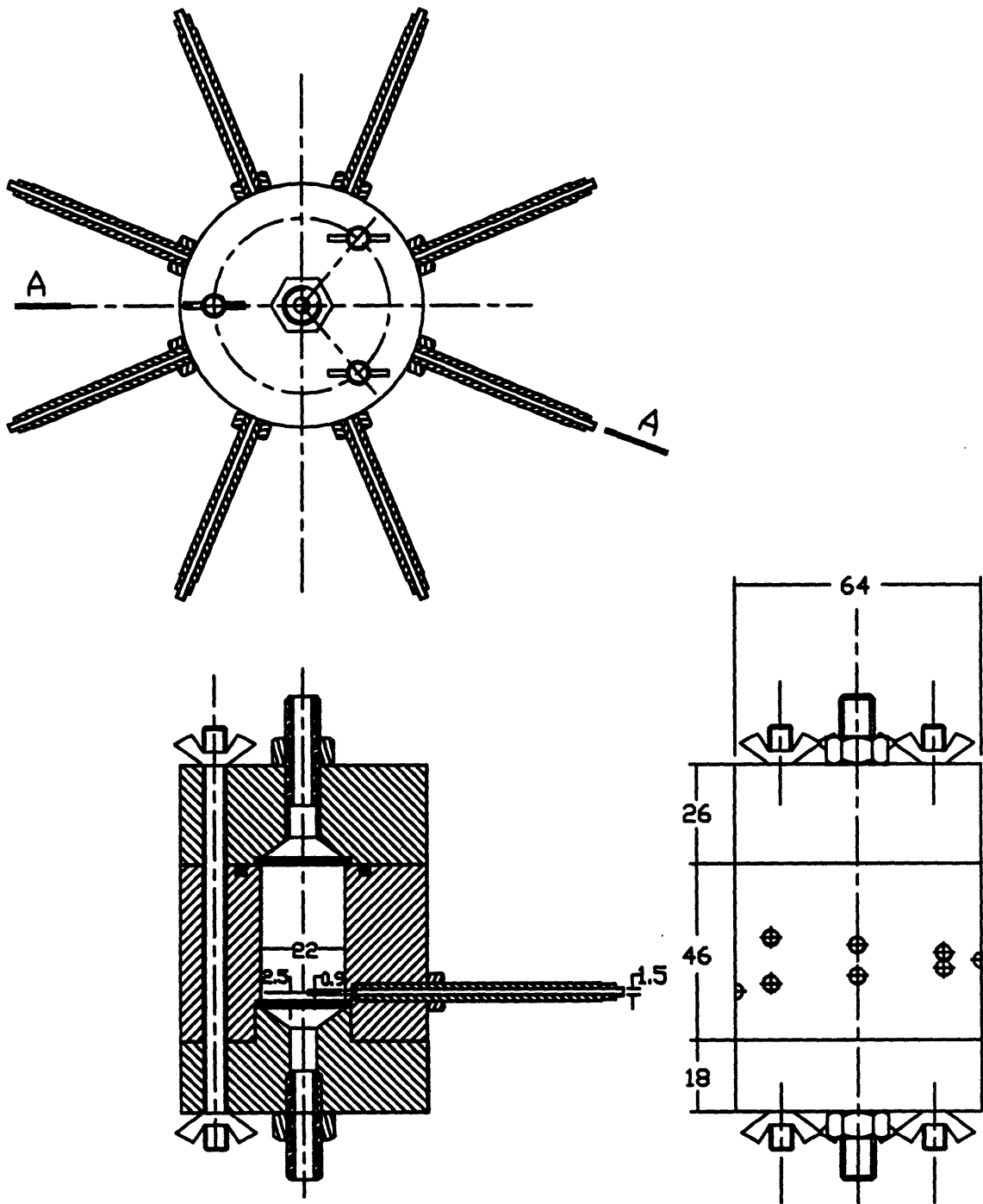
Fig. 4.2.2. Orthogonal Projections of The Osmotic Cell

(Dimensions in mm, not drawn to scale)

The diameter of the measurement holes is 0.9 mm while the outside diameter of the taps is 5.0 mm. The taps are removable so that we can choose different membranes. There are 10 measurement holes distributed in a spiral along the side wall of the filtration cell. During measurement when all of the gaskets and membranes are in place, the center of the lowest hole is 2.5 mm from the membrane surface. The distance between the tap membranes and the interior of the side wall is 2.0 mm.

4.3   Measurement With the Osmotic Cell

The entire osmotic cell assembly for the filtration experiment is shown in Fig 4.3. Four pressure transducers (Omega, PX 142-2.5 BD 5v), each in a closed aluminum shielding box with a custom made adapter, were threaded onto measurement taps whose distance from the membrane surface is 2.5 mm, 5.5 mm, 10.5 mm and 15.5 mm respectively. The transducers were powered by a constant voltage supplier (Omega, PST-4130). The osmotic pressure readings were registered by a computer data acquisition system (MINC 11-23, DEC, Mayland, MA).
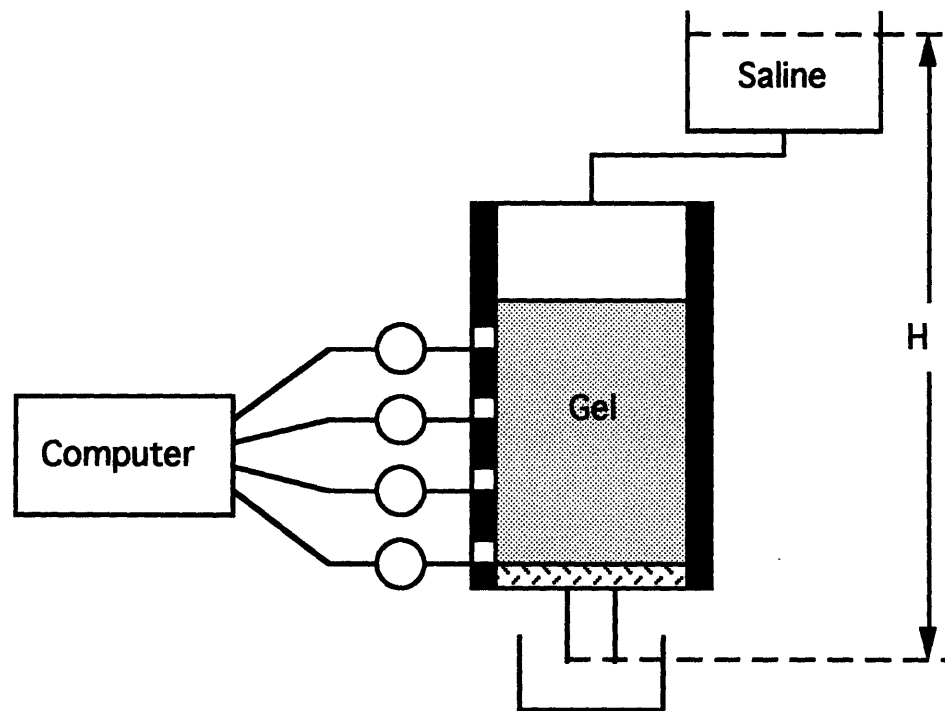
Fig. 4.3   The Osmotic Cell Assembly for Filtration Experiment

Prior to each filtration experiment, the osmotic cell assembly has to be tested. Firstly, all pressure transducers were calibrated before tap membranes were assembled to the filtration cell. In doing so, the saline column was set at different heights to produce transducer voltage outputs. The calibration process generates a pressure vs. voltage curve for each transducer. These curves were then used to convert voltage outputs to pressure readings during measurement. After assembling tap membranes onto the osmotic cell, the "hydrostatic test" was performed. This test provided a further calibration of zero, positive and negative pressure by the saline column with the tap membranes in position. Any obstruction or leakage in the measurement hole-membrane-tap-transducer linkage will be revealed through zero shift and/or readings which are either higher or lower than

the applied pressure. After the hydrostatic head test, osmotic pressure calibrations were carried out with solutions of known osmotic pressure to check the integrity of the tap membranes. A successful set-up of the osmotic cell assembly typically should have hydrostatic test and osmotic pressure calibration results as shown in Fig. 4.4 and Fig. 4.5
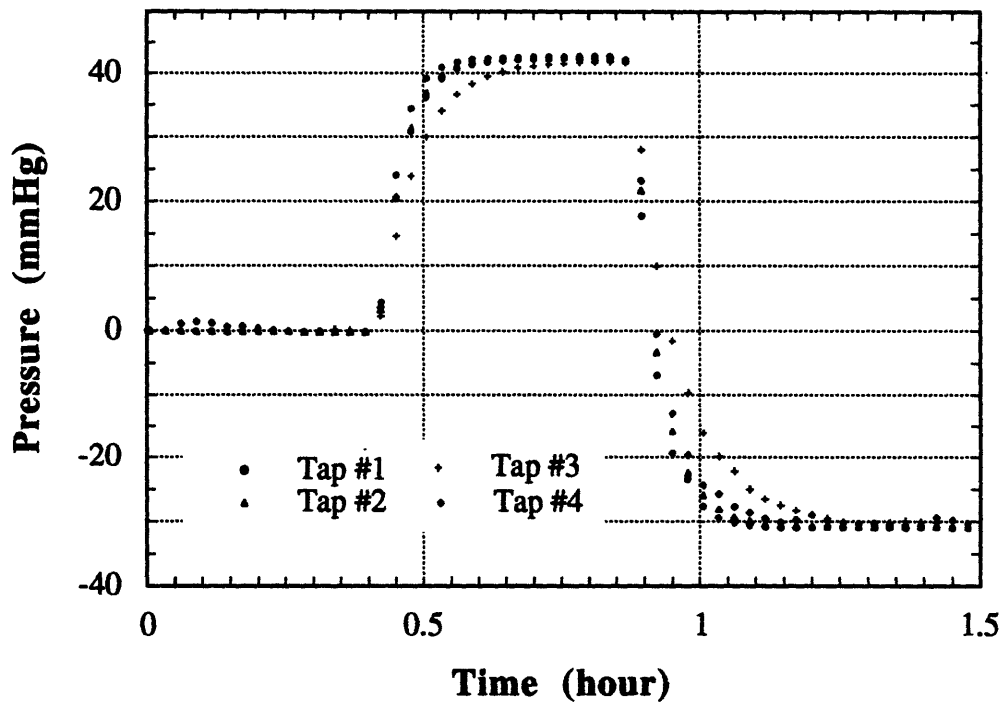
Fig. 4.4 Normal Hydrostatic Test Result of the Osmotic Cell Assembly.

Tap membranes are in position. Plotted are pressure transducers' readings when the saline column was placed at zero from time zero to approximately time 0.4 hour; at 42 mmHg from time 0.4 hour to time approximately 0.87 hour; and at -30 mmHg from approximately time 0.87 hour to time 1.5 hour.

40

35   Reference Osmotic Pressure ~ 19.0 to 20.0 mmHg
      Current Values: 18.5 mmHg to 20.5 mmHg
30   P.T. Accuracy: +/- 1.o mmHg
       Membrane: Millipore PTGC013 10
25   BSA: Boehringer Mannheim 100 030

Osmotic Pressue (mmHg)

20

15   •   x=2.5 mm

                                ○   x=5.5 mm
10
                                ι   x=10.5 mm

5   ✦   x=15.5mm

0

    0   5   10   15   20   25

                Time (Hour)
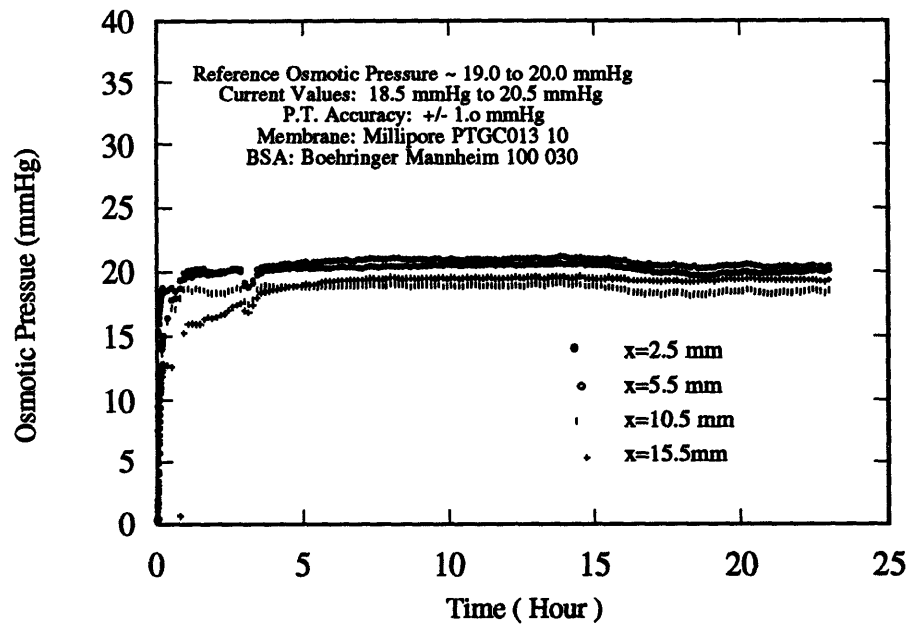
Fig. 4.5   Normal Osmotic Pressure Calibration of the Osmotic Cell Assembly.

Plotted are the osmotic pressure readings of the pressure transducers. The
calibration solution was bovine serum albumin (Boehringer Mannheim 100 030) in
physiological saline of 0.05 g/ml with reference osmotic pressure of 18 to 20
mmHg. The accuracy of the pressure transducer is +/- 1.0 mmHg.

After passing both the hydrostatic test and osmotic pressure calibration, a specified
volume of a well-mixed macromolecular solution is placed into the cell. The rest of the
osmotic cell, the reservoir and the tubing linking the two are all filled with the fluid to be
transported through the macromolecular network. The reservoir is set at a given height to
provide the hydrostatic head and the filtration experiment begins. The diameter of the
reservoir is approximately 8 times larger than that of the filtration cell to eliminate any

sensible drop in the hydrostatic height due to the outflow of the filtrate. The filtration flow rate is determined by weighing the filtrate over a certain interval of time (Kim, 1989). Without membrane in place, transducers connected to taps measure the pressure distribution. With tap membranes, application of modified Darcy's law across the tap membrane reveals that transducers measures the difference of pressure and osmotic pressure, p-π. Combining the measurement with and without tap membranes, we can obtain osmotic pressure distribution. With a membrane which can selectively block only one type of solute while letting all others to pass freely in addition, we can obtain the distribution of the corresponding partial osmotic pressure according to the discussions presented in Section 3.1.

After we obtain osmotic pressure distribution, the concentration distribution is also known because we already know the relation of osmotic pressure as a function of solute concentration. In principle we can also obtain species distributions for multi-component filtration systems given the relationship between all partial osmotic pressures and the solute concentrations. Hence, the osmotic cell can measure the filtration flow rate, the concentration distribution, and both the pressure and osmotic pressure distributions.

Chapter 5

Saline Filtration through an Albumin Layer

Albumin is a widely distributed protein, found in both plasma and tissues (Katz et al, 1970; Bill, 1960). Albumin participates in the transport through tissues by both contributing to the osmotic pressure and by possibly imposing resistance to other moving components (Kim, et al, 1991). It is of interest to learn how albumin behaves in a simple two-component transport system before we study its role in more complicated multi-component transport systems.

The bovine serum albumin molecule, globular in shape, is similar to human serum albumin in shape, molecular weight, partial specific volume, friction factors (Loeb and Scheraga, 1956). It is available commercially with well-specified molecular properties. Hence, bovine serum albumin was chosen in this study.

This chapter will begin with a discussion of filtration experiments where the albumin layer is retained by a 100 % rejection membrane to the solute. A theoretical analysis will follow and experimental data will be compared to theoretical predictions.

5.1   Initial Filtration Experiments

A filtration cell with a needle probe was built and initial filtration experiments were carried out by Kim (1989). The needle probe measured no pressure gradient during

Kim's experiment as theory predicts (Silberberg, 1980,1989), which confirmed that all pressure drop occurred at the membrane osmotically, namely $\Delta p = \pi$ across the membrane. The predicted osmotic pressure at the membrane surface by Kim, however, differ significantly from the applied filtration pressure head (Kim, 1989). Thus we first repeat Kim's experiment with the same apparatus, material and procedures and the results were given in a previous publication (Kim et al, 1991). We briefly describe our repeating experiment in this section.

The pressure distribution measurement was made with a 33-GA (0.02 cm OD) needle probe in Kim's filtration cell. During the filtration experiment, saline (Dulbecco's phosphate buffered saline, pH = 7.3, Life Science Technologies, Chagrin Falls, OH) carrying albumin (Fraction V, Boehringer Mannheim Biochemical, Indianapolis, IN) moves towards the membrane (PTGC 025 10, Millipore) which selectively rejects the albumin while letting saline pass freely. Due to the membrane rejection and the balance between back diffusion and forward convection of albumin, a concentration profile forms. The concentration profile, known as a "concentration polarization layer" (Vilker, 1976), is depicted in Fig. 5.1 with fluoresceinated bovine serum albumin (Sigma No. A-9771, St. Louis, MO).
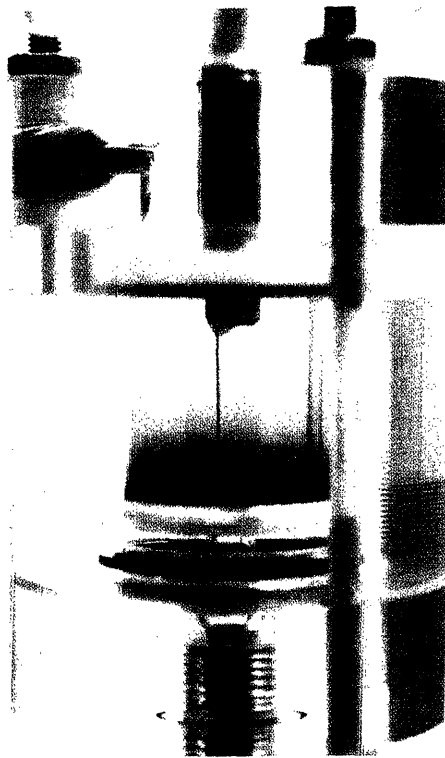
Fig. 5.1 Photograph of Fluoresceinated Albumin Concentration Polarization Layer. The needle probe is shown inside the concentration polarization layer. The total mass of albumin in filtration cell, $m = 0.4$ g. Pressure drop applied, $\Delta p = 460$ mmHg. See Kim et al, 1991 for details.

The concentration polarization layer contributes to the gross flow resistance (the membrane's resistance is less than 1% of the entire resistance). Nevertheless, the pressure measurement inside the layer given in Fig. 5.2 confirms that the pressure gradient is approximately zero everywhere other than at the membrane surface where all the pressure loss occurred osmotically.
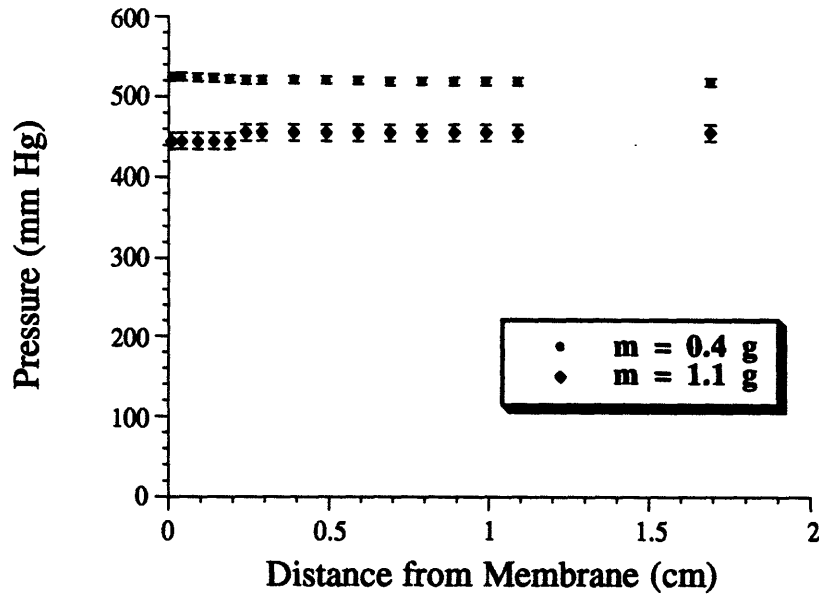
Fig. 5.2 Experimental Data of Pressure Distribution Inside the Concentration Polarization Layer. Results are measured by the needle probe. Error bars reflect uncertainty in the measured pressure. See Kim et al, 1991 for details.

5.2 Filtration in the Osmotic Cell Assembly

Further experiments were carried out using the osmotic cell assembly described in Chapter Four. All the materials used are identical to those used in the initial filtration experiment, except for the membrane (YM 10, Amicon, Beverly, MA). The saline solution of bovine serum albumin was prepared by adding buffered saline (Dulbecco's phosphate buffered saline, Life Science Technologies, Chagrin Falls, OH) with 0.05% sodium azide. All the solution and perfusion saline were degassed by ultrasonic bath for

30 minutes under low vacuum. Following the procedure described in Chapter Four, the flow rate and the distribution of p-π were obtained. We will show these results later in Section 5.5 with the comparison between theory and the experimental data.

5.3 Measurement of Osmotic Pressures

The osmotic pressure has to be determined as a function of solute concentration in order to solve the transport equation of saline through a layer of albumin. There are a variety of methods for measuring the osmotic pressure of a solution (Adams, 1985; Wagner, 1945). We used a self-made membrane osmometer shown schematically in Fig. 5.3.
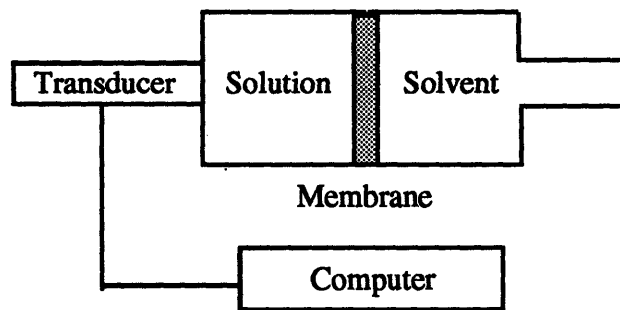
Fig. 5.3 Schematics of an membrane osmometer

The measurement chamber (solution and solvent chambers) is a stainless steel membrane holder (Millipore xx30 012 00, Millipore, MA) of 13 mm diameter. The membranes used were obtained from Millipore as well (PTGC 013, Millipore, MA). The pressure transducer was supplied by Omega (PX 143-015 BD 5v, Omega, CT). The saline solution of bovine serum albumin of different concentrations was prepared as described

in Section 5.2. The measured osmotic pressure is given in Fig. 5.4. For comparison, Vilker's osmotic pressure measurement results of bovine serum albumin/saline solution with same pH value (Vilker, 1981) and Kim's data (Kim, 1989) are also shown in Fig. 5.4.

Our experimental data are similar to Vilker's but differ significantly from Kim's at high concentration. Like Vilker, we use a "positive pressure" measurement method in which the solution is placed in contact with the pressure transducer in the measurement chamber; and the pressure developed in the measurement chamber due to osmosis is positive. Kim (1989) used "negative pressure" measurement in which the saline was placed in the measurement chamber and the solution in the other. In this approach, when the negative pressure developed inside the measurement chamber exceeds the vapor pressure of saline, it is no longer possible to measure the real osmotic pressure of the solution. The vapor pressure of saline is about the same as that of water, approximately 25 mmHg at 25 °C (Keenan et al, 1969). Kim delayed the osmotic pressure reading at which deviation would occur between the positive and negative pressure methods by raising the pressure inside the measurement chamber (Fig 2.2 of Kim, 1989).
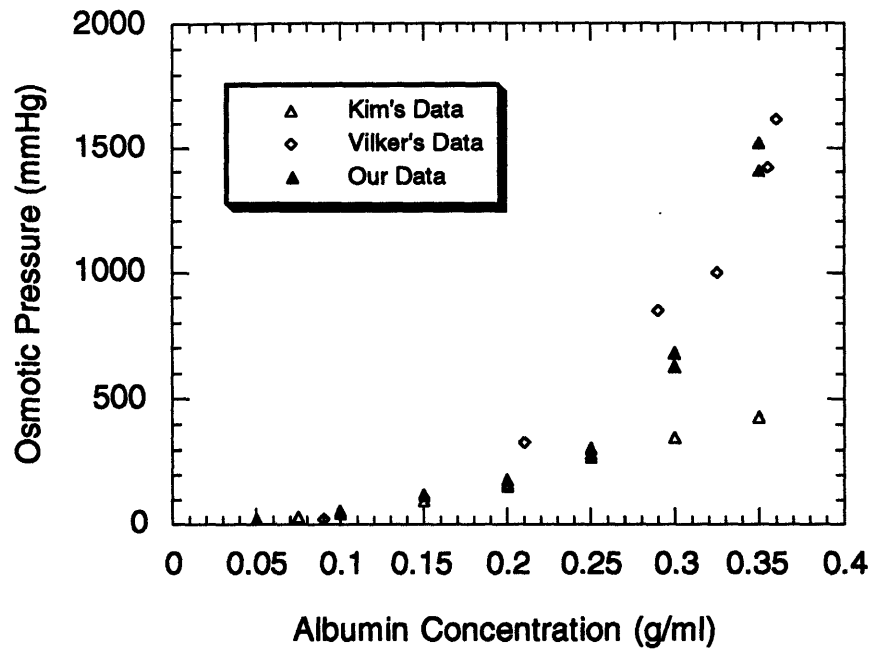
Fig. 5.4 Experimental Data of Osmotic Pressure of Bovine Serum Albumin Solutions. All measurements were obtained at pH = 7.0 approximately.

It should be emphasized that some commercial membrane osmometers, such as the Wescor Colloid Osmometer (Wescor, Inc., Logan, UT), use the negative pressure measurement method. The osmotic pressure obtained by the negative pressure method is reliable only when the osmotic pressure of the solution under the investigation is less than the vapor pressure of the solvent in the measurement chamber. In the osmotic cell discussed in Chapter Four, we used the negative pressure method. Fortunately however, the pressure inside the measurement chamber during the filtration is the difference between the pressure and the osmotic pressure, p-π, which is always greater than zero as

long as there is a filtration flux. We will discuss this further in Chapter Eight.

5.4 Theoretical Solutions

We have derived the transport equation in a two-component system in Chapter Two. Noticing that the matrix stress is zero, from Eq. (2.15) and (2.16), we have

$$\frac{d(p-\pi)}{dx} = -\frac{\mu Q}{KA}$$

$$\frac{dp}{dx} = 0$$

(5.1)

To solve Eq. (5.1), we have to provide the osmotic pressure π and permeability K as functions of albumin concentration. Osmotic pressure measurements described in the last section provide the osmotic pressure relation. Furthermore, the permeability K of bovine serum albumin in buffered saline is given semi-empirically by Kim (1989):

$$K = 1.6 \times 10^{-14} c^{-1} (1 - 1.348c)^{5.1} \quad (cm^2)$$

$$0 < c < 0.3 \quad g/ml$$

(5.2)

where c is the albumin concentration in g/ml.

K does not depend on the pH of the albumin solution for the concentration range under consideration (Kim et al, 1991).

The boundary condition of Eq. (5.1) is

$$c\big|_{x=0} = c_m \quad , \quad c\big|_{x=\infty} = 0$$

$$\pi\big|_{x=0} = \pi(c_m) = \Delta p$$

(5.3)

By the fact that π is function of concentration, Eq. (5.1) can be rewritten as

$$\frac{d\pi}{dc}\frac{dc}{dx} = \frac{\mu Q}{KA}$$

(5.4)

Multiplying Eq. (5.4) by concentration and integrating over $x = (0,\infty)$ gives

$$Q = \frac{A^2}{\mu m}\left(\Delta p K(c_m)c_m - \int_0^{c_m} \pi(c)\frac{d(cK)}{dc}dc\right)$$

(5.5)

where A, μ, m are the cross sectional area of the filtration cell, the viscosity of saline and the total mass inside the filtration cell respectively.

Integrating Eq. (5.4) from $x=0$ to x gives

$$x = \frac{A}{\mu Q}\{f(c) - f(c_m)\}$$

(5.6)

where

$$f(c) = \int_0^c K(c)\frac{d\pi}{dc}dc$$

Numerical integration of Eq. (5.5) and Eq. (5.6) will enable us to find the flow rate Q (

Δp, m) and concentration distribution c (Δp, m, x). Knowing the relation $\pi(c)$, we can then obtain the osmotic pressure distribution π (Δp, m, x) as well as Δp-$\pi(\Delta p$, m, x) since Δp is constant over all x > 0.

5.5 Comparison of Theory and Experimental Data

The flow rate Q, concentration profile c(x), osmotic pressure distribution $\pi(x)$ and Δp-$\pi(x)$ as functions of Δp and m can be calculated from theory. Only those to be compared with experimental data are presented here. In Fig. 5.5, the calculated albumin concentration profiles under applied pressures of 20 mmHg and 41.7 mmHg are given. Fig. 5.4 and 5.5 show that $\Delta p = \pi$ at the membrane surface determines the concentration at the membrane surface. Fig 5.6 compares the calculated flow rate with the experimental data. The distributions of p-π from theory are compared with experiment in Fig 5.7. Theory agrees well with the experimental data.
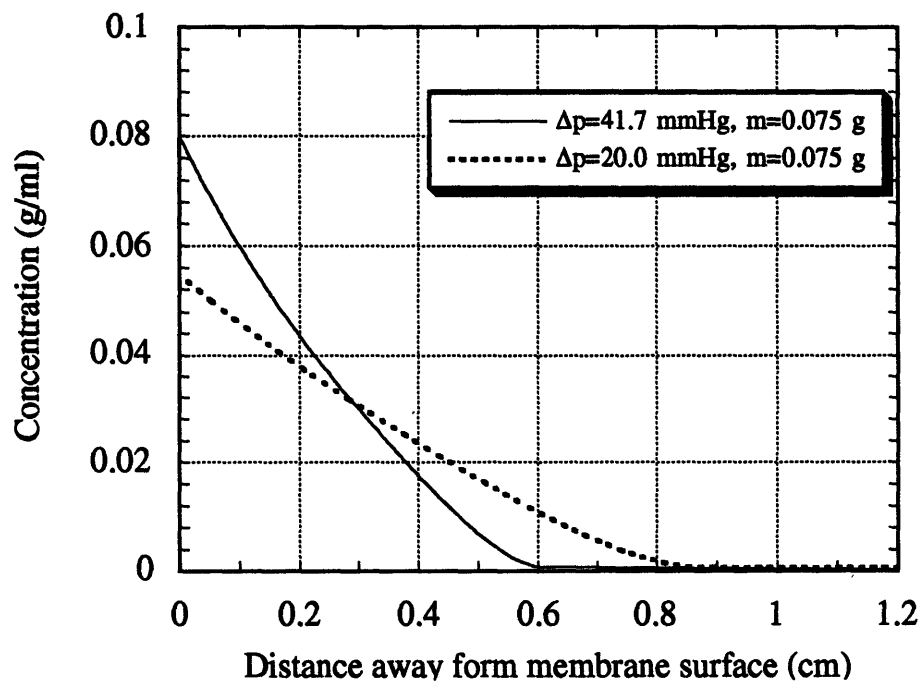
Fig 5.5 Numerical Solution of Albumin Concentration Profile

Albumin distribution along the flow path during saline filtration through a layer of bovine serum albumin. The cross-sectional area of the filtration cell is 3.88 cm^2.
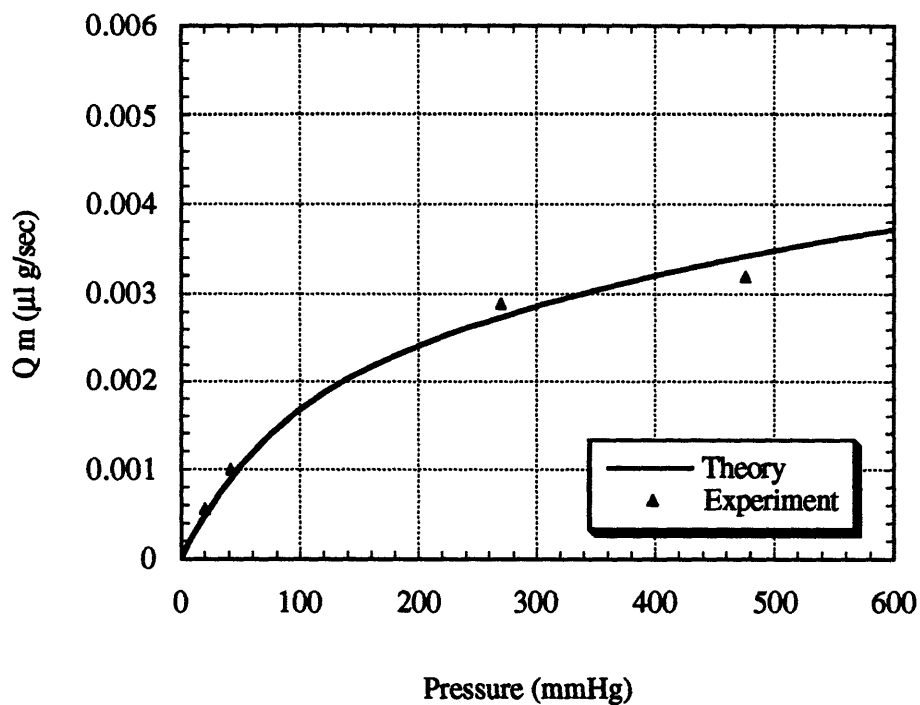
Fig. 5.6 Comparison between Theory and Data of Filtration Flow Rate
for Saline Filtration through an Albumin Layer

The product of the predicted filtration flow rate Q and the total albumin
mass inside the filtration cell as a function of applied pressure Δp.
m=0.075g for both low pressure data points. m=0.4g and 0.75g for
Δp=265 mmHg run and m=0.4g for Δp=490 mmHg test. The two low
pressure data points were obtained using the osmotic cell while the two
high pressure data points were obtained using Kim's filtration cell.
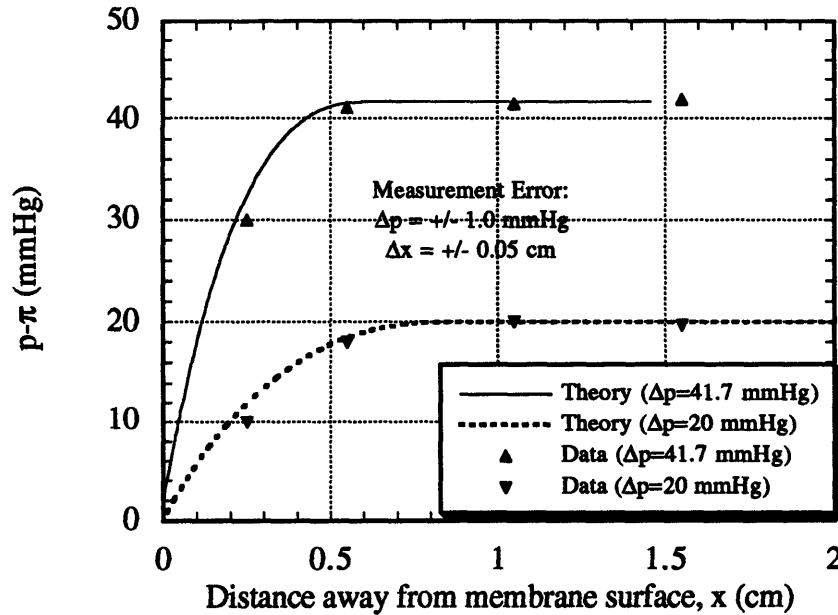
Fig. 5.7 Comparison between Theory and Data of p-π for Saline Filtration through an Albumin Layer. Total mass of albumin in filtration cell m=0.075 g. Main and tap membranes: PM 10, Amicon

5.6 Conclusions

In summary, during the filtration of saline through a layer of albumin solution, there is no macroscopic pressure drop along the flow path. The total pressure loss occurred at the membrane surface osmotically and thus established an albumin concentration at the membrane surface. An osmotic cell, a filtration cell with side osmotic taps, can be used to monitor the driving force loss and the distribution of solute. Using osmotic pressure measurement and knowledge of the permeability K(c), transport equations (5.1) determine all quantities of interest for saline filtration through albumin. Theory and

experiment are in good agreement.

This chapter also revealed the important fact that one should be careful in using the "negative pressure method" to measure the osmotic pressure of a solution. When the osmotic pressure of a solution is larger than the vapor pressure of the solvent involved, osmometers using negative pressure method are no longer able to measure the true osmotic pressure of the solution.

Chapter 6

Saline Filtration Through an Hyaluronic Acid Layer

Hyaluronic acid is a long chain linear anionic polysaccharide with a molecular weight between 100 to 10,000 thousand Dalton. The length and radius of a repeating unit of hyaluronic acid, the dimer, are approximately 0.95 nm and 0.5 nm, respectively (Ethier, 1983). A dimer has a molecular weight of approximately 400 Dalton. Thus a hyaluronic acid molecule of molecular weight 1,000 thousand Dalton has an end-to-end length of 2.4 µm, a long molecule indeed (Johnson, 1987).

Hyaluronic acid is a member of the glycosaminoglycan family (GAGs), which along with collagen, elastin and fibronectin are the main constituents of the extracellular matrix (Grodzinsky, 1983; Granger, 1981; Ogston, 1970). Soluble in water, hyaluronic acid has a much higher surface to volume ratio compared to that of globular molecules like albumin, can form extremely viscous aqueous solutions and is thought to be involved in controlling connective tissue transport characteristics (Johnson, 1987). Hence it is important to study saline filtration through a hyaluronic acid layer. This study will prepare us for examining saline filtration through a mixture of albumin and hyaluronic acid.

6.1 Filtration Experiment

Filtration experiments were carried out in the osmotic cell assembly as described in Chapter Four to measure the filtration flow rate and the distribution of the driving force, p-π. Saline solutions of hyaluronic acid were prepared by adding specified amount of buffered saline (Dulbecco's phosphate buffered saline, Life science Technologies, Chagrin Falls, OH), with 0.05% sodium azide, into a container of hyaluronic acid (H 1751, Sigma, St. Louis, MO) and leaving the sealed container in the refrigerator at 4 ^{0}C for 5 to 10 days. After hyaluronic acid was completely dissolved into the saline, the mixture was very slowly stirred mechanically (Flexa-Mix, Fisher) and degassed using a low vacuum line for about 45 minutes. The osmotic cell underwent the zero, positive, and negative pressure tests as described in Chapter Four. Then a specified volume of the well-mixed solution was added to the osmotic cell with its main and the tap membranes (PM 10, Amicon, Beverly, MA) in place, and the osmotic pressure test was carried out. After obtaining the expected osmotic pressure readings from all four tap transducers, the rest of the osmotic cell, the reservoir, and the tubing linking the two were filled with the buffered saline. Then the reservoir was raised and filtration started. The filtration pressure is provided by the hydrostatic head from the filtrate outlet to the saline surface in the reservoir. The applied pressure head was between 20 and 35 mmHg. The distance from the membrane surface to the filtrate outlet is approximately 9.2 cm in this case.

The osmotic pressure of the hyaluronic acid solutions was determined by the osmometer described in Chapter Five. It was found that the osmotic pressure of the hyaluronic acid solution varies from one lot to another, as earlier studies have observed (Wiederhielm, 1976). The average value of the osmotic pressures, however, approximately followed the relation given by Johnson (1987)

$$\pi = 5.8 \times 10^7 \times c^2 \quad (dyne / cm^2) \quad\quad (6.1)$$

78

where c is the concentration of hyaluronic acid in g/ml.

6.2 Theoretical Solutions

The transport equations, as discussed in Chapter Five, are as follows

$$\frac{d\pi}{dc}\frac{dc}{dx} = \frac{\mu Q}{KA}$$

$$\frac{dp}{dx} = 0$$

$$(6.2)$$

The boundary conditions for Eq. (6.2) are

$$c\big|_{x=0} = c_m \quad , \quad c\big|_{x=\infty} = 0$$

$$\pi\big|_{x=0} = \pi(c_m) = \Delta p$$

$$(6.3)$$

The osmotic pressure is given by Eq. (6.1). Given permeability K, Eq. (6.2) with (6.3) can be solved to obtain the solute distribution with the filtration flow rate Q as a parameter. The additional constraint of mass conservation (the fact that total solute mass in the filtration cell equals the integration of the entire concentration profile over all cross-sectional area) determines the filtration flow rate Q.

For macromolecules having a high surface to volume ratio, the permeability K usually has different dependence on concentration at different concentration regimes, known as the dilute regime, the semi-dilute regime and the homogeneous regime (Johnson et al, 1987). The power law dependence of permeability K on hyaluronic acid concentration is

-1, -1.5 and -1.17 respectively for the dilute, semi-dilute and homogeneous regimes (Johnson et al, 1987). The dilute regime spans a concentration from zero to approximately 10^{-5} g/ml, followed by the semi-dilute regime over a concentration between 10^{-5} and 10^{-3} g/ml. For hyaluronic acid concentrations higher than 10^{-3} g/ml in physiological buffered saline, we enter the homogeneous regime where the permeability can be expressed as (Johnson et al, 1987; Ethier, 1986)

$$K(c) = 1.24 \times 10^{-15} \times c^{-1.17} \quad (cm^2)$$

(6.4)

According to the boundary condition (6.3) and the osmotic pressure expression (6.1), the hyaluronic acid concentrations at the membrane surface at the applied pressure head of 20 mmHg and 35 mmHg are approximately 0.02 g/ml and 0.03 g/ml. Although hyaluronic acid concentration approaches zero as the distance from the membrane becomes large, we expect the hyaluronic acid mass in the region near the membrane surface to have a dominant effect on the transport process. Hence, we use the homogeneous regime relation of permeability, Eq. (6.4), over the entire solution domain of the filtration problem under consideration.

Integration of Eq. (6.2), as shown in Chapter 5, gives

$$Q = \frac{A^2}{\mu m} \left(\Delta p K(c_m) c_m - \int_0^{c_m} \pi(c) \frac{d(cK)}{dc} dc \right)$$

(6.5)

$$f(c) - f(c_m) = \frac{\mu Q x}{A}$$

(6.6)

where

$$f(c) = \int_0^c K(c) \frac{d\pi}{dc} dc$$

and m is the total hyaluronic acid mass inside the filtration cell.

With $\pi(c)$ and $K(c)$ given in Eq. (6.1) and (6.4), we have, from Eq. (6.5) and (6.6):

$$Q = 1.128 \times 10^{-4} \frac{c_m^{1.83}}{m} \quad (ml/sec)$$

$$c = \left(c_m^{0.83} - \frac{10^5 Qx}{6.545} \right)^{1.205} \quad (g/ml)$$

(6.7)

with distance x and mass m units in cm and gram, respectively.

Furthermore, from Eq. (6.1) and the boundary condition that osmotic pressure at the membrane surface balances the pressure drop across the membrane, we have

$$c_m = \sqrt{\frac{\Delta p}{43244}} \quad (g/ml)$$

(6.8)

In deriving Eq. (6.8), we have made use of the fact that there is no pressure drop in the concentration polarization layer along the filtration path for all $x > 0$.

Substituting Eq. (6.8) into Eq. (6.7), we have

$$Q = 6.463 \times 10^{-9} \frac{(\Delta p)^{0.915}}{m} \quad (ml / sec)$$

$$\tag{6.9}$$

$$c = \left(1.185 \times 10^{-2} \times (\Delta p)^{0.415} - 9.876 \times 10^{-5} \frac{(\Delta p)^{0.915} x}{m} \right)^{1.025} \quad (g / ml)$$

where m is in gram, Δp in mmHg and x in cm.

We can see that Q changes in inverse proportion to total mass in the filtration cell and approximately linearly with applied pressure head, Δp.

6.3   Results and Comparisons

The osmotic pressure of hyaluronic acid solution, given by Eq. (6.1), and that of bovine serum albumin solutions, given by the best fit of the experimental data shown in Fig. 5.4, is compared in Fig. 6.1. The permeability of the hyaluronic acid, Eq. (6.4), is also compared with that of the bovine serum albumin, Eq. (5.2), in Fig. 6.2. The differences are remarkable both in osmotic pressure and in permeability due to the large surface to volume ratio of the hyaluronic acid compared to that of the albumin.
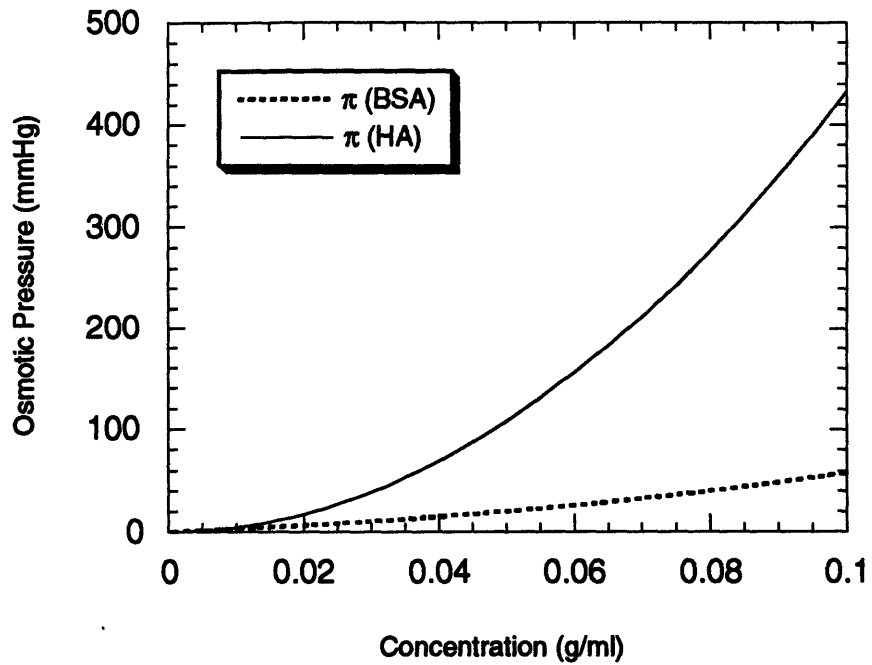
Fig. 6.1 Comparison of osmotic pressure of bovine serum albumin and hyaluronic acid in biological buffered saline. Osmotic pressure of hyaluronic acid was calculated from Eq. (6.2) while osmotic pressure of bovine serum albumin was obtained from the best fit of our experimental data given in Fig. 5.4.
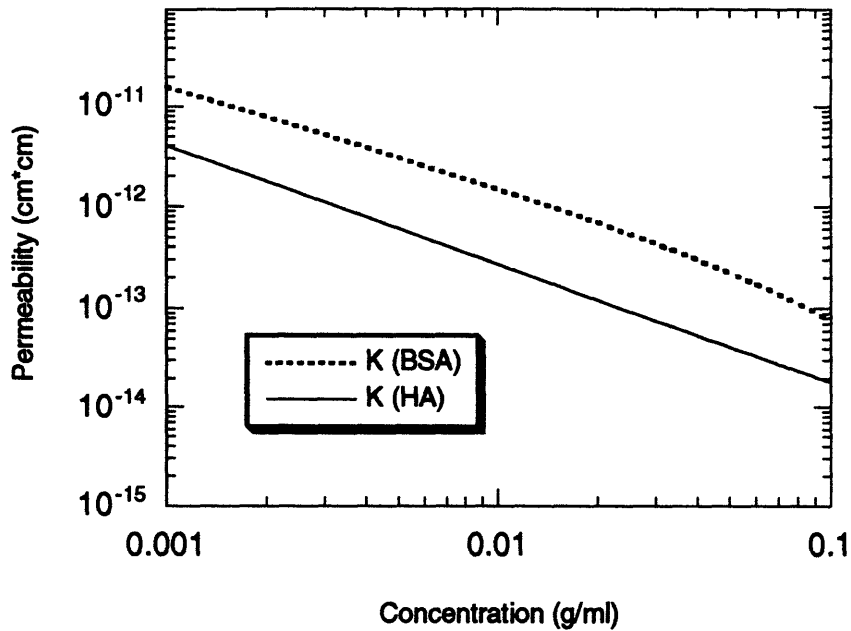
Fig. 6.2 Comparison of permeability of bovine serum albumin and hyaluronic acid in biological buffered saline. The permeability of hyaluronic acid was calculated from Eq. (6.4) while that of bovine serum albumin was calculated from Eq. (5.2)

The predicted flow rate of saline filtration through an albumin layer and that of saline filtration through a hyaluronic acid layer is compared in Fig. 6.3. When filtration pressure is low, where most physiological transport occurs, the filtration flow rate of saline through an albumin layer is much higher than that of saline through a hyaluronic acid layer. The concentration distribution of saline through an albumin layer and that of saline through a hyaluronic acid layer is compared in Fig. 6.4. As expected, hyaluronic acid molecules are much more dispersed in the filtration cell than albumin molecules under the same experimental conditions.
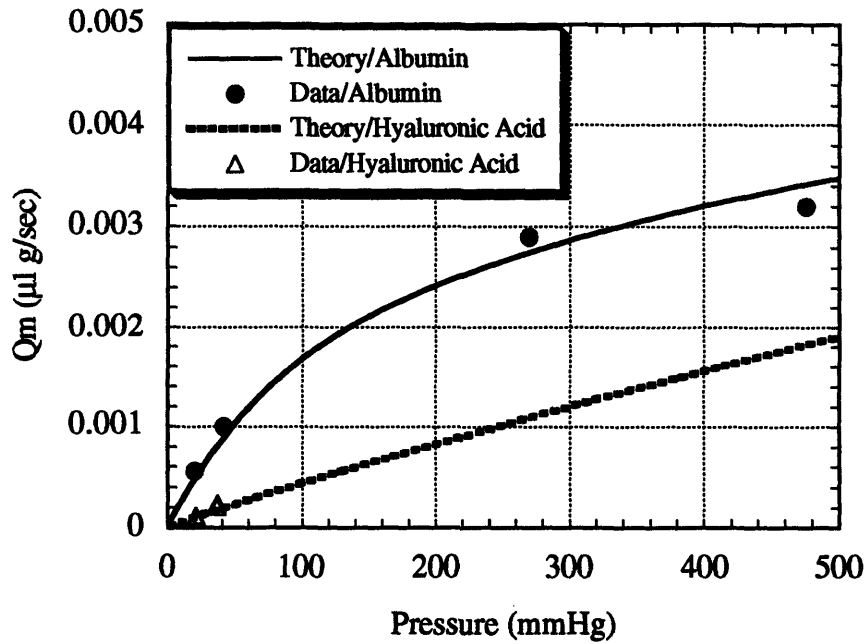
Fig. 6.3 Comparison between Qm under various filtration pressure heads of saline filtration through bovine serum albumin, Eq. (5.5), and that of saline filtration through hyaluronic acid, Eq. (6.7). The cross-sectional area of the filtration cell is 3.88 cm^2 in both cases. The albumin data shown in Fig. 5.6 and the hyaluronic acid data which will be compared with theory again in Fig. 6.7 are plotted in this figure as well.
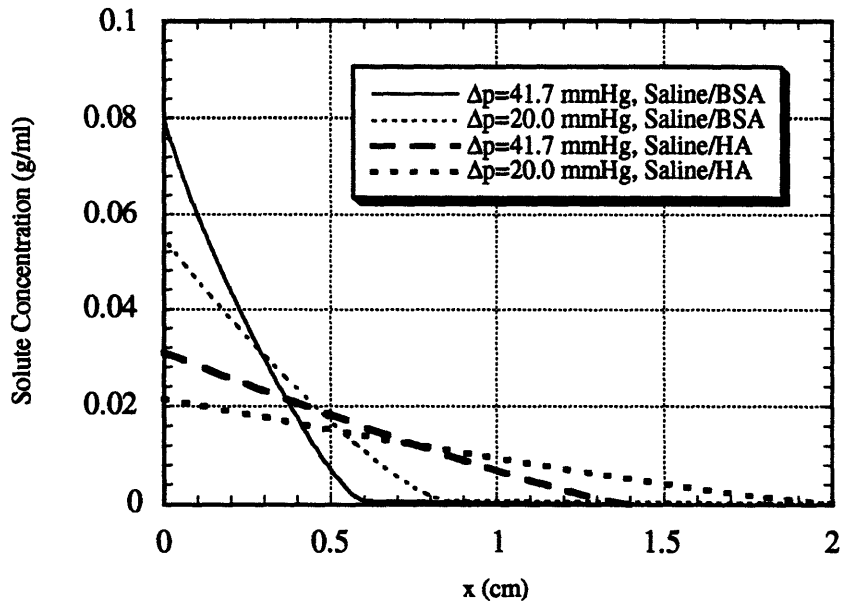
Fig. 6.4 Comparison of solute distribution during saline filtration through a bovine serum albumin layer, Eq. (5.6), and saline filtration through a hyaluronic acid layer, Eq. (6.7). Total solute mass in the filtration cell for both cases is 0.075 g. The cross-sectional area of the filtration cell is 3.88 cm^2.

The experimental results of filtrate volume as function of filtration time under different pressure heads are given in Fig. 6.5. The equilibrium flow rate Q was calculated as the slope of corresponding curve approaches a constant. Typical measurements of the osmotic taps are given in Fig. 6.6, the equilibrium values of which will be compared with the theory.

The comparison of the experimental and the calculated flow rate was given in Fig. 6.7. The agreement is good in general. The largest deviation between the theory and the data is approximately 20 % under the pressure head of 36.6 mmHg. Because the filtration

experiments of $\Delta p = 36.6$ mmHg in both tests are made after the completion of $\Delta p = 21.6$ mmHg measurement, which in both cases takes about 15 days, degradation of hyaluronic acid or a small amount of hyaluronic acid passage through the membrane might contribute to the deviation observed in Fig. 6.7.
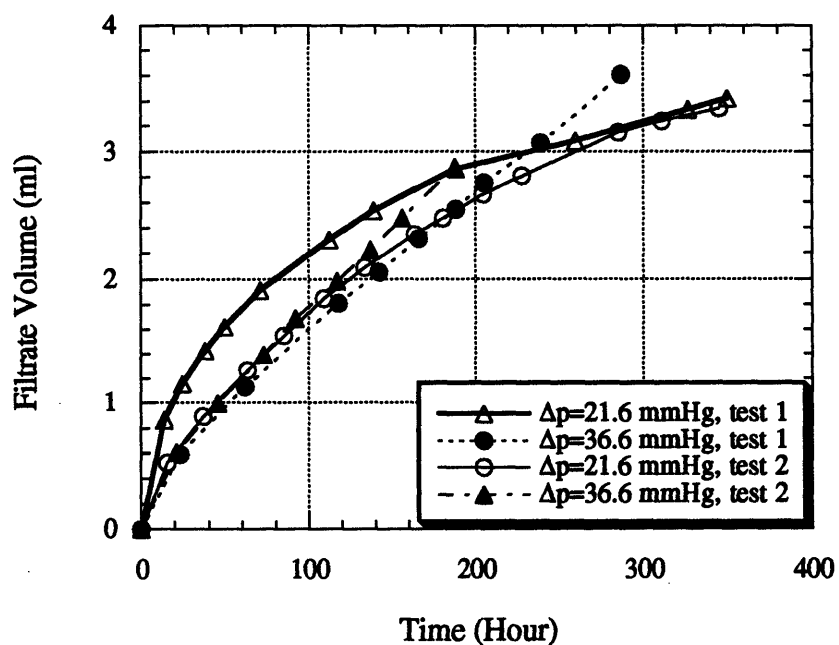
Fig. 6.5   Filtration under different pressure heads. Total amount of hyaluronic acid in the filtration cell, m = 0.076 g. Main and tap membranes: PM 10, Amicon. Measurement error: $\Delta p = +/-1.0$ mmHg, $\Delta V = 0.005$ ml.
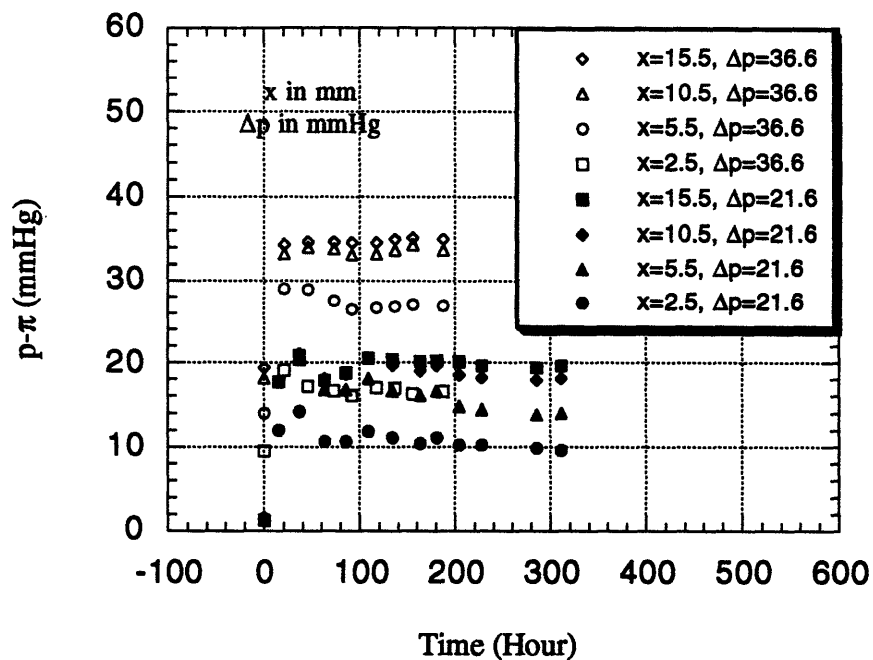
Fig. 6.6 Typical measurements of osmotic taps during saline filtration through a layer of hyaluronic acid. Total hyaluronic acid mass in filtration cell, m = 0.076 g. Main and tap membranes: PM 10, Amicon. Experiments were carried in the osmotic cell assembly as described in Chapter 4. Measurement errors: $\Delta x = +/-0.05$ cm; $\Delta p = +/-1.0$ mmHg.
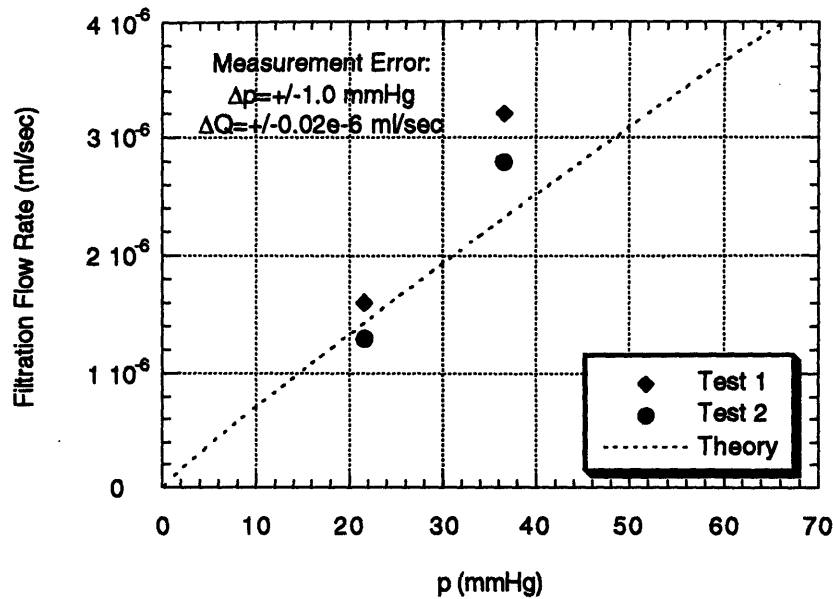
Fig. 6.7   Comparison between the theory and the experimental data of filtration flow rate. Total hyaluronic acid in the filtration cell, m = 0.076 g. Main and tap membranes: PM 10, Amicon.

Finally, the predicted distributions of the driving force of the filtration, p-π, are compared in Fig. 6.8 with the measurements of the osmotic taps. Theory agrees well with the experimental measurement under the two experimental pressure heads in both tests.
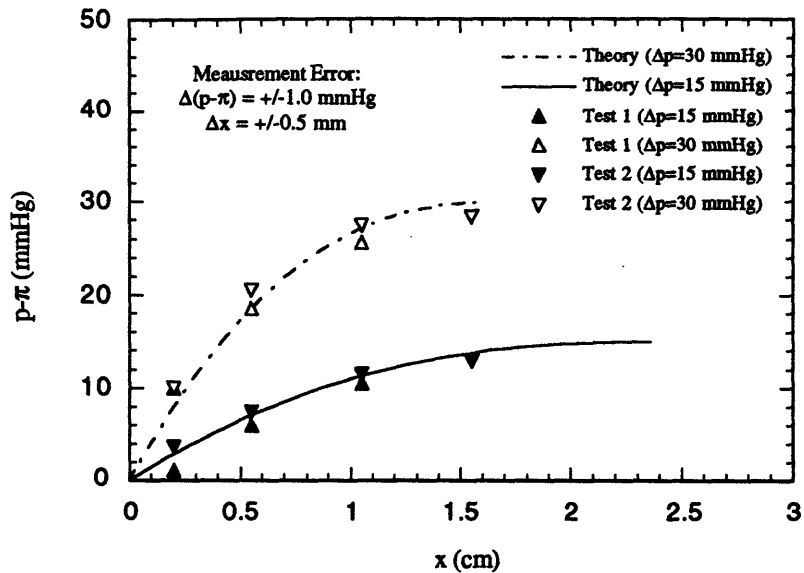
Fig. 6.8   Comparison between the theory and the experimental data. x = distance away from the membrane surface. p–π is the difference between the pressure and the osmotic pressure in the filtration cell. Total mass of hyaluronic acid in the filtration cell, m = 0.076 g. The main and the tap membranes: PM 10, Amicon. Measurement error: Δx=+/-0.05 cm; Δp=+/-1.0 mmHg. p–π and p reference is at the membrane surface. The distance from the membrane surface to the filtration outlet is approximately 9.2 cm.

6.4   Summary

In conclusion, theoretical and experimental studies of saline filtration through a layer of hyaluronic acid were presented in this chapter. The filtration experiments were performed in the osmotic cell assembly as described in the Chapter Four. The filtration flow rate and the distribution of the driving force of the filtration, p–π, have been measured.

The osmotic pressure and the permeability as functions of hyaluronic acid concentration given in the literature were used to provide a closure for the transport equations. The transport equations were then solved to obtain the filtration flow rate, the solute distribution, and the driving force, p-π, distribution. It is found that the flow rate is inversely proportional to the total mass of hyaluronic acid in the filtration system and is approximately proportional to the applied filtration pressure head. Theoretical predictions about the flow rate and the distribution of p-π, and hence the solute concentration profile, agree well with the experimental data.

It is found that due to much higher surface to volume ratio of the hyaluronic acid molecules than that of the albumin, the osmotic pressure of the hyaluronic acid is much higher while the permeability is much smaller than that of the albumin. This in turn makes it much more difficult for saline to filtrate through a hyaluronic acid layer than to filtrate through an albumin layer. The distribution of the hyaluronic acid molecules is also much more dispersed than that of the albumin molecules during the filtration experiment.

Chapter 7

Transport in Ternary Mixtures of Saline, Albumin and Hyaluronic Acid

We discussed in Chapter Five the filtration of saline through a layer of bovine serum albumin, a globular macromolecule. In Chapter Six, the filtration of saline through a layer of hyaluronic acid, a long chain macromolecule, was presented. The comparison between saline filtration through albumin and through hyaluronic acid has shown remarkable differences in terms of the flow resistance and the solute distribution. In natural transport processes in living tissues, we commonly encounter multi-component filtration systems where bodily fluid carrying nutrients permeates through an extracellular matrix. Hyaluronic acid is one of the main constituents of the extracellular matrix and albumin one of the main nutrient proteins. Hence it is interesting to see how these two types of macromolecules interact with each other in a three-component filtration system. Although albumin and hyaluronic acid are chosen with biological applications in mind, the method developed here is applicable to general three-component solution systems, provided that gelation does not occur so that there are no elastic stresses in the macromolecular networks.

In this chapter, we will first study the filtration of saline through a layer of albumin and hyaluronic acid mixtures. Then the filtration of three-component mixtures of saline, albumin and hyaluronic acid through a membrane which partially rejects hyaluronic acid will be discussed. In both cases, experimental data and theoretical predictions will be obtained and compared.

7.1 Experimental Studies

We will first discuss the filtration experiment and then the measurement of partial osmotic pressure for three-component mixtures.

7.1.1 Filtration Experiment

The mixture of albumin and hyaluronic acid was made by first dissolving the hyaluronic acid (H 1751, Sigma Chemicals, St. Louis, MO) into buffered saline (Dulbecco's phosphate buffered saline, Life Science Technologies, Chagrin Falls, OH) with 0.05% sodium azide according to the procedure described in Chapter Six. A given amount of bovine serum albumin (Fraction V, Boehringer Mannheim Biochemical, Indianapolis, IN) was then added to the hyaluronic acid solution. The three-component mixture was mixed with a magnetic stirrer very slowly inside a sealed container in a 4 ^{0}C environment for approximately an hour. The prepared mixture was then refrigerated at 4 ^{0}C in a sealed container for later use. The storage time of the prepared mixture was always a week or less.

The main membrane (pm 10, Amicon for total rejection or plhk 100, Millipore for partial rejection, see each figure for information) and tap membranes (ym 30 of Amicon. We started with pm 10 and later found that ym 30 encounters less protein binding, which is one of the main concerns for tap measurement) were placed into a beaker half filled with buffered saline, and then the beaker was placed under high vacuum from a vacuum pump (Disto-pump, model 1399, Fisher Scientific) for half an hour. The air trapped inside the membrane would thus be mostly replaced by the saline. There afterwards, the membrane would thus be mostly replaced by the saline. There afterwards, the

membranes are placed in the osmotic cell. In the meantime, the prepared mixture of saline, albumin and hyaluronic acid is degassed with a low vacuum line. After the osmotic cell assembly has gone through the hydrostatic head test, a specified volume of the three-component mixture is placed into the osmotic cell and the osmotic pressure test starts. Often this process has to be repeated several times so that both the hydrostatic test and the osmotic pressure test give the expected readings. After these initial tests, the osmotic cell, the reservoir, and the tubing linking the two are filled with the perfusion fluid. The perfusion fluid in the case of saline filtration through a layer of albumin and hyaluronic acid is saline, while in the case of filtration through a partially rejecting membrane, the perfusion fluid is the three-component mixture itself. The reservoir is then raised to a given level to provide the filtration pressure head and the experiment begin. The filtrate volume and the tap transducers' readings are obtained as functions of time until equilibrium is reached. The reservoir's level is then changed so that the flow rate and the driving force distribution under a new pressure head can be measured.

7.1.2 Partial Osmotic Pressure Measurement Trial

Partial osmotic pressures have to be provided in order to solve the transport equations for three-component filtration systems. A scheme was developed in Chapter Two to measure the partial osmotic pressure in the three-component mixture of saline, albumin and hyaluronic acid. The key issue now is to find a membrane which rejects hyaluronic acid completely while letting albumin pass freely. Much to our surprise, the test of osmotic pressure of more than ten membranes from four different manufacturers revealed that it is impossible to find such a membrane. The experimental results are summarized in Table 7.1.

94

Membrane	π (HA) mmHg (Exp. Time (h))				π (BSA) mmHg (Exp. T (h))		
0.01 μm	-6.2 (3)				-6.0 (3)		
0.015 μm	-4.9 (24)						
0.03 μm	-4.9 (3)	-5.7(24)			-0.6 (8)	-0.7 (24)	
0.05 μm	-3.1 (24)	-3.8(24)			0.0 (24)	-0.1 (24)	
pm 10k	-11. (24)	-9.2(24)	-9.8 (24)		-16. (24)	-21. (24)	
pltk 30k	-5.4 (3)	-11.(24)	-15. (24)	-7.8 (42)	-9.8 (8)	-18. (24)	-12. (17)
xm 50k	-10. (42)	-11.(24)			-15. (17)	-16. (24)	
plhk 100k	-6.0 (24)	-5.1(24)	-4.1 (42)		-2.1 (24)	-2.5 (24)	-0.4 (17)
ym 100k	-4.4 (24)						
plmk 300k	-4.6 (3)	-1.8(24)			-0.6 (8)	0.0 (24)	
xm 300k	-5.7 (3)						

Table 7.1   Osmotic pressure of two-component mixtures of albumin in saline and hyaluronic acid in saline measured by different membranes. Albumin and hyaluronic acid concentration in the solution used were 0.05 g/ml and 0.01g/ml, respectively. The corresponding reference osmotic pressure for the albumin and the hyaluronic acid solution tested are 19 mmHg and 10 mmHg respectively (Kim et al, 1991, Wiederhielm et al, 1976). Membrane #1 and #2 are from Poretics (Poretics Co., CA), while #3 and #4 are from Nuclepore (Nuclepore Lab., MA). The pm, xm and ym series membranes are from Amicon. The pltk, plhk and plmk membranes are from Millipore. The osmometer used is shown in Fig. 5.3.

The molecular weight of hyaluronic acid is several orders of magnitude larger than that of bovine serum albumin. However, the experiment reveals that hyaluronic acid, which is a linear chain molecule, is much more difficult to block. It is impossible to find a membrane, from those commercially available, which completely rejects hyaluronic acid while letting albumin pass freely. Thus we are forced to use the alternative scheme

discussed in Chapter Two to determine the partial osmotic pressures.

For the study of mixture filtration through a partial rejecting membrane, we choose the plhk 100 membrane from Millipore to provide certain blockage to hyaluronic acid while letting albumin to pass nearly freely. Although the 0.03 μm membrane from Nuclepore has similar rejection characteristics to albumin and hyaluronic acid, it is a polycarbonate screen membrane which is difficult to handle.

In order to obtain a numerical solution to the transport equations for mixture filtration through a membrane of partial blockage to solutes, we need the solute retention property of the membrane. A membrane's solute retention property can be obtained from osmotic pressure measurement. Suppose the concentration difference across the membrane in an osmometer is initially ΔC_0 and is ΔC_e at the osmotic equilibrium, $(\Delta C_e / \Delta C_0)$ is a measure of the solute retention ability of the membrane. For a dilute solution, the osmotic pressure across a membrane is linearly related, through the Van't Hoff equation (Tanford, 1963), to the concentration difference across the membrane. Hence for a dilute solution, we have

$$R = \frac{\Delta C_e}{\Delta C_0} \approx \frac{C_e}{C_0} \approx \frac{\pi_e}{\pi}$$

where C_e and π_e are the equilibrium concentration and corresponding osmotic pressure while C_0 and π are that of the testing solution. R is defined here as the membrane solute retention coefficient. The solute concentration in the solvent chamber is assumed zero all the time during the measurement. Thus, from the osmotic pressure measurement results given in Table 7.1, we find that for the plhk 100 membrane,

$$R_2 \approx \frac{1.7}{19} \approx 0.1 \ , \quad R_3 \approx \frac{5.0}{10} \approx 0.5 \tag{7.1}$$

where R_2 and R_3 are membrane retention coefficients of plhk 100 for albumin and hyaluronic acid, respectively.

During mixture filtration through a membrane that partially rejects solutes, the initial concentration difference across the membrane is C_∞ because the fluid downstream of the membrane is pure solvent. When steady-state is established, the concentration difference across the membrane is $(C_{x=0} - C_\infty)$. Assume the filtration flux does not affect the retention property of the membrane, we have, by the definition of R we gave earlier

$$R = \frac{C_{x=0} - C_\infty}{C_\infty}$$

This equation will be used to determine the solute concentration at the membrane surface.

Further osmotic pressure measurements were made with the mixture of saline, albumin and hyaluronic acid and the results are summarized in Table 7.2

Solution	1%HA+1%BSA	1%HA+1%BSA	.5%HA+1%BSA
π (mmHg)	-5.0	-5.2	-5.8

Table 7.2   Osmotic pressure of saline / albumin / hyaluronic acid measured by plhk 100 membrane. The reference osmotic pressure for 1% HA+1% BSA solution is approximately 15 mmHg, while that for 0.5% HA+1% BSA solution is approximately 12 mmHg (Wiederhielm et al, 1976). The osmotic pressure for two-component 1% and 0.5% HA+saline solution are approximately 10 and 5 mmHg, respectively (Wiederhielm et al, 1976) and that for two-component 0.5% albumin+saline solution is approximately 2 mmHg (Landis and Pappenheimer, 1963).

The comparison of the data from 1% HA+1% BSA solution measurement in Table 7.2 and that of the plhk 100 membrane in Table 7.1 revealed that the presence of albumin in the three-component mixture would not affect the plhk 100 membrane's retention of hyaluronic acid. The concentration of hyaluronic acid appears not to affect the outcome of the measurements either, which seems unrealistic and requires further examination. For the purpose of determining solute concentrations at the membrane surface during three-component mixture filtration through a plhk 100 membrane, Eq.(7.1) will be used as a reasonable approximation.

7.2   Theoretical Studies

7.2.1 Transport Equations and Constitutive Relations for Closure

The transport equations for a three-component filtration system have been derived in Chapter Two. Since there are no matrix stresses in the solution considered here, Eq. (2.18) yields:

$$v_1 - v_3 = \alpha \frac{dp}{dx} + \beta \frac{d\pi_2}{dx} + \vartheta \frac{d\pi_3}{dx}$$

$$v_2 - v_3 = \xi \frac{dp}{dx} + \eta \frac{d\pi_2}{dx} + \zeta \frac{d\pi_3}{dx} \tag{7.2}$$

$$\frac{dp}{dx} = 0$$

where

$$\alpha = -\frac{\phi_1 \gamma_{12} + \phi_1 \gamma_{23} + \phi_2 \gamma_{12}}{\delta}$$

$$\beta = \frac{\phi_1 \gamma_{23}}{\delta}$$

$$\vartheta = \frac{\phi_1 \gamma_{12} + \phi_1 \gamma_{23}}{\delta}$$

$$\xi = -\frac{\phi_2 \gamma_{12} + \phi_2 \gamma_{13} + \phi_1 \gamma_{12}}{\delta}$$

$$\eta = -\frac{\phi_1 \gamma_{23}}{\delta}$$

$$\zeta = \frac{\phi_1 \gamma_{12}}{\delta}$$

$$\delta = \gamma_{12} \gamma_{23} + \gamma_{12} \gamma_{13} + \gamma_{13} \gamma_{23}$$

Again, subscript 1, 2, 3 stands for saline, albumin and hyaluronic acid respectively. γ_{ij} is the frictional coefficient between component i and j in a unit volume of the mixture, ϕ_i is the volume fraction, and π_i is the "partial osmotic pressure" of component i defined as follows

$$\frac{d\pi_2}{dx} = \frac{\phi_2}{\phi_1} \frac{RT}{\upsilon_2} \frac{d}{dx}(\ln a_2)$$

$$\frac{d\pi_3}{dx} = \frac{\phi_3}{\phi_1} \frac{RT}{\upsilon_3} \frac{d}{dx}(\ln a_3)$$

(7.3)

The frictional coefficients between saline and the solutes can be determined, as described in Chapter Three, from the literature (Ethier, 1986; Johnson, 1987; Kim et al, 1991)

$$\gamma_{12} = 6.25 \times 10^{11} c_b (1 - 0.734 c_b)^2 (1 - 1.348 c_b)^{-5.1}$$

$$c_b \leq 0.3 \quad g/ml$$

$$\gamma_{13} = 3.425 \times 10^{13} c_h^{1.47} (1 - 0.541 c_h)^2$$

$$c_h \leq 0.008 \quad g/ml$$

and (7.4)

$$\gamma_{13} = 8.065 \times 10^{12} c_h^{1.17} (1 - 0.541 c_h)^2$$

$$0.008 \quad g/ml \leq c_h \leq 0.02 \quad g/ml$$

The frictional coefficient between albumin and hyaluronic acid can be determined from the sedimentation data (Laurent et al, 1960, 1963) and the analysis of the sedimentation process presented in Chapter Two:

$$\gamma_{23} = \frac{\gamma_{12}(\phi_1 + \phi_2)(\rho_2 - \rho_1) + \gamma_{13}\phi_2(\rho_2 - \rho) - \gamma_{12}\gamma_{13}s_0 Ae^{-B\sqrt{c_h}}}{\phi_1(\rho_1 - \rho) + (\gamma_{12} + \gamma_{13})s_0 Ae^{-B\sqrt{c_h}}} \quad (7.5)$$

where ϕ_i, ρ_i are the volume fraction and the density of species i respectively. ρ is the density of the whole mixture. A=1.03 and B=6.05 are experimental constants determined by Laurent, et al (1960, 1963). c_h is the hyaluronic acid concentration in g/ml. s_0 is the sedimentation coefficient of bovine serum albumin in saline given by Eq. (3.32)

$$s_0 = \frac{c_2^0(1 - \rho^0 \upsilon_2)}{\gamma_{12}^0} \quad (7.6)$$

where superscript "0" stands for quantities in a binary mixture of albumin sedimenting in saline.

100

Thus all three frictional coefficients are available through Eq. (7.4), (7.5) and (7.6).

The partial osmotic pressures of a ternary mixture can be determined by the "excluded volume" concept described in Section 3.2 with empirical osmotic pressure relations in the two corresponding binary mixtures. For the osmotic pressure of hyaluronic acid in saline, we use Ogston's empirical formula (1966), which is almost identical to Johnson's expression (1987) for the concentration range under our consideration. We used Johnson's expression which is in a much simpler form in Chapter Six in order to obtain an analytic solution there.

$$\pi_{ha} = 1.4c_h + 42500c_h^2 + 135000c_h^3 \tag{7.7}$$

Given that our albumin osmotic pressure measurement was performed mainly for concentrations much higher than the range we are interested in this particular study, and that at low concentrations, the osmotic pressure as a function of concentrations is well established, the empirical formula of Landis and Pappenheimer (1963) was used for the osmotic pressure of bovine serum albumin in saline

$$\pi_{bsa} = 280c_b + 1800c_b^2 + 12000c_b^3 \tag{7.8}$$

Following the procedure described in Section 3.2, with Eq. (7.7) and (7.8), we can calculate partial osmotic pressure of albumin and hyaluronic acid as functions of solute concentrations in the three-component mixture of saline / albumin / hyaluronic acid.

7.2.2 Equations and Boundary Conditions for Concentration Profiles

The previous discussions established that the three frictional coefficients and the two partial osmotic pressures are functions of albumin and hyaluronic concentration, c_2 and c_3. Hence, the transport equation (7.2) can now be written as

$$a_{12}\frac{dc_2}{dx} + a_{13}\frac{dc_3}{dx} = b_1$$

$$a_{22}\frac{dc_2}{dx} + a_{23}\frac{dc_3}{dx} = b_2$$

(7.9)

where

$$a_{12} = \beta\frac{\partial\pi_2}{\partial c_2} + \vartheta\frac{\partial\pi_3}{\partial c_2}$$

$$a_{13} = \beta\frac{\partial\pi_2}{\partial c_3} + \vartheta\frac{\partial\pi_3}{\partial c_3}$$

$$a_{22} = \eta\frac{\partial\pi_2}{\partial c_2} + \varsigma\frac{\partial\pi_3}{\partial c_2}$$

$$a_{23} = \eta\frac{\partial\pi_2}{\partial c_3} + \varsigma\frac{\partial\pi_3}{\partial c_3}$$

$$b_1 = \frac{Qc_{1\infty}}{Ac_1} - \frac{Qc_{3\infty}}{Ac_3}$$

$$b_2 = \frac{Qc_{2\infty}}{Ac_2} - \frac{Qc_{3\infty}}{Ac_3}$$

β, θ, η, and ς are coefficients given in (7.2). From Eq. (7.9) we can solve for the concentration gradients

$$\frac{dc_2}{dx} = f(c_2, c_3, Q, c_{2\infty}, c_{3\infty})$$

$$\frac{dc_3}{dx} = g(c_2, c_3, Q, c_{2\infty}, c_{3\infty})$$

(7.10)

102

where

$$f = \frac{a_{23}b_1 - a_{13}b_2}{a_{12}a_{23} - a_{13}a_{22}}$$

$$g = \frac{a_{12}b_2 - a_{22}b_1}{a_{12}a_{23} - a_{13}a_{22}}$$

(7.11)

In the case of saline filtration through a layer of albumin and hyaluronic acid mixture, we have

$$c_{2\infty} = 0 \quad , c_{3\infty} = 0$$

An additional boundary condition at the membrane surface for saline filtration through a layer of albumin and hyaluronic acid is

$$\left(\pi_2 + \pi_3\right)_{x=0} = \Delta p$$

(7.12)

For the case where the membrane completely rejects both albumin and hyaluronic acid, the total mass of both solutes is conserved

$$\int_0^\infty c_2(x)Adx = m_2$$

(7.13)

$$\int_0^\infty c_3(x)Adx = m_3$$

where m_2 and m_3 are the total mass of albumin and hyaluronic acid respectively, inside the filtration cell.

In the case of a mixture of saline, albumin and hyaluronic acid filtration through a plhk

103

100 membrane, which partially rejects hyaluronic acid, solute concentrations at infinity are specified and the boundary conditions at the membrane surface are determined by the membrane's solute retention coefficients, as discussed in Section 7.1.2:

$$c_2\big|_{x=0} = (1+R_2)c_{2\infty}$$
$$c_3\big|_{x=0} = (1+R_3)c_{3\infty} \tag{7.14}$$

During mixture filtration, the plhk membrane poses frictional resistance to hyaluronic acid, and to a lesser extent, to albumin. The retention coefficients are approximate measures of the resistances. The fact that the equilibrium osmotic pressure difference across a plhk 100 membrane for the 1% hyaluronic solution is approximately 5 mmHg, suggests that the friction force per unit area between the membrane and the hyaluronic acid is approximately 5 mmHg. Thus when the osmotic pressure of the initial hyaluronic acid solution is higher that 5 mmHg, the net force of osmosis and membrane friction causes hyaluronic acid molecules to filtrate through the membrane until the osmotic pressure difference across the membrane equals approximately 5 mmHg. A Similar argument holds for albumin molecules, although the membrane's frictional force on the filtrating albumin molecules is smaller. Hence, for mixture filtrates through a plhk 100 membrane, there is a drop in the driving force p-π across the membrane and we no longer have

$$\left(\pi_2 + \pi_3\right)_{x=0} = \Delta p \tag{7.15}$$

The information embedded in the retention coefficients of the frictional interactions between the membrane and the solutes, however, might allow us to determine the filtration flow rate Q. We will further discuss this issue in Section 7.4 and 7.5.

In summary, we have equations and proper conditions to determine the solute concentration distributions numerically.

7.2.3   Numerical Solutions of Concentration Distributions

Specifying the flow rate Q, which appears in the transport equation (7.9), and given concentration boundary conditions at the membrane surface, we can solve the transport equations numerically for solute distributions, $c_2(x)$ and $c_3(x)$.

First, the partial osmotic pressures were obtained in discrete form numerically as functions of c_2 and c_3 by procedures described in Chapter Three. Then the fourth order Runge-Kutta method (Press et al, 1988) was used to obtain solutions for the first three steps required to initiate the forth order Adams-Bashforth (Press et al, 1988) method. There afterwards, the Adams-Bashforth predictor-corrector method was used to obtain the solute concentrations step by step until both of them approached the concentrations specified at infinity.

The two solute concentrations obtained at each step are usually different from the discrete concentration values of c_2 and c_3 where the partial osmotic pressures were defined. Hence two-dimensional interpolation has to be used at every step to find the partial osmotic pressure values. For functions of one variable, we have the classical Lagrange's interpolation formula (Press et al, 1988). For a function $F(x,y)$ with two variables, we can decompose it into a product of two single-variable functions, as has been done in deriving most modern finite difference schemes for multi-dimensional problems

(Anderson et al, 1984). Thus, we obtain the two-dimensional interpolation formula
(Press et al, 1988)

$$F(x,y) \approx \sum_{i=k-1}^{i=k+1} \sum_{L=n-1}^{L=n+1} F_{iL} \left\{ \prod_{\substack{j=k-1 \\ j \neq i}}^{j=k+1} \left(\frac{x-x_j}{x_i-x_j} \right) \prod_{\substack{L=n-1 \\ L \neq m}}^{L=n+1} \left(\frac{y-y_m}{y_L-y_m} \right) \right\} \qquad (7.16)$$

For a mixture of saline, albumin and hyaluronic acid filtration through a plhk 100 membrane, the numerical calculation is rather straight forward. The boundary condition (7.14) determines both solute concentrations at the membrane surface and once we specify the flow rate Q, we can solve for $c_2(x)$ and $c_3(x)$. Then, we obtain the distributions of the total and partial osmotic pressures, as well as the driving force distribution, p-π. We have no explicit condition at the moment, however, to determine the flow rate Q. As discussed in the Section 7.2.2, Eq. (7.15) is not valid for mixture filtration through a plhk 100 membrane. We will use the experimental filtration flow rate in the simulation and obtain p-π to compare with the experiment. Furthermore, the calculated p-π value at the membrane surface would allow us to verify the discussion presented in Section 7.2.2 regarding the membrane resistance to the filtrate.

In order to obtain numerical solutions which can be compared with experiments for saline filtration through a layer of albumin and hyaluronic acid, we need further analysis which will be detailed in the next section.

7.2.4 A Numerical Iteration Scheme for Saline Filtration through a Layer of Albumin and Hyaluronic Acid

In the case of saline filtration through a layer of albumin and hyaluronic acid, experiments were carried out by specifying the filtration pressure head Δp and the total mass of albumin and the hyaluronic acid in the filtration cell, m_2 and m_3. To solve Eq. (7.9), however, we need to specify $c_2(x=0)$, $c_3(x=0)$ as well as Q. In order to compare the numerical solutions with the experimental data, the following procedure was used. First, the pressure head, Δp and one of the concentrations at the membrane surface, say $c_3(x=0)$, were specified. Then $c_2(x=0)$ was calculated numerically from the boundary condition (7.12). By further specifying flow rate Q, Eq. (7.9) can be solved for $c_2(x)$ and $c_3(x)$. Integration of $c_2(x)$ and $c_3(x)$ gives the total mass in the filtration cell. Q and $c_3(x=0)$ are adjusted until m_2 and m_3 each equal the amount of albumin and hyaluronic acid placed into the filtration cell, respectively. In this way we obtain the flow rate Q, albumin distribution $c_2(x)$ and hyaluronic acid distribution $c_3(x)$ for specified Δp, m_2 and m_3. Then the partial osmotic pressures $\pi_2(x)$ and $\pi_3(x)$, as well as the total osmotic pressure distribution $\pi(x)$ were calculated. Thus, we can compare theory and experimental data in terms of the flow rate Q and the driving force distribution, p-π, under given Δp, m_2 and m_3.

To speed up the solution process, an optimization scheme -- the Powell method (Press et al, 1988) was used which minimizes the objective function defined as follows

$$J = \left[m_2 - m_2^n(c_{30},Q)\right]^2 + \left[m_3 - m_3^n(c_{30},Q)\right]^2 \qquad (7.21)$$

where m_2^n and m_3^n are the calculated mass of albumin and hyaluronic acid in the filtration cell during the nth iteration.

7.3 Results and Comparisons for Cases with A Completely Rejecting Membrane

The filtrate volume as a function of time under different filtration pressures in saline filtration through a layer of albumin and hyaluronic acid is given in Fig. 7.1. The filtration flow rates, which will be compared later with theoretical predictions, were calculated when equilibrium was reached.
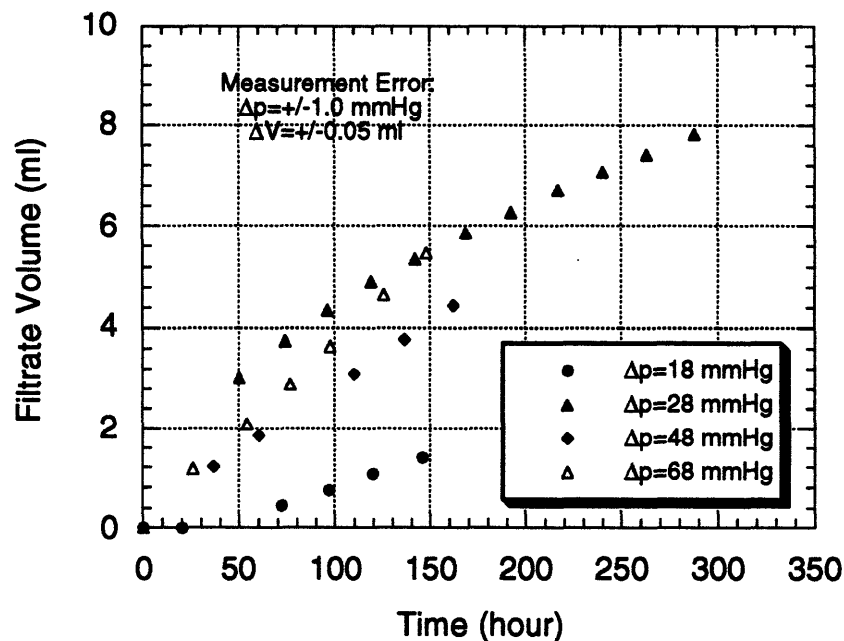
Fig 7.1 Experimental Results of Saline Filtration Through a Layer of Bovine Serum Albumin and Hyaluronic Acid Mixture, with a total rejecting membrane (pm 10, Amicon). Saline filtrate volumes are as functions of experimental time under different filtration pressures. Total albumin and hyaluronic acid mass in the filtration cell, m (bsa) =0.06 g, m (ha) = 0.022g.

It shows that each filtration experiment takes a very long time to reach steady-state.

Typical measurement of the osmotic taps are given in Fig. 7.2
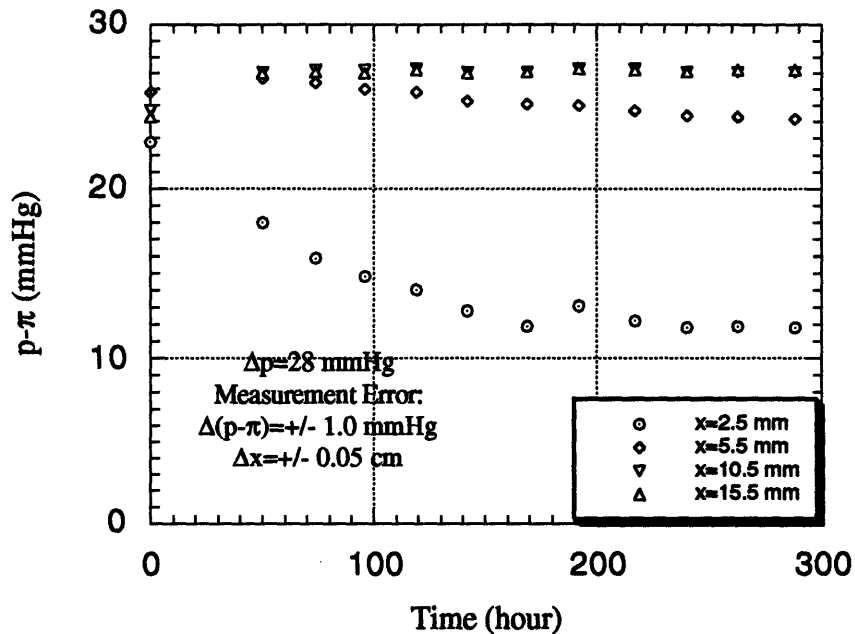
Fig 7.2 Typical osmotic taps' measurement during saline filtration through a layer of albumin and hyaluronic acid mixture. Applied filtration pressure head = 28.0 mmHg. Total mass of albumin and hyaluronic acid in the filtration cell, m (bsa) = 0.06 g and m (ha) = 0.022 g. Main membrane: pm 10; Tap membranes: ym 30; both of Amicon.

The p-π data will be compared later with numerical solution in Fig. 7.5.

Typical concentration distributions calculated for saline filtration through a layer of albumin and hyaluronic acid are shown in Fig 7.3.
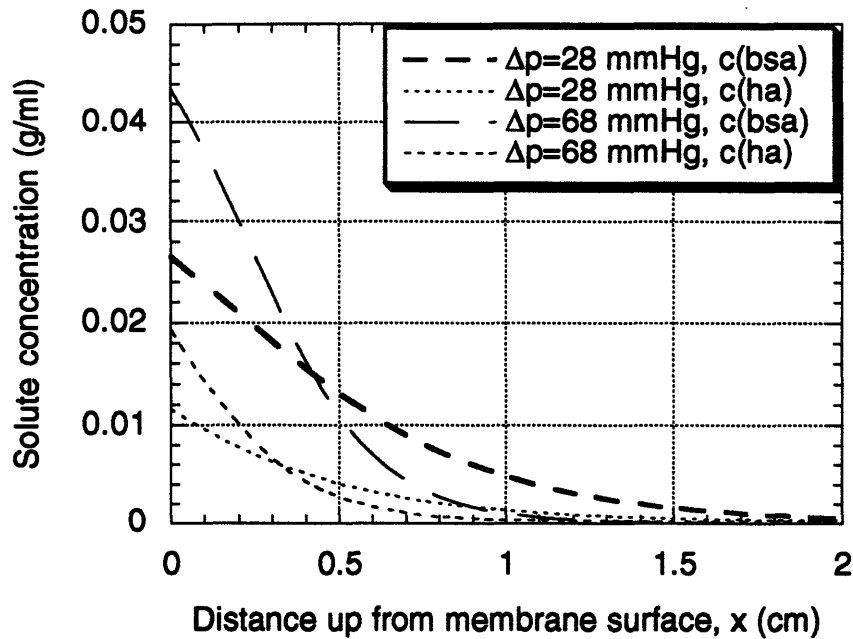
Fig 7.3 Concentration profiles of albumin and hyaluronic acid in the filtration cell during saline filtration through a layer of albumin and hyaluronic acid retained by a completely rejecting membrane (pm 10, Amicon), from numerical simulation. Total albumin mass, m(bsa) = 0.06 g. Total hyaluronic acid mass, m(ha) = 0.022 g.

The numerical solutions of the filtration flow rate are compared with the experimental data in Fig 7.4. The agreement between the prediction and the data is good with the largest deviation of approximately 15 % occuring under a large pressure head. As the filtration pressure head approaches zero, the agreement becomes better. The results confirmed the assumption that for filtration problems under the physiological pressure difference, the friction coefficients between each solute and the solvent in a three-component system can be approximated with the frictional coefficients in a corresponding

110

binary mixture. However, it should be emphasized that the interaction between solutes still plays an important role in multi-component filtration systems both through the elevated osmotic pressure (Weilderhielm, 1976) and though the non-zero frictional coefficients between solutes.
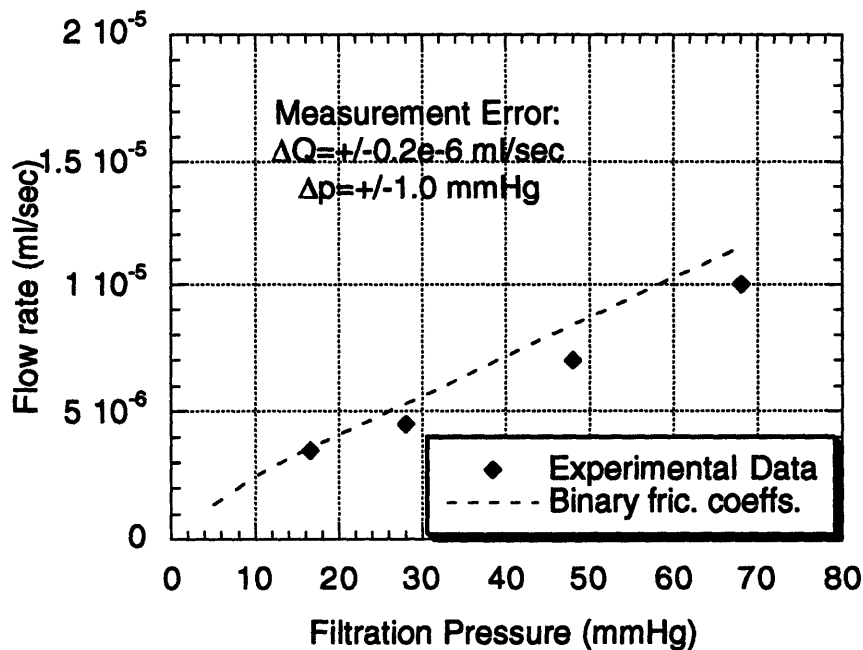
Fig 7.4 Comparison between theory and experimental data of filtration flow rate for saline filtration through a layer of albumin and hyaluronic acid mixture. Total mass of albumin and that of hyaluronic acid in the filtration cell, m (bsa) = 0.06 g, m (ha) = 0.022 g. Main membrane: pm10, Amicon

Numerical solutions of p–π are compared with experimental data in Fig 7.5. Experimental data agree well with numerical solutions.
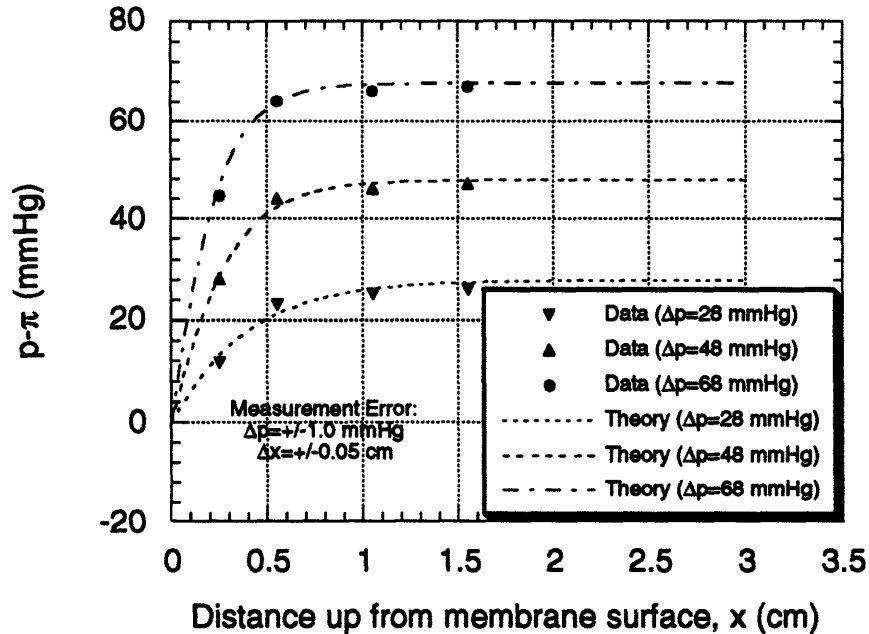
Fig 7.5 Comparison of predicted and measured driving force distribution. Saline filtration through a layer of albumin and hyaluronic acid mixture. Main membrane: pm10; tap membranes: ym 30; both of Amicon. Total mass of albumin and that of hyaluronic acid in the filtration cell, m (bsa) = 0.06 g, m (ha) = 0.022 g.

The comparisons for both the filtration flux and the driving force p-π distribution revealed that theory agrees well with experimental data. Based on the studies presented in Chapter Five, Six and Seven, a comparison of the required filtration head to acquire a given flow rate in a three-component system and its corresponding two-component systems is given in Fig 7.6.

112
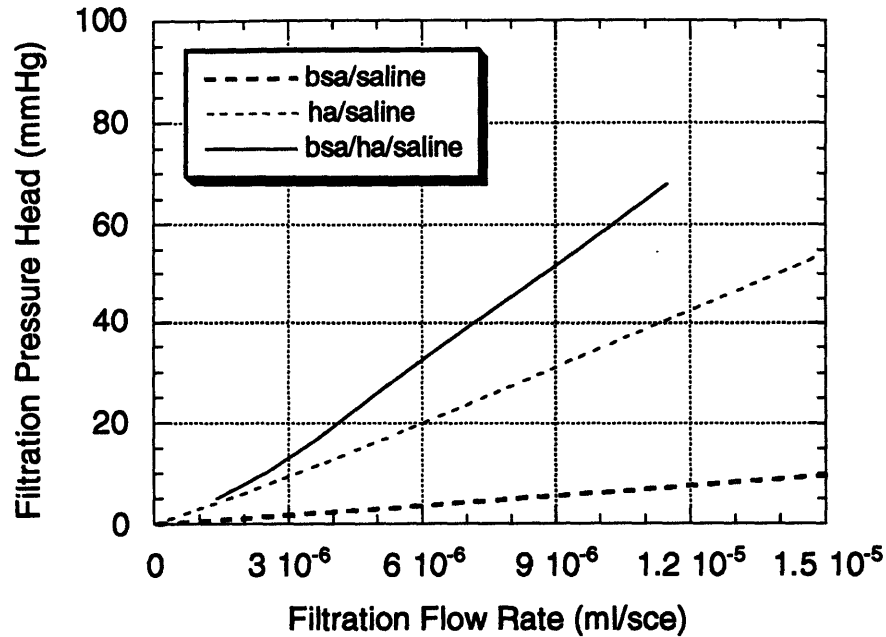
Fig 7.6 Comparison of required filtration pressure to acquire a given filtration flux for binary filtration systems of 0.06 g albumin and saline; 0.022 g hyaluronic acid and saline, and for ternary system of 0.06g albumin , 0.022g hyaluronic acid and saline. From numerical solution with boundary conditions of a totally rejecting membrane to both albumin and hyaluronic acid.

This comparison shows that under low filtration pressure, the pressure required to maintain a given flow rate for the ternary system is the sum of the pressure required to drive the same flux in the two corresponding binary systems. Under higher filtration pressures, however, the interaction between solutes significantly increases the required pressure in order to drive the given flow rate in the ternary system over that for a non-interactive system.

7.4 Results and Comparisons for Cases with A Partially Rejecting Membrane

Filtrate volume as a function of time under different filtration head and mixture concentration are presented in Fig. 7.7 for mixture of saline, albumin and hyaluronic acid filtration through plhk 100 membrane.
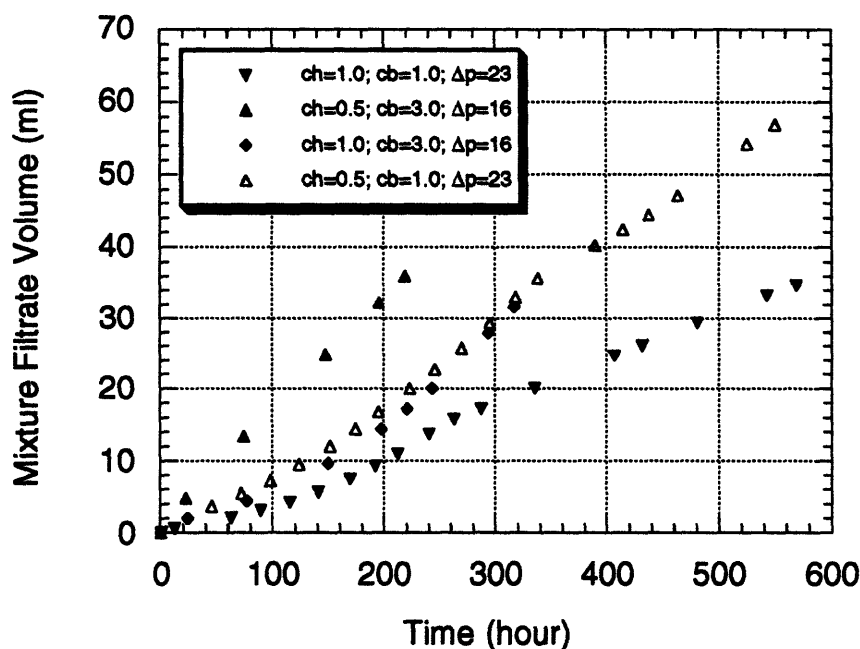
Fig 7.7 Experimental results of the mixture of saline, bovine serum albumin and hyaluronic acid filtrating through a partially rejecting membrane (plhk 100, Millipore). Filtrate volumes are given as a function of time at different pressures (Δp in mmHg), hyaluronic acid concentration (ch, in g/ml) and albumin concentration (cb, in g/ml). The short duration runs were followed by the long duration runs and hence reached equilibrium much faster.

We can see that equilibrium is reached after a very long experimental time. The steady-

state filtration rate has been calculated at the equilibrium for each case and will be given in Table 7.3.

Typical measurements of the osmotic taps are given in Fig 7.8. The equilibrium values of the tap measurement will be compared with theoretical predictions later in Fig. 7.11.
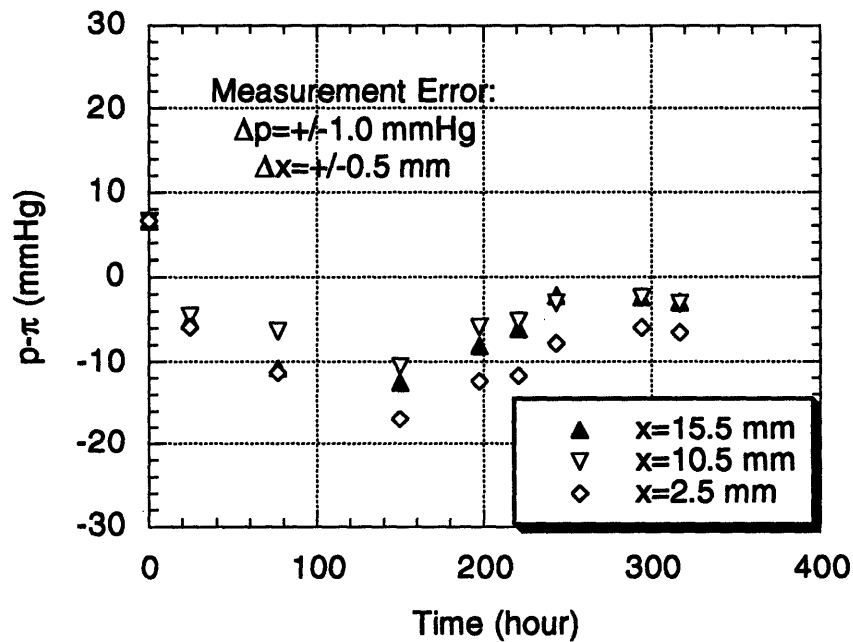
Fig. 7.8 Osmotic taps' reading during mixture filtration through plhk 100 membrane. Tap membranes: ym 30, Amicon. Hyaluronic acid concentration = 0.01 g/ml. Bovine Serum Albumin concentration = 0.03 g/ml. Applied filtration pressure, Δp = 16.6 mmHg. Osmotic pressure of the mixture, π = 20.67 mmHg

Concentration profiles from the numerical solution of albumin during mixture filtration through membranes with different solute retention coefficients are given in Fig. 7.9 and the concentration profiles of hyaluronic acid are given in Fig 7.10.
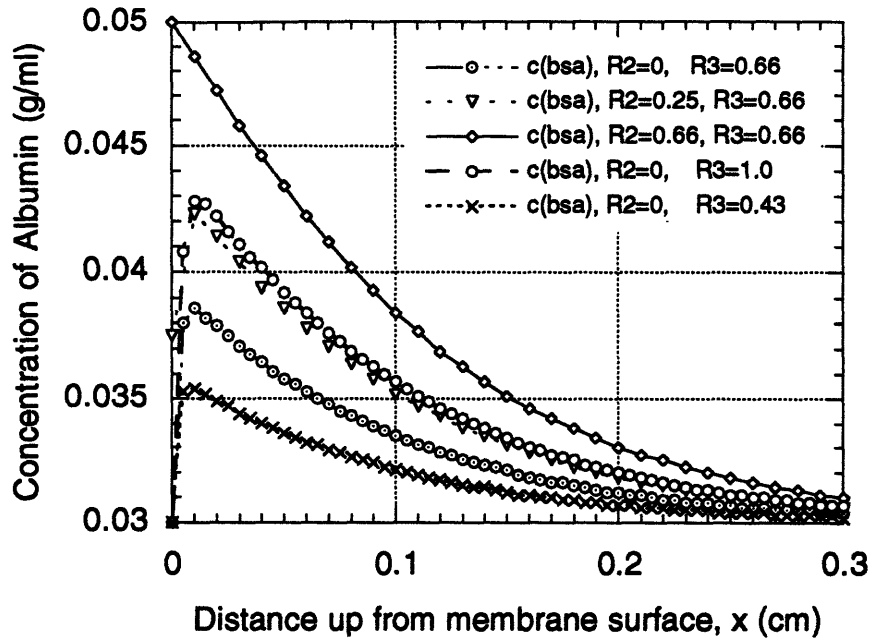
Fig. 7.9 Distribution of albumin during mixture filtration through a partially rejecting membrane both to albumin and to hyaluronic acid. Results are from the numerical simulation. Applied filtration pressure head, $\Delta p=16.6$ mmHg, R_2 and R_3 are membrane retention coefficients of albumin and hyaluronic acid, respectively. The flow rate was specified with the measured experimental flow rate, $Q=3.5e-5$ ml/sec.

The albumin concentration at the membrane surface is solely determined by the albumin retention coefficient of the membrane, as Eq. (7.14) dictates. With a membrane of zero albumin retention, the concentration of albumin at the membrane surface is zero regardless of the filtration pressure head and the hyaluronic acid concentration. Immediately away from the membrane, however, the blockage of albumin by hyaluronic acid effectively retains albumin even though the membrane has a zero albumin retention

rate. Hence, membranes with small albumin and large hyaluronic acid retention coefficients would create a sharp albumin concentration gradient near the membrane surface. For a membrane with similar retention rates for both albumin and hyaluronic acid, the distribution of albumin is much smoother, as the highest curve in the figure shows.
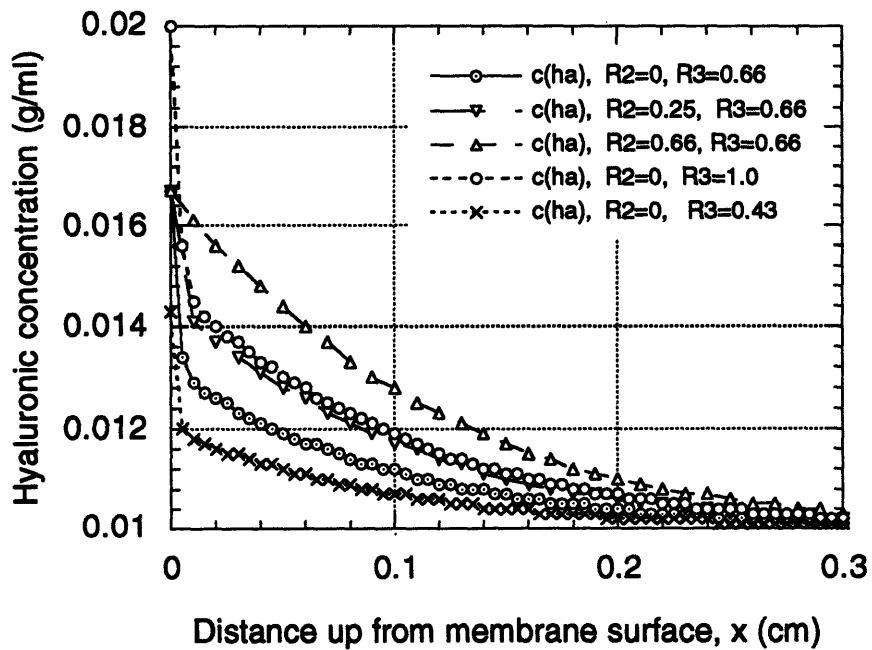
Fig 7.10 Concentration profile of hyaluronic acid during mixture filtration through a partially rejecting membrane to both albumin and hyaluronic acid. R_2, R_3 are membrane retention coefficients of albumin and hyaluronic acid, respectively. Applied filtration pressure head, $\Delta p=16.6$ mmHg. Flow rate is from the experimental data, $Q = 3.5e-5$ ml/sec. Filtrate concentration: C(ha) = 0.01 g/ml. C(bsa) = 0.03 g/ml.

Similarly, the concentration of hyaluronic acid at the membrane surface is solely

determined by the membrane retention of the hyaluronic acid. The hyaluronic acid concentration immediately away from the membrane, however, is severely affected by the presence of albumin through osmotic repulsion, and thus creates a sharp gradient in the hyaluronic acid concentration. For mixture filtration through a membrane with similar retention coefficients of albumin and hyaluronic acid, the concentration profile of hyaluronic acid, like that of albumin, is much smoother.

The filtration flow rates for the mixture of various concentrations filtrating through a plhk 100 membrane under different pressure heads are given in Table 7.3. Although a second order polynomial fits Q very well as a function of ($\Delta p \cdot C_2/C_3$), more experimental results are required to justify this functional dependence.

c(ha) g/ml	c(bsa) g/ml	Δp(mmHg)	$\Delta p(c_2/c_3)$	$Q*10e5$ (ml/sec)
0.005	0.03	16.6	108.0	4.4
0.01	0.03	16.6	54.0	3.5
0.005	0.01	21.6	46.0	2.8
0.01	0.01	21.6	23.0	2.0
0.01	0.01	21.6	23.0	1.7

Table 7.3   Filtration rates for mixtures of saline, albumin and hyaluronic acid under different filtration pressure head - partially rejecting main membrane (plhk 100, Millipore). The preliminary data of filtration flux Q correlates well with the quantity $\Delta p \cdot (c_2 / c_3)$, as seen in the table. In fact, a second order polynomial fits Q very nicely to $\Delta p \cdot (c_2 / c_3)$ for the five data points given in the table.

Finally, the numerical solution of p-π distribution are compared with experimental data in Fig. 7.11.
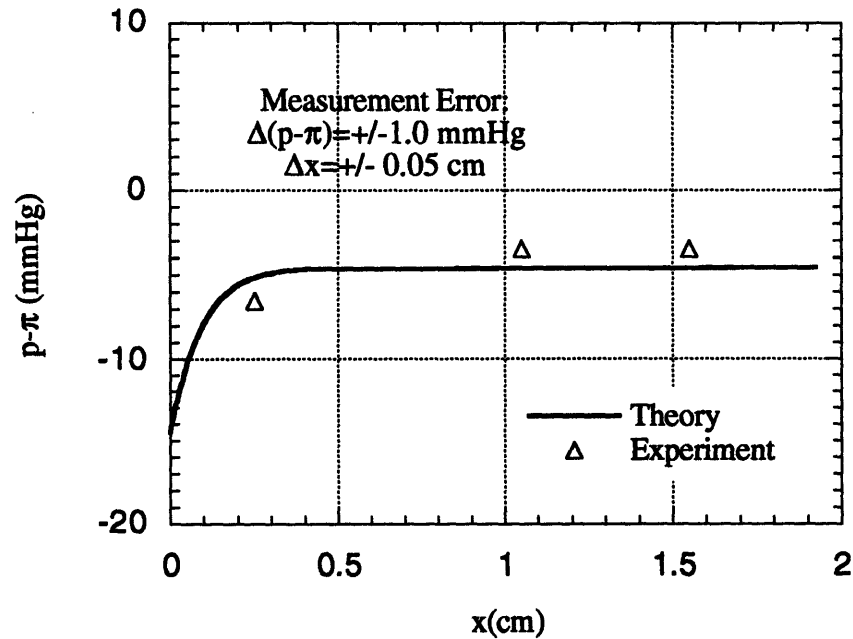
Fig 7.11   Mixture of saline, albumin and hyaluronic acid filtration through a plhk 100 membrane. Comparison between theory and experimental data of p-π. Tap membranes: ym 30K, Amicon. Albumin concentration = 0.03 g/ml. Hyaluronic acid concentration = 0.01 g/ml. Applied pressure head, Δp = 16.6 mmHg. Osmotic pressure of the mixture, π = 20.67 mmHg

Again, theory agrees well with the preliminary data. More experiments should be carried out in future studies so that one can obtain more data points within the concentration polarization layer for a better comparison.

During computation of the p-π curve shown in Fig. 7.11, we have used the filtration flux Q determined experimentally, as discussed in Section 7.2.2. In Section 7.2.2, we also

postulated that the difference of p-π across the plhk 100 membrane should be approximately 7 mmHg, with 5 mmHg contributed by the jump in chemical potential of hyaluronic acid across the membrane and 2 mmHg by that of albumin. We haven't used this postulation in our computation of the p-π distribution so that we can separate the comparison of p-π from the determination of Q. Now that we have calculated the p-π, we can read from Fig. 7.11 the p-π jump across the membrane. p-π at $x=0^+$ is approximately -14 mmHg. The osmotic pressure of the filtrate is approximately 20.67 mmHg. Hence $(p\text{-}\pi)_{x=0-}$ equals -20.67 mmHg. Thus there is approximately a jump of 6.5 mmHg across the membrane during the filtration experiment, as indicated in the osmotic pressure measurement. It should be cautioned, however, that p-π from numerical computation is sensitive to the membrane retention coefficients and that these retention coefficients are approximately determined from the osmotic pressure measurement by Van't Hoff equation. Van't Hoff equation is only valid for dilute solutions and hence the retention coefficients thus determined are only approximations. More accurate determination of the retention coefficients, further filtration experiments and analysis are required to further validate the discussions regarding the determination of the flux Q. Preliminary discussions and comparisons between theory and experimental data, however, suggested that we might be able to determine the filtration flow rate through the p-π jump across the membrane determined by the osmotic pressure measurement.

7.5   Summary

Filtration experiments of saline through a layer of albumin and hyaluronic acid retained by a membrane which completely rejects both solutes were carried out in the osmotic cell

described in Chapter Four. The filtration flow rate as well as the driving force distribution, p-π, were measured. The partial osmotic pressures were calculated according to the "excluded volume" concept, and the frictional coefficients were obtained through the closure scheme described in Chapter Three. Numerical solutions of filtration flow rate, solute concentration distributions and the driving force p-π distribution under various filtration pressures were obtained. It is found that due to the interaction between the albumin and the hyaluronic acid, the filtration pressure head required to maintain a given permeation flux is much higher than that required if there were no interactions. The comparisons of predicted flow rates and p-π distribution to the measured values show that theory agree well with the experiment.

Extensive membrane osmosis tests were performed with albumin solution and hyaluronic acid solution of known osmotic pressure. It is found that although the molecular weight of the hyaluronic acid is several orders of magnitude larger than that of albumin, it is impossible to find a membrane which can completely block hyaluronic acid while letting albumin pass freely. Given similar molecular weight, it is much easier for a size selective membrane to block globular molecules than to block long chain molecules like hyaluronic acid. The retention coefficient of the plhk 100 membrane for hyaluronic acid is determined to be approximately 0.5 and that for albumin is approximately 0.1.

Mixtures of saline, albumin and hyaluronic acid were perfused under different filtration heads through plhk 100 membranes. The filtration flux and the distribution of p-π were measured. The filtration flux correlates very well with $\Delta p(c_2/c_3)$ for the five data points obtained. Filtration flux increases with increase of the pressure head or albumin concentration and decreases with increase of the hyaluronic acid concentration in the filtrates. The increase with the pressure head and the decrease with the hyaluronic acid

concentration of the flux are easy to understand. The increased flux as albumin concentration increases, however, is less obvious. Actually this also makes physical sense because first of all the membrane used only partially blocks the hyaluronic acid while imposing a small resistance to the albumin. Secondly, the equilibrium condition requires that what flows in from upstream, flows out as the filtrate, namely, the concentration of the filtrate equals that of the mixture in the reservoir. Thirdly, there are frictional interactions between saline, albumin and hyaluronic acid. Thus as the albumin concentration increases, albumin molecules "drag" with them more hyaluronic acid and thus reduce the concentration polarization layer and hence increase the filtration flux. More experiments and analysis are required to validate this argument and the functional dependence.

With experimentally determined membrane rejection coefficients and the filtration flux, the transport equations were solved and the distribution of p-π is compared with preliminary experimental data. The agreement between the two is good. In order to predict the filtration flux, however, we have to provide either the membrane resistance to the filtrate, or the Δ(p-π) across the membrane during filtration. From Fig. 7.11 we know that by specifying Q, numerical solution of the transport equations give Δ(p-π) across the membrane. Hence knowing the actual Δ(p-π) across the membrane will allow us to determine filtration flux Q by numerical iteration with different Q until Δ(p-π) from the numerical solution equals the actual value. Equivalently, knowing the membrane resistance R to the filtrates would allow us to determine the filtration flux. The numerical iteration procedure is to choose different Q, solve for the Δ(p-π) across the membrane, then calculate the membrane resistance according to the modified Darcy's law until the numerical membrane resistance equals the real value. The information about the membrane resistance and the p-π across the membrane during filtration is embedded in

the osmotic pressure measurement as we have discussed in Section 7.2.2 and 7.4. One approximation would be that p-π across the membrane during filtration experiment is the same as that during the osmotic pressure measurement. Preliminary comparison shows that this is a very good approximation. Future studies should be carried out to further verify this approximation so that we can solve the filtration flux numerically as well for mixture filtration through a partially rejecting membrane.

Chapter 8

Saline Filtration through Collagen Gels

Collagen, with its many different types, is one of the most abundant structural proteins found in bone, cartilage, skin, blood vessels, connective tissues, and most organs (Nimni, 1983). A single collagen molecule typically has a triple helical structure with a length of approximately 300 nm and a radius of approximately 0.75 to 1.5 nm (Yannas, 1972, Visvanadham et al, 1978). In most tissues however, collagen molecules tend to aggregate to form massive micro-fibrils (Nimni, 1983). Because collagen is one of the main components in most living tissues and can be crosslinked to form a gel, we choose it for our study of transport through macromolecular gels.

A gel is a crosslinked macromolecular network which can support load. The transport equations derived in Chapter Two show that if there is no matrix stress in the macromolecular networks, there would be no pressure loss along the flow path during filtration processes. This prediction has been verified directly by the measurement of pressure distribution during saline filtration through a layer of bovine serum albumin, as described in Chapter Five. The comparisons of theory and experimental data in binary and ternary filtration systems in solution forms, as discussed in previous chapters, have further confirmed the prediction. In a collagen gel, however, the crosslinked network can support elastic stresses. The transport equations, Eq. (2.15), indicate that one would then be able to measure a pressure gradient along the filtration path in the gel. Hence the measurement of pressure distribution in a collagen gel under the saline filtration is one of the main goals of this chapter.

Filtration experiments were first performed in a filtration cell (Kim, 1989) with a needle probe to measure pressure distribution. Then the same experiment was repeated in the osmotic filtration cell described in Chapter Four to measure the distribution of p-π. We will discuss both experiments in the following sections.

8.1. Initial Filtration Experiment

Saline filtration through gels can be described by Eq. (2.15):

$$\nabla(p - \pi) = -\frac{\mu}{K}\vec{v}_{av}$$

$$\nabla p = \phi_m \nabla \sigma \qquad (8.1)$$

where σ is the matrix stress (positive if tensile) and x is the distance from the membrane surface (positive up away from the membrane). The osmotic pressure π, the average velocity $\vec{v}_{av}$ and the hydraulic conductivity K are defined as

$$\pi = -\frac{kT}{\upsilon_1}\ln a_1 \quad , \quad \vec{v}_{av} = \frac{\vec{Q}}{A} = \phi_1\vec{v}_1 \quad , \quad K = \frac{\mu\phi_1^2}{\gamma_{12}} \qquad (8.2)$$

Due to the compression in the gel caused by the frictional interaction between the saline and the collagen gel retained by the supporting membrane, the matrix stress σ is negative. σ becomes more negative as the distance from the membrane surface, x, decreases. Hence the gradient of σ is positive. From the second equation of (8.1), the pressure

gradient is also positive, and thus we expect to measure a pressure drop along the filtration path. From the first equation of (8.1), the modified Darcy's law, the pressure gradient minus the osmotic pressure gradient is also positive. Thus we should measure a p-π drop along the filtration path as well.

8.1.1   Experimental Procedure

Collagen gels were made from a 3 mg/ml collagen solution (Vitrogen 100, Collagen Co., Palo Alto, CA), Hank's Balanced Salt Solution (HBSS) and the cross-linking agent, glutaraldehyde solution .

To start with, 1 ml of 25 % glutaraldehyde solution (49630, Fluka Chemika, Switzerland) was mixed with 100 ml HBSS (Sigma H4385, 10x, Sigma Chemical Co., St. Louis, MO) to make a 0.025 % glutaraldehyde solution. 0.2 M NaOH solution and 0.2 M HCL solution were also prepared with NaOH beads (7708-03, Mallinckrodt Inc., Paris, KY), a 37 % HCL solution (UN 1789, Mallinckrodt Inc., Paris, KY) and distilled water filtered with 0.2 μm filter (N0. 4192, Gelman Sciences, Ann Arbor, MI). Then 9 ml of Vitrogen and 0.5 ml HBSS was added into a beaker, which is cooled by an ice-water bath, and the pH of the collagen / HBSS mixture was adjusted to 7.2 by 0.2 M HCL and 0.2 M NaOH solution. Afterwards, 0.5 ml 0.025 % glutaraldehyde solution was added to the collagen / HBSS mixture. The beaker was shaked gently during the entire process. The mixture, called the pre-gel solution, was subsequently degassed for about 20 minutes with the beaker placed in an ice-water bath to prevent early gelation. After the degassing, the pre-gel solution was used immediately to make a collagen gel inside the filtration cell at room temperature.

The membrane (pltk 30, Millipore, MA) was mounted inside the filtration cell and its resistance was measured. Typically the resistance of the membrane was less than 5% compared with the resistance of the gel. The interior wall of the filtration cell was then coated carefully with Sigmacote (SL-2, Sigma Chemical Co., St. Louis, MO) to reduce collagen binding to the wall. After allowing the Sigmacote to air dry for approximately 20 minutes, 7 ml of the pre-gel solution was added into the filtration cell and a 33 gage needle probe (Kim et al, 1991) was positioned into the middle of the pre-gel solution. Then the filtration cell was covered with parafilm (American National Can, CT) and left at room temperature over night (12 - 24 hours), forming an elastic collagen inside the filtration cell. Then we filled the filtration cell with saline and connected it to a saline reservoir to start the filtration experiment. Because of the deformation caused by the saline filtration and the binding of the gel to the side wall, the top surface of the collagen gel deformed into a stable downward convex shape during the filtration process. After equilibrium was reached, the pressure distribution was measured by moving the needle probe along the filtration path. We waited approximately 20 minutes after each move and then took a pressure reading.

8.1.2 Measurement and Comparison of Filtration Rate

Typical filtration flow rate measurement results are given in Fig. 8.1. The filtration flow rate changes linearly with the applied filtration pressure difference, which suggests that the deformation of the collagen gel under the filtration is small.
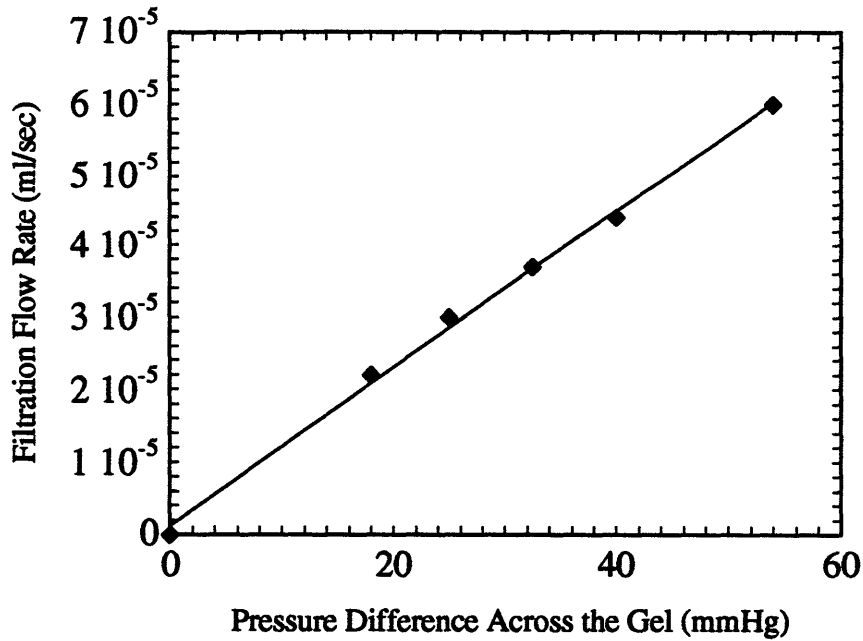
Fig. 8.1 Filtration flow rate as a linear function of the filtration pressure head during saline filtration through a collagen gel. The volume fraction of the collagen gel = 0.0022. Total length of the collagen is approximate 2 cm. The area of the filtration cell is 3.88 cm². Membrane: pltk 30, Millipore. Detailed experimental procedure is given in Section 8.1.1.

To compare with literature data, the permeability, or the hydraulic conductivity, K is calculated by Darcy's Law (Jackson and James, 1986) from our experimental results. K is also calculated from sedimentation data (Obrink, 1971) according to Eq. (3.31) as well as from the fiber matrix model (Either, 1986), namely

$$K = 0.31 \times a^2 \phi^{-1.17} \quad (cm^2)$$

where a is the collagen fiber radius in Å and ϕ is the volume fraction of collagen. The radius of collagen fiber has been determined to be approximately 7.5 to 15 Å (Yannas,

1972; Viswanadham et al, 1978).

The permeability of collagen from the sources described above, as well as literature data from filtration experiment of Jackson and James (1986) are given in Fig. 8.2.
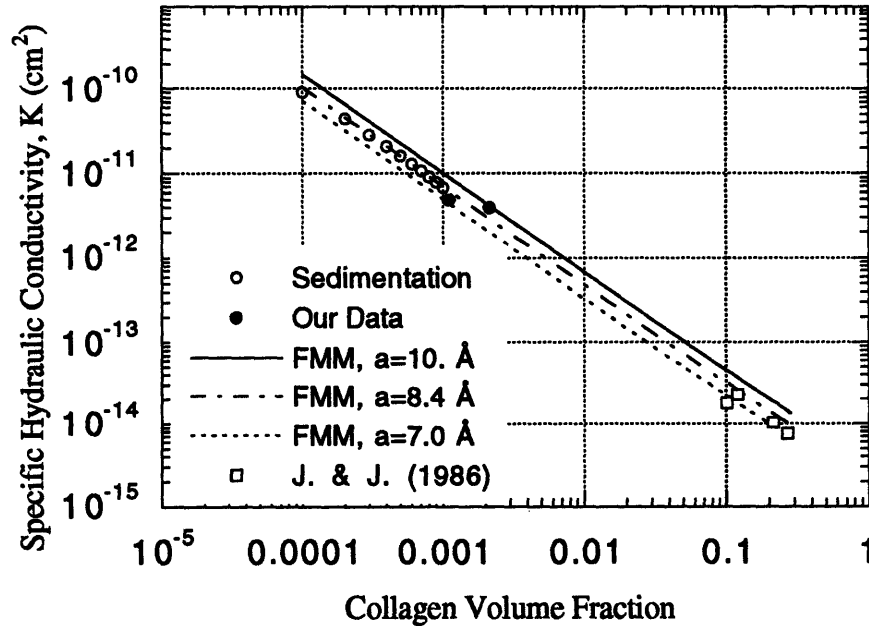
Fig. 8.2 Comparison of collagen permeability from different sources. FMM stands for values of K calculated from the fiber matrix model. a is the fiber radius used in the calculation.

8.1.3 Results and Discussions of Initial Needle Pressure Measurement

The measurement of collagen permeability is consistent with literature data as given in Fig. 8.2. The measurement of the needle probe, however, gave an inconsistent negative pressure reading as shown in Fig 8.3.
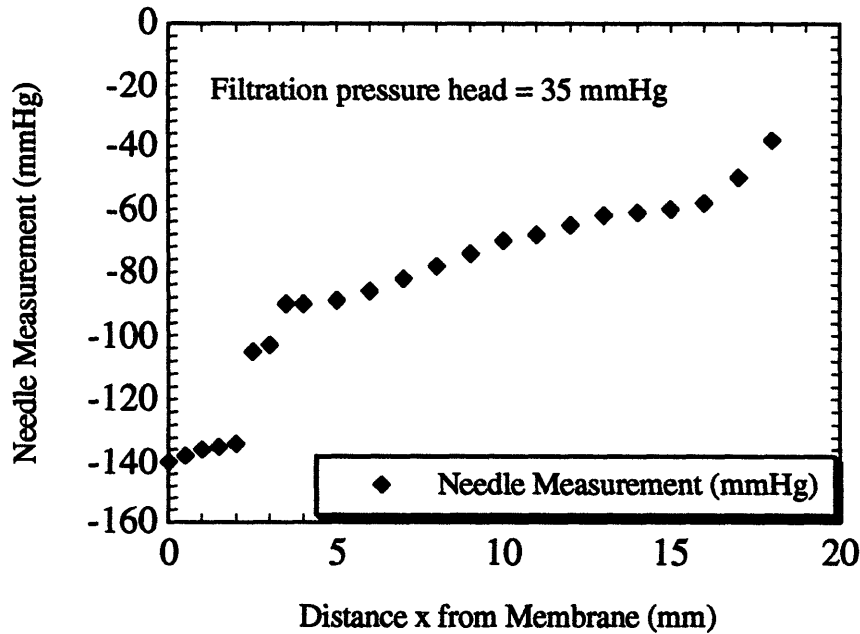
Fig 8.3 Initial needle measurement results of the pressure distribution in a collagen gel under saline filtration as described in Section 8.1. Total length of the gel is approximately 2 cm. The needle probe was initially positioned at the bottom of the gel (x=0) and was slowly moved upwards by a micrometer fixed on the filtration cell (Kim et al, 1991). The time interval between each data point is approximately 20 minutes.

One might think that there exists some osmotic effect in the needle measurement results. Osmotic pressure test of the collagen gel, however, reveals that fully crosslinked collagen networks have near zero osmotic pressure (on the order of 1 mmHg, within our pressure transducer's error). Furthermore, Stokes-Einstein's formula of diffusivity (Wijmans et al, 1985) relates osmotic pressure, permeability and diffusivity

$$D = \frac{K\phi}{\mu_1} \frac{d\pi}{d\phi}$$

where μ_1 is the viscosity of saline and D is the diffusivity of collagen in saline. Integrating over volume fraction gives

$$\pi(\phi) = \int_0^\phi \left(\frac{\mu_1 D(\phi)}{K(\phi)\phi} \right) d\phi$$

The diffusivity of collagen in saline is on the order of 7×10^{-8} cm^2/sec (Obrink, 1972). The permeability has been given in Fig. 8.2. Given the volume fraction of the collagen gel we use in our experiment, the osmotic pressure can be calculated to be on the order of 0.5 mmHg. Hence Fig 8.3 clearly indicates that there are some additional mechanisms other than osmosis that affect the measurement results. It is possible that the negative pressure was caused by the extra compression and relaxation of the collagen gel due to the movement of the needle probe. It is also possible that there are significant interfacial interactions between the needle and the gel, as well as effects due to temperature fluctuation. Hence a series of controlled tests were planned.

8.1.4 Needle Pressure Probe Tests in Collagen Gels

The test apparatus was depicted in Fig. 8.4. The gels was made the same way as described before. The water bath was used to provide a constant temperature. The pressure transducer was zeroed when the probe was in its final position inside the gel and immediately before the measurement started. To elucidate the effect of the needle movement on the measurement, probes were positioned both before and after gels were formed. The possible interfacial effect was to be checked by using needles of different

131

size and material.
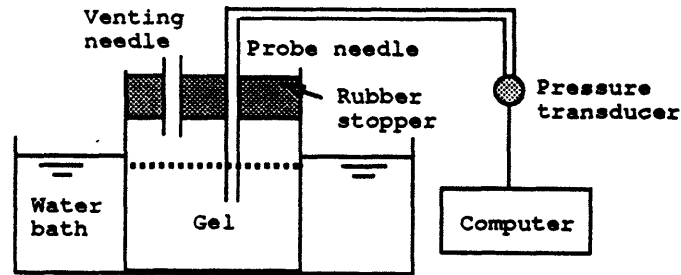
Fig 8.4 Experimental Set-up to test possible needle-gel interactions. The temperature is kept constant by the water bath. The venting needle provided the passage for the air trapped inside the bottle. Stainless steel needles of different size were used as the probe, as described in Section 8.2. Gels were made according to the procedure described in Section 8.1. The transducer is of accuracy +/-1.0 mmHg (PX 142-2.5 BD 5v, Omega, CT).

Tests immediately showed that the movement of the needle probe inside a gel damaged the gel and hence contributed to the inconsistency in the measurement results. But the inconsistency remained even if the probe was positioned before the gel was formed. Hence tests of stainless steel needle probes of different size were performed. The results are summarized in Fig 8.5.
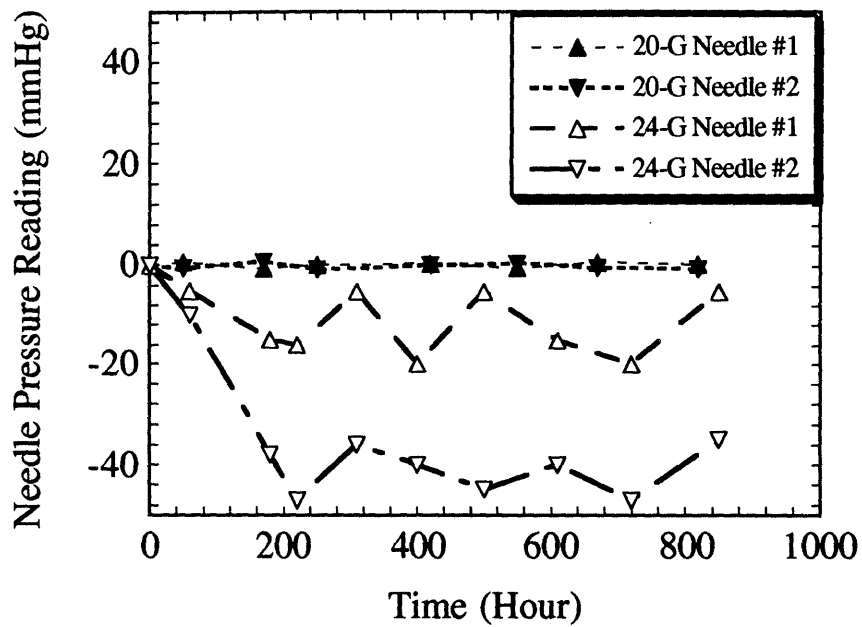
Fig 8.5. Results of needle test for possible needle-gel interaction. The apparatus of the test was shown in Fig. 8.4. Large needle measures the real zero pressure inside the gel.

We concluded that by using a large stainless steel needle placed in the pre-gel collagen solution before gelation, we would be able to measure the true pressure caused by the filtration flux inside the gel. Hence, a double-port needle probe with larger stainless steel needles (20 gage), as shown in Fig 8.6, was made. With the double-port probe, we do not have to move the probe during the measurement and are still able to verify if there is a pressure gradient along the filtration path.
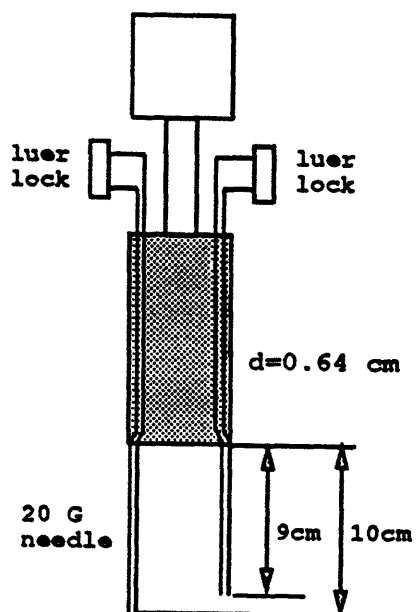
Fig 8.6. Schematics of a double-port needle probe made from two 20 G stainless steel needles. The probe holder is a stainless steel tube. Needles are epoxied inside the holder and the holding tube is filled with epoxy to prevent leakage.

8.2 Pressure Measurement by the Double-Port Needle Probe

The experimental apparatus is schematically shown in Fig 8.7. The filtration experiment and measurements were carried out following the same procedure as described in the last

section but without moving the needle probe. The flux vs. pressure curve as given in Fig. 8.1 was obtained. The pressure readings of the two ports are shown in Fig 8.8.
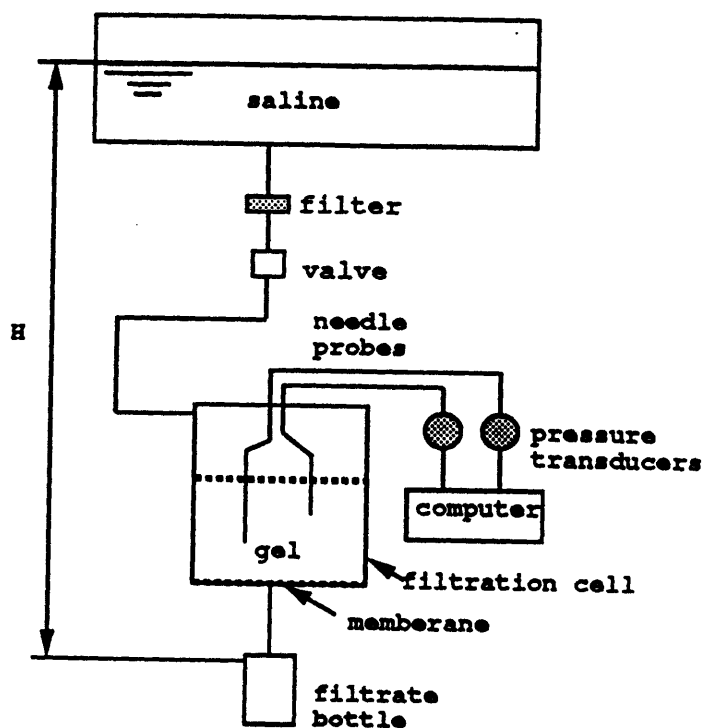
Fig 8.7 Schematics of the filtration apparatus with the double-port needle probe. The filtration head was provided by the saline in the filtration reservoir. The pressure distribution was measured by the needle probes and the transducers (PX 142-2.5 BD 5v, Omega)
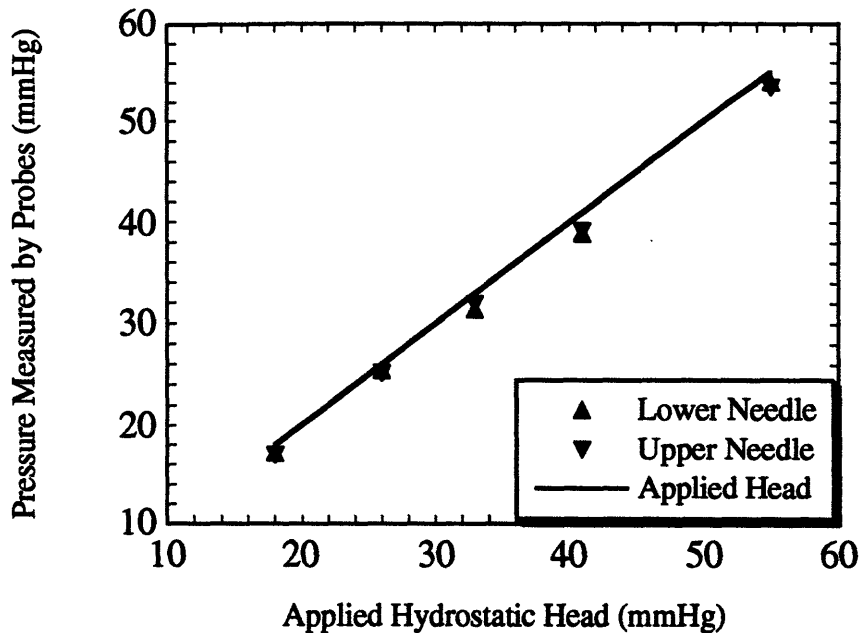
Fig 8.8 Pressure readings of the double-port needle probe during saline filtration through a collagen gel. Both needles measure the same pressure as the applied filtration head. Schematics of the experimental set-up was shown in Fig. 8.7. The total gel length is approximately 2 cm. The distance between the bottom of the gel to the tip of the lower needle, the distance between the two needle tips, and the distance between top surface of the gel and the tip of the upper needle are all approximately one third of the total gel length.

The results show that there is no pressure gradient along the filtration path, a clear contradiction to the theoretical prediction! We initially suspected leakage along the side of the needle probe. Nevertheless, the comparison of the flow rates with or without the needle probe in position, as shown in Fig 8.9, convinced us that there was no leakage alongside the needle. The leakage along the interior wall of the filtration cell was not

likely since collagen gel was bounded to the wall even with Sigmacote.
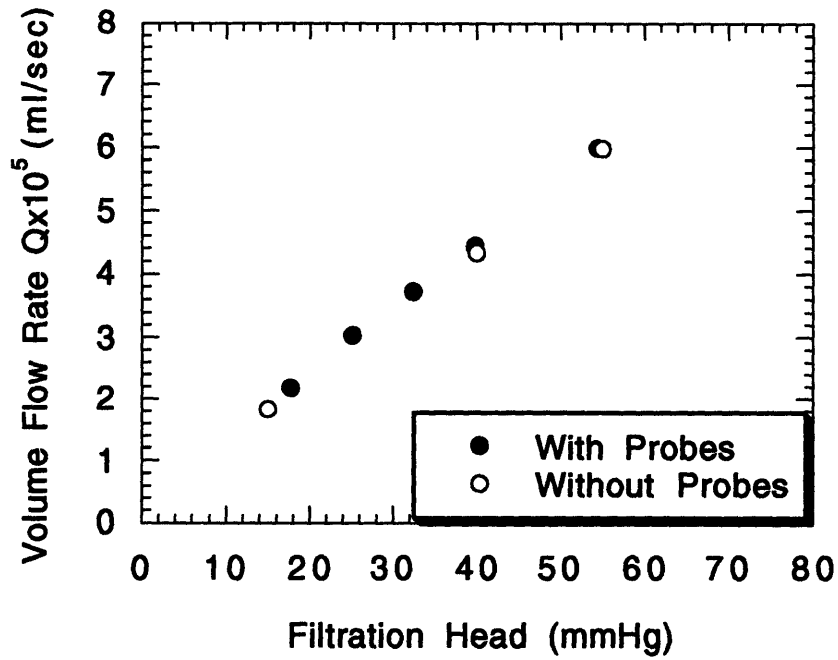
Fig 8.9 Comparison of flow rate for saline filtration through collagen
gels with or without the double-port needle probe in position. Collagen
gels used in the two tests were the same and were made according to the
procedure described in Section 8.1.1.

On the other hand, there are questions about the matrix stress term in the transport
equations. The general force balance equation on gel / saline mixture would give Eq.
(8.3) (Silberberg, 1989). Whereas the force balance on a one-dimensional slab of gel
/saline gives Eq. (8.4) (Silberberg, 1980).

$$\frac{dp}{dx} = \phi \frac{d\sigma}{dx}$$
(8.3)

$$\frac{dp}{dx} = \frac{d(\phi\sigma)}{dx} \qquad\qquad (8.4)$$

In our case, Eq. (8.3) and Eq. (8.4) differ very little because the deformation of the gel is very small, as discussed in Section 8.1.1. Thus we may assume Eq. (8.4) holds. An analysis depicted in Fig 8.10 with Eq (8.4) would lead to the conclusion of Eqs. (8.5).
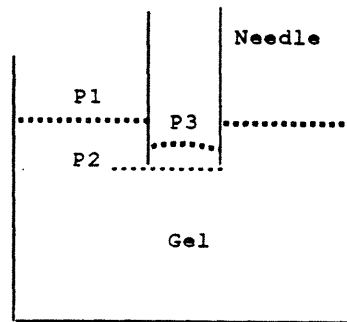
Fig 8.10 Analysis of the pressure measurement of a needle probe in a gel. The needle was filled with buffered saline and was connected to a pressure transducer (PX142-2.5 BD 5v). The gel is the same as that used in the filtration experiment described in Section 8.2. P_1 and P_3 are values of local fluid pressure right above the gel in the saline at the indicated positions, while P_2 is the local fluid pressure inside the gel.

$$p_1 - p_2 = (\phi\sigma)_1 - (\phi\sigma)_2$$

$$p_3 - p_2 = (\phi\sigma)_3 - (\phi\sigma)_2 \qquad\qquad (8.5)$$

$$p_3 \equiv p_2 + (\phi\sigma)_2 \equiv p_1$$

Eqs. (8.5) state that the needle probe can only measure the combination of the pressure and the matrix stress, a "total pressure" which is constant everywhere inside the gel and equal to the source pressure which drives the filtration.

If Eqs. (8.5) hold, they will have significant implications on variety of clinical tests. In micro circulation studies, one occasionally measures the tissue fluid pressure (Intaglietta and Tompkins, 1989; Fein, 1972; Wiederhielm et al, 1964). A device frequently used to measure the tissue fluid pressure and the pressure inside gel filled micro cavities (Maepea and Bill, 1989) is the Servo-Nulling Micropressure Monitor (Intaglietta and Tompkins, 1989; Fein, 1972; Wiederhielm et al, 1964). The applications of such instrument are also found in more fundamental research such as transport through cell membranes (Intaglietta and Tompkins, 1989). The main components of this apparatus are a highly sensitive bridge circuit and a pressure probe known as microelectrode. The microelectrode is a micropipette with a tip diameter of 0.5 to 5 microns filled with electrolyte solutions. When the probe is placed into the tissue or gel filled cavities, the difference between the sample pressure and the initial sensor chamber pressure displaces the electrolyte solution. This displacement in turn switches on a servo to adjust the sensor chamber pressure until an equilibrium in pressure is reached (Wiederhielm, 1964). Thus it is obvious that all the discussions we have had for our needle measurement in gel is relevant to the measurement made by the servo-nulling micropressure monitor. What people used to believe to be the local fluid pressure measured by the instrument might actually be the

139

"total pressure", not to mention the possibility of interfacial interaction between the tiny micropipette and the tissue or the gel.

8.3   Measurement and Analysis of Driving Force Losses

Failing to measure any pressure gradient with the double-port needle probe in a gel, we wanted to determine if we could measure a gradient in the driving force, p-π, as the theory predicted. Filtration experiments were performed in the osmotic cell according to the procedure described in Chapter Four. After the membrane resistance test, the hydrostatic head test and the osmotic pressure test (with 0.05 g/ml albumin saline solution), a collagen gel was made according to the procedure described in Section 8.1. The filtration flow rate was measured and was the same as measured previously, within experimental error of approximately 5 %. The p-π measurements were made at filtration pressure of zero, 5 mmHg and 10 mmHg. The results are shown in Fig 8.11.
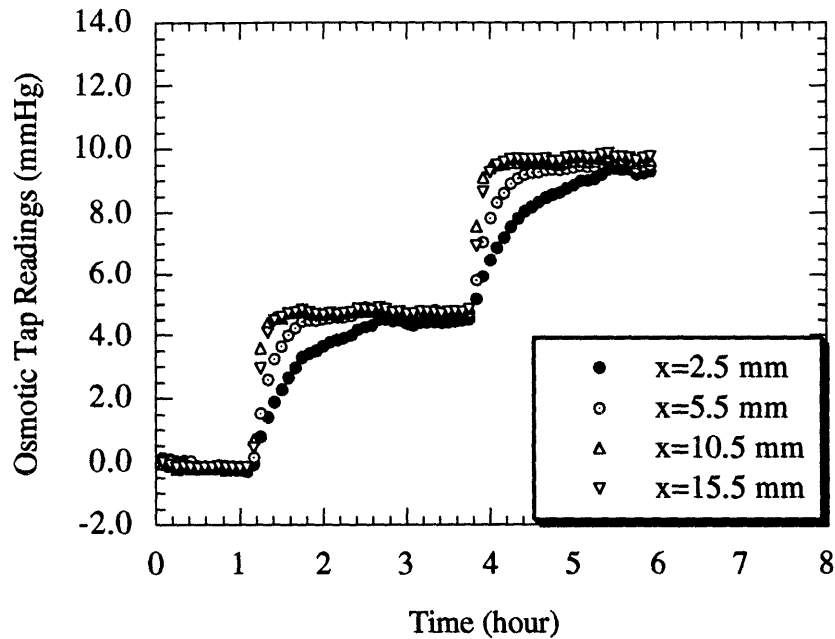
Fig 8.11 Osmotic tap readings of p-π during saline filtration through a collagen gel. Collagen gel was made as described in Section 8.1.1. Main and tap membranes are pltk 30 (Millipore, MA).

All readings of the four osmotic probes stayed at zero when applied filtration head is zero. Approximately one hour each time after the filtration head was raised, all readings of the osmotic probes approached the same applied pressure. Once again the osmotic taps fail to detect any gradient of the driving force, p-π. This result is not a surprise considering the fact that a fully crosslinked gel acts as a membrane by itself. There should not be any difference between the results obtained with a needle probe and those obtained with an osmotic probe. However, the experimental data clearly contradict the theory. As discussed in Section 8.1, we expect to detect a gradient in p-π. In fact the filtration of saline through a collagen gel can be schematically shown in Fig 8.11.
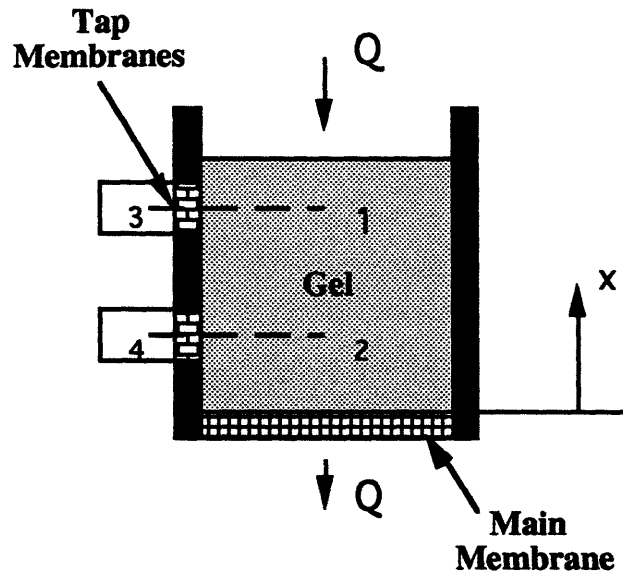
Fig 8.12 Analysis of the osmotic probe measurement during saline filtration through a collagen gel. Positions 1 and 2 are inside the gel, whereas positions 3 and 4 are inside osmotic taps which are separated from the gel by tap membranes.

Applying the modified Darcy's law between point 1 and 2 gives

$$(p-\pi)_1 - (p-\pi)_2 = \int_1^2 \frac{\mu Q}{KA} dx \ > 0 \qquad (8.7)$$

Since there is no flow between point 1 and 3, and between points 2 and 4, we have, again by the modified Darcy's law

$$p_3 = (p-\pi)_1 \qquad p_4 = (p-\pi)_2 \qquad (8.8)$$

Thus, according to the modified Darcy's law, we conclude the osmotic taps should measure a gradient in p-π as shown in Eq (8.9)

$$p_3 > p_4 \qquad (8.9)$$

Since the modified Darcy's law is an independent transport equation in addition to the mechanical force balance equation for binary systems, this conclusion clearly revealed that there is a discrepancy between the theory and the measurement.

8.4 Summary and Discussions

Experiments of saline filtration through a collagen gel have been carried out. The osmotic pressure of the collagen gel and the filtration flow rate measured agree well with literature data. The needle probe test revealed that there might be an interfacial interaction between the needle and the collagen gel when the needle size is small. This interaction apparently diminishes as the size of the needle increases. The measurement of the pressure and the driving force distributions, however, revealed a contradiction between the theory and the experimental data. Experimental errors are unlikely other than a possible leakage along the interior wall of the filtration cell. Although direct experimental check of the leakage, which may be very difficult to conduct, has not been performed, the visible binding of the collagen gel to the wall suggests that it is very unlikely to have a significant leakage along the wall. Another possible source of error is the effect of the surface curvature of the gel. Due to gel binding at the side wall of the filtration cell and the gel deformation under filtration, the top surface of the collagen gel is a downward convex during experiment. The curvature of gel would cause flow non-uniformity. The horizontal velocity caused by the non-uniformity alone, however, cannot explain the constant pressure and constant p-π measured. The closest tap to the membrane surface, which is approximately 2.5 mm away from the membrane surface in a gel with a length of

143

approximately 2.0 cm, would still be able to detect a difference in p-π, if there is any.

The experimental observations from the needle measurement and the osmotic cell measurement of saline filtration through a collagen gel are significant and relevant to important issues regarding clinical testing, microcirculation and other fundamental studies involving transport through crosslinked macromolecular networks. Further studies are called for in order to resolve the discrepancy between the theory and the experimental observations. Regardless of the outcome, resolving this controversy would be very exciting.

Chapter 9

Conclusions, Discussions and Suggestions for Future Studies

This thesis described a series of studies aimed at obtaining a better understanding of transport in multi-component macromolecular networks, a phenomena widely found in many biological and industrial processes. This was accomplished by establishing a theoretical framework, developing experimental methods, and studying binary and ternary macromolecular systems. The objective of this chapter is to summarize this research project in a step-by-step manner, to discuss some remaining controversies, and to suggest the direction of future studies.

9.1 A Theoretical Framework for Studying Transport through Macro-molecular Networks

As discussed in Chapter One, current theories are based on linear phenomenological equations, which is a fundamental set of empirical formula in non-equilibrium thermodynamics. The phenomenological equations balance all actions and reactions on each individual component and thus they describe the dynamics of each component. Therefore, if a theory is intended to study the motion and the state of each individual component, it is natural to use the phenomenological equations as the starting point. For permeation through macromolecular systems, which typically have very low Reynolds numbers, the linear phenomenological equations are an excellent approximation. The

difficulties in applying linear phenomenological equations, however, rise from the fact that they are empirical formulae involving formidable number of unknown coefficients for multi-component systems, as we have discussed in Chapter Two. Transport equations based on the phenomenological equations (Silberberg, 1980, 1989) were adopted in this study, but they are incomplete and additional relations are required to provide closure. A closure scheme based on equilibrium thermodynamics (with a local equilibrium assumption), fluid mechanics, and experimentation has been proposed in Chapter Three. The transport equations and the closure schemes we proposed provide a theoretical framework for studying transport through macromolecular networks.

9.2 Experimental Studies of the Transport Phenomena

There are two purposes in conducting the experimental studies. First, to obtain additional empirical relations required for the closure of the theoretical framework. Secondly, to validate the theoretical framework developed in this research. The determination of osmotic pressures is the focus of the first category. The filtration experiment, on the other hand, was adopted for the purpose of validating the latter. By designing and fabricating an osmotic cell, a filtration cell with side pressure and osmotic pressure taps, we measured the filtration flow rate, the pressure and the osmotic pressure distribution during filtration of saline through binary and ternary macromolecular solution and gels.

The theoretical framework and the experimental apparatus developed in this study provided complete tools necessary for the study of transport through the macromolecular networks.

9.3 Observations, Discussions and Suggestions

9.3.1 Filtration through Solutions Retained by a Complete Rejecting Membrane

(1)   The measurement of pressure distribution during saline filtration through an albumin layer confirmed the theoretical prediction that there is no pressure loss along the filtration path, despite that the albumin layer generates enormous flow resistance (Chapter Five). We also observed that:

(I)   The surface-to-volume ratio of macromolecules is an important parameter in deciding the filtration resistance of a macromolecular solution (Chapter Six).

(II)   The interaction between macromolecular solutes in multi-component mixtures retained by a completely rejecting membrane generally increases the flow resistance (Chapter Seven).

Moreover, it is noted that in such filtration systems, it is the total mass rather than the initial concentration of the macromolecular solute in the filtration system that determines the filtration resistance and subsequently the flux. For example, bodily fluids transported through tissues are usually mixtures of macromolecules. If for some reason the tissue begins to retain solute over time, we would see a corresponding increase in filtration resistance. In such macromolecular networks, a large filtration pressure difference has to be applied across the network in order to maintain the original filtration flux.

(2)   The measurement of osmotic pressure of albumin solutions revealed that when the osmotic pressure of a solution exceeds the vapor pressure of the solvent involved, commercial osmometers based on the negative pressure method are not reliable (Chapter Five).

(3)   The distribution of the concentration, pressure and osmotic pressure, as well as the filtration flow rate can all be determined by solving the transport equations. As discussed in Chapter Five through Seven, theoretical solutions agree well with the experimental data, indicating that the theoretical framework developed in this thesis is applicable for filtration through multi-component macromolecular solutions.

(4)   The analysis of the sedimentation process is described in Chapter Three for the purpose of determining the frictional interaction between solutes. The analysis altered our original belief that sedimentation experiments cannot reveal detailed aspects concerning the filtration in macromolecular systems. By developing transport equations for the sedimentation process, the effect of the chemical activities can be revealed from the shape of the sedimenting front. Hence it would be fruitful for future studies to explore the possibility of using sedimentation instead of the filtration experiments to understand the transport phenomena.

(5)   The future application of the modeling and the experimental method of the unsteady osmosis developed in Chapter Four would be valuable. In many biological and industrial systems, we would encounter processes where the potential is established through a convective diffusion process.

9.3.2 Mixture Filtration through a Partially Rejecting Membrane

(1)   The determination of membrane rejection coefficients reveals that a size selective membrane is more effective in blocking a globular molecule than in blocking a long chain molecule.

(2)   The flow rate, Q, increases with the increase of albumin concentration during the mixture filtration through a partially rejecting membrane. It would be valuable for future studies to verify the preliminary functional dependence of Q with the quantity ($\Delta p \cdot c_2/c_3$) as discussed in Section 7.3.

(3)   It is also valuable to further verify the method, discussed in Sections 7.2, 7.4 and 7.5, of theoretically determining filtration flow rate Q in mixtures filtration through a partially rejecting membrane.

9.3.3 Filtration through Collagen Gels

(1)   In the process of using a needle probe to measure the pressure distribution during saline filtration through a collagen gel, we discovered a possible needle-gel interation which diminishes as the size of the probe increases. The damage to the gel due to the movement of the needle also caused an artifact during the measurement. Experiments revealed that a needle probe can only measure a constant pressure, which is the combination of the local matrix stresses and the fluid pressure. The pressure measurement is in contradiction with the theory. The experimental results may have significant implications in the measurement of the tissue fluid pressure and the pressure

149

inside micro-cavities by a servo-nulling micropressure monitor.

(2)   The osmotic pressure measurement in the osmotic cell during saline filtration through a collagen gel give constant p-π along the filtration path. This result again is in contradiction with the theory. Further experiments are required to verify the experimental results. An examination into the theoretical framework, especially when matrix stress is involved, should also be conducted so that the discrepancy between the theory and the experimental observations can be resolved.

To conclude this chapter, the most interesting future project would be to apply and to further develop the methodology presented in this study to solve real world problems, examples of which have been mentioned at the beginning of this thesis.

Bibliography

Adams, E. T. (1985), Osmometry, in Encyclopedia of Polymer Science and Engineering, vol. 10, John wiley & Sons, New York.

Albertson, P. A. (1986), Partition of cell particles and macromolecules, 3 rd Ed., John Wiley & Sons, New York.

Anderson, D. A, Tannehill, J. C. and Pletcher, R. H. (1984), Computational fluid mechanics and heat transfer, Hemisphere Publishing Co., New York.

Andrade, J. D. (ed.) (1976), Hydrogels for medical and related applications, ACS Symposium Series, No. 31, Washington, D. C., American Chemical Society.

Bear, J. (1972), Dynamics of fluids in porous media, Elsevier, New York.

Bear J. and Corapcioglu M. Y. (1984), Fundamentals of Transport Phenomena in Porous Media, Martinus Nijhoff Publishers.

Bert, J. and Pearce, R. H. (1984), The interstitium and microvascular exchange, in Handbook of Physiology, the Cardiovascular System, Microcirculations, Ed. Renkin, E. M. and Michael, C. C., American Physiology Society, Bethesda.

Bill, A. (1968), A method to determine osmotically effective albumin and gamma globulin concentrations in tissue fluids, its application to the uvea and a note on the effects of capillary "leaks" on tissue fluid dynamics, Acta Physiol. Scand., vol 73, p511.

Biot, M.A. (1956), Theory of deformation of porous viscoeleastic anisotropic solid, J. Appl. Phys, vol. 27, p459.

Bird, R. B., Stewart, W. E. & Lightfoot, E. N. (1960), Transport Phenomea, John Wiley & Sons, New York.

Bonnorris, J. K. G. and Sellers, A. L. (1970), Extravascular albumin in human tissues, Clinical Science, vol. 39, p725.

Brinkman, H. C. (1948), On the permeability of media consisting of closely packed porous particles, Appl. Sci. Res., vol. A1, p81.

Colton, C. K. and Lowrie, E. G. (1981), Hemodialysis: Physical principles and technical considerations, in The Kidney, 2nd Ed., B. M. Brenner and F. C. Rector, eds., W. B. Saunders Co., Now York, p2425.

de Gennes (1971), Scaling concepts in Polymer Physics, Cornell University Press, Ithaca, New York.

Debye, P. and Buche, A. M. (1948) Intrinsic viscosity, diffusion and sedimentation rate of polymers in solution, J. of Chemical Physics, vol. 16, pp573-579.

Deen, W. M., Bohrer, M. P. and Brenner, B. N. (1979), Macromolecule transport across glomerular capillaries: Application of pore theory, Kidney Ins., vol. 16, p353.

Eisenberg, S. R. and Grodzinsky, A. J. (1987), The kinetics of chemically induced nonequilibrium swelling of articular cartilage and corneal stroma, J. of Biomechanical Engineering, vol. 109, p79.

Ethier, C. R. (1983), Hydrodynamics of flow through gels with applications to the eye, M.S thesis, Dept. of Mechanical Engineering, MIT

Ethier, C. R. (1986), The hydrodynamic resistance of hyaluronic acid: estimates from sedimentation studies, Biorheology, vol. 23, p99.

Ethier, C. R. (1992), Creeping flow through heterogeneous fibrous materials, personal communications.

Fein, H. (1972), Microdimensional pressure measurements in electrolytes, J. of Applied Physiology, vol. 32, no. 4, p560.

Flory, P. J. (1953), Principles of polymer chemistry, Cornell University Press, Ithaca, New York.

Granger, H. J. (1981), Physicochemical properties of the extracellular matrix, in Tissue Fluid Pressure and Composition, Ed. Hargens, A. R., Williams and Wilkins & Inc.

Grodzinsky, A. J. (1983), Electromechanical and physicochemical properties of connective tissue, CRC critical Reviews in Biomedical Engineering, vol. 9, no. 2, p133.

Gu, W. Y., Lai, W. M. and Mow, V. C. (1993), Transport of fluid and ions through a porous-permeable charged hydrated tissue, and streaming potential data on normal bovine articular cartilage, J. of Biomechanics, vol. 26, no. 6, p709.

Gyftopoulos, E. P. and Beretta, G. P. (1991), Thermodynamics, Foundations and Applications, Maxwell Macmillan International, New York.

Happel, J. and Brenner, H. (1965), Low Reynolds Number Hydrodynamics, Prentice Hall, New Jersey.

Hiemanz, P. C. (1986), Principles of Colloid and Surface Chemistry, Marcel Dekker Inc.

Horkay, F. and Zrinyi, M. (1986), Studies on mechanical and swelling behavior of polymer networks on the basis of the scaling concept. 6., gels immersed in polymer solutions, J. Macromol. Sci.-Phys., B25(3), p307.

Horkay, F. and Zrinyi, M. (1988), Studies on mechanical and swelling behavior of polymer networks on the basis of the scaling concept. 7., effect of deformation on the swelling equilibrium concentration of gels, Macromolecules, vol. 21, p3260.

Horowitz, P. and Hill, W. (1989), The art of electronics, Cambridge University, Cambridge.

Hossain, M. M., Do, D. D. and Bailey, J. E. (1986), Immobilization of enzymes in porous solids under restricted diffusion conditions, AIChE j., vol. 32, p1088.

Intaglietta, M. and Tompkins, W. R. (1989), Simplified micropressure measurements via bridge current feedback, Microvascular Research, vol. 39, p386.

Intaglietta, M., Pawula, R. F. and Tompkins, W. R., Pressure Measurements in the mammalian microvasculature, Microvascular research, vol. 2, p212

Jackson, G. W. and James, D. F. (1982), the hydrodynamic resistance of hyaluronic acid and its contribution to tissue permeability, Biorheology, vol. 19, p317.

Jackson, G. W. and James, D. F. (1986), The permeability of fibrous porous media, The Canadian Journal of Chemical Engineering, vol. 64, no. 3, p364.

Johnson, M. (1987), Transport through the aqueous outflow system of the eye, Ph.D. thesis, Dept. of Mechanical Engineering, MIT.

Johnson, M., Kamm, R. D., Ethier, C. R., and Pedley, T. (1987), Scaling laws and the effects of concentration polarization on the permeability of hyaluronic acid, PhysicoChemical Hydrodynamics, vol. 9, no. 3/4, p427.

Katchalsky, A and Curran, P. F. (1965), Nonequilibrium Thermodynamics in Biophysics, Harvard University Press, Cambridge, Massachusetts.

Katz, J., Bonnorris, G. and Sellers, A. L. (1970), Extravascular albumin in human tissues, Clinical Science, vol. 39, p725.

Kesting, R. E. (1971) Synthetic Polymer Members, McGraw Hill, New York.

Kim, A. (1989), The hydraulic permeability of serum albumin solutions, MS thesis, Dept. of mechanical engineering, MIT.

Kim, A., Wang, C. H., Johnson, M. and Kamm, R. D. (1991), The specific hydraulic conductivity of bovine serum albumin, Biorheology, vol. 28, p401.

Kirkwood, J. G. and Riseman, J. (1948), The intrinsic viscosities and diffusion constants of flexible macromolecules in solutio, J. of Chemical Physics, vol. 16, pp565-573

Klibanov, A. M. (1983), Immobilized enzymes and cells as practical catalysts, Science, vol. 219, pp723-727.

Kuwabara, S. (1959), The force experienced by randomly distributed parallel circular cylinders or spheres in a viscous flow of small Reynolds numbers, J. Phys. Soc. Japan, vol. 14, p527.

Lai, W. M., Hou, J. S., Mow, V. C. (1991), A triphasic theory for the swelling and deformation behaviors of articular cartilage, J. of Biomechanical Engineering, vol. 113, p245.

Landis, E. M. and Pappenheimer, J. R. (1963), Exchange of subtances through the capillary walls, In: Handbook of Physiology, Circulation. Washington, D. C., Am. Physiol. Soc., Sec. 2, vol. II, pp961-1034.

Langer, R. (1980), Polymeric delivery systems for controlled drug release, Chem. Eng. Commun., vol. 6, p1.

Laurent, T. C. and Pietruszkiewicz, A. (1961), The effect of hyaluronic acid on the sedimentation rate of other substances, Biochemica et Biophysica Acta, vol 49, p258.

Laurent, T. C., Bjork, I., Pietruszkiewicz, A. and Persson, H. (1963), On the interation between polysaccharides and other macromolecules, II. The transport of globular particles through hyaluronic acid solutions, Biochemica et Biophysica Acta,vol. 78, p351.

Leob, G. I. and Scheraga, H. A. (1956), Hydrodynamic and thermodynanic properties of bovine serum albumin at low pH, J. of Phys. Chem., vol. 60, p1633.

Levich, V. G. (1962), Physicochemical Hydrodynamics, Prentice-Hall, New Jersey.

Maepea, O. and Bill, A. (1989), The pressures in the episcleral veins, Schlemm's canal and the trabecular meshwork in Monkeys: Effects of changes in intraocular pressure, Exp. Eye Res., vol. 49, p645.

Mijnlieff, P. F. and Jaspers, W. J. M. (1971), Tras. Faraday Soc., vol. 67, p1837.

Mow, V. C., Holmes, M. H. and Lai, W. M. (1984), Fluid transport and mechanical properties of articular cartilage: A review, J. Biomechanics, vol. 17, no. 5, p377.

Nimni, M. E. (1983), Collagen: Structure, function and metabolism in normal and fibrotic tissues, Seminars in Arthritis and Rheumatism, vol. 13, no. 1, p1.

Obrink, B. (1972), Non-aggregated tropocollagen at physiological pH and Ionic strength, Eur. J. Biochem. vol. 25, pp563-572.

Ogston, A. G. (1966), On water binding, Federation Proc., vol. 25, pp986-988.

Ogston, A. G. (1970), The biological function of the glycosaminoglycans, in chemistry and Molecular Biology of the intercellular Matrix, Ed. Balazs, E. A., Academic Press, vol 3, p1231.

Pedley, T. J. (1980), The interaction between stirring and osmosis, part 1, J. of Fluid Mech., vol. 101, p 843.

Pedley, T. J. (1981), The interaction between stirring and osmosis, part 2, J. of Fluid Mech., p 281.

Probstein, R. F. (1989), Physicochemical Hydrodynamics, Butterworths Publishers, Reading,, Massachusetts.

Press, W. H., Plannery, B. P., Teukolsky, S. A. and Vetterling, W. T. (1988), Numerical Recipes, Cambridge University Press, Cambridge.

Reid, R. C., Prausnitz, J. M. and Sherwood, T. K. (1977), The properties of gases and liquids, McGraw-Hill, New York.

Schafer, J. A. and Andreoli, T. E. (1972), Water transport in biological and artificial membranes, Arch. Internal Med., vol 129, p279.

Schesdegger, A. E. (1974), The physics of flow through porous media, University of Toronto Press, Toronto.

Silberberg, A. (1980), The role of matrix mechanical stress in swelling equilibrium and transport through networks, Macromolecules, vol. 13, p742.

Silberberg, A. (1989), Transport through deformable matrixes, Biorheology, 26, 291-313.

Tanaka, T. (1981), Gels, Scientific American, vol. 244, p124.

Tanford, C. (1963), Physical Chemistry of Macromolecules, John Wiley and Sons, New York.

Treloar, L. R. G. (1975), The physics of rubber Elasticity, Clarendor Press, Oxford.

Truesdell, C. (1962), Mechanical Basis of Diffusion, J. of Chemical Physics, vol. 37, no. 10, p2336.

Vilker, V. (1976), Ultrafiltration of biological macromolecules, Ph.D. thesis, Dept. of Chemical Engineering, MIT.

Vilker, V. L., Colton, C. K., and Smith, K. A. (1981), The osmotic pressure of concentrated protein solutions, J. Colloid and interface Sci., vol. 79, p548.

Viswanadham, R., Agrawal D. C. and kramer, E. J. (1978), Water transport through reconstructed collagen hollow-fiber membranes, J. of Appl. Poly. Sci., vol. 22, pp1655-1663.

Wales, M. (1981), Pressure drop across polarization layers in ultrafiltration, Amer, Chem. Soc. Symp. Ser., vol. 154, p159.

Wagner, R. H. (1945), Determination of osmotic pressure, in Physical Methods of Organic Chemistry, ed. Weissberger, A, Vol. 1, p253

Wiederhielm, C. A., Woodbury J. W., Kirk, S. and Rushmer, R. F. (1964), Pulsatile pressures in the microcirculation of frog's mesentery, Am. J. Physiol., vol. 207, p173.

Wiederhielm, C. A., Fox, J. R. and Lee, D. R. (1976), Ground substance mucopolysaccharides and plasma proteins: their role in capillary water balance, Ameri. J. of Physio., vol 230, no. 4, p1121.

Wijmans, J. G., Nakao, S., Berg J. W. A., Troelstra, F. R., Smolders, C. A. (1985), Hydrodynamic resistance of concentration polarization boundary layer in ultrafiltration, J. Membr. Sci., vol 22, p117.

Winlove, C. P. and Parker, K. H. (1984), Diffusion of macromolecules in hyaluronate gels, I. Development of methods and preliminary results, Biorheology, vol. 21, p347.

Yamamoto, S., Nomura, M. and Sano Y. (1990), Predicting the performance of gel-filtration chromatography of proteins, J of Chromatography, vol. 512, pp77-87.

Yannas, I. V. (1972), Collagen and gelatin in the solid state, J. Macromol. Sci-Revs. macromol. Chem., C7(1), p49.